

Distribution Agreement

In presenting this thesis as a partial fulfillment of the requirements for a degree from Emory University, I hereby grant to Emory University and its agents the non-exclusive license to archive, make accessible, and display my thesis in whole or in part in all forms of media, now or hereafter now, including display on the World Wide Web. I understand that I may select some access restrictions as part of the online submission of this thesis. I retain all ownership rights to the copyright of the thesis. I also retain the right to use in future works (such as articles or books) all or part of this thesis.

Patrick Czabala

March 31, 2023

Triazene Coarctate Cyclization for the Synthesis of Fluorescent Cyclic Peptides

by

Patrick Czabala

Dr. Monika Raj
Adviser

Chemistry

Dr. Monika Raj
Adviser

Dr. Elena Cholakova
Committee Member

Dr. Richard Himes
Committee Member

Dr. Tracy McGill
Committee Member

Dr. Matthew Weinschenk
Committee Member

2023

Triazene Coarctate Cyclization for the Synthesis of Fluorescent Cyclic Peptides

By

Patrick Czabala

Dr. Monika Raj

Adviser

An abstract of
a thesis submitted to the Faculty of Emory College of Arts and Sciences
of Emory University in partial fulfillment
of the requirements of the degree of
Bachelor of Science with Honors

Chemistry

2023

Abstract

Triazene Coarctate Cyclization for the Synthesis of Fluorescent Cyclic Peptides

By Patrick Czabala

Fluorescent cyclic peptides have transformed the way we study biological systems by tracking interactions with proteins and other biomolecules *in situ* or imaging biological events in real-time with high spatial resolution. Current methods mainly rely on functionalizing side chains of cyclic peptides with fluorophores, which could change the physicochemical properties of the parent cyclic peptides and influence their ability to bind and localize in cells. None of the current methods are capable of generating cyclic peptides with in-built fluorescence for cell imaging studies. Herein, we introduce a simple, chemoselective triazene coarctate cyclization (TCC) reaction that combines N-terminal proline or methylated lysine with ortho-alkyne functionalized phenyl diazonium ions to generate highly stable, fluorescent isoindazole 3-carbaldehyde peptides. The peptides exhibit fluorescence only after formation of the isoindazole 3-carbaldehyde, and the photophysical properties of the product can be tuned through late-stage modifications of the in-built aldehyde. We envision the application of this method to cellular imaging in both UV and IR regions. The scope of this reaction is broad, opening up a powerful new approach for the synthesis of in-built fluorescent cyclic peptides and for diverse applications in biological systems.

Triazene Coarctate Cyclization for the Synthesis of Fluorescent Cyclic Peptides

By

Patrick Czabala

Dr. Monika Raj

Adviser

A thesis submitted to the Faculty of Emory College of Arts and Sciences
of Emory University in partial fulfillment
of the requirements of the degree of
Bachelor of Science with Honors

Chemistry

2023

Acknowledgements

I would like to thank Dr. Monika Raj for her tireless support of me as a scientist. I would also like to thank all the current and past members of the Raj Lab for their guidance, mentorship, patience, and help during my time with the lab.

The achievement of presenting an Honors Thesis is decidedly not my own. I could not be here today without the support of the many mentors I have had throughout my life, especially Mrs. Scotti Frese, Mrs. Annette Escala, Dr. Cindy Robertson, Dr. Beth Gereben, Mrs. Julie Wilborn, Mrs. Vivian Ferrari, Mr. Chad Longe, Mr. Michael Young, Mrs. Leigh Ann Wearne, and the St. John Bosco Academy community.

I thank Dr. Tracy McGill for her personal support of me during my undergraduate career, both inside and outside the classroom. I credit Dr. McGill with much of my development as a chemist and as a Catholic.

I thank Dr. Kuei Tang and Dr. Ogonna Nwajobi, Raj lab graduates, for their previous work on this chemistry and willingness to let me extend the application of this method to the present study, as well as for their support and mentorship of me during their time at the Raj lab.

I thank Raj Lab Postdoctoral Scholar Dr. Samrat Sahu for his efforts to synthesize fluorescent small molecule products for this project. He has been an invaluable addition to this work.

I thank Raj Lab student John Talbott for his help in reviewing my honors thesis.

I thank Raj Lab student Angele Bruce for allowing me to re-produce one of her beautiful figures (Fig. 1) in my thesis. I also thank Angele for her mentorship in peptide synthesis and for her tireless efforts to keep our instruments running.

I thank Raj Lab student Rachel Wills for her training and expertise in running the spectrophotometer used to analyze our products.

I thank Raj lab undergraduate Shreyas Rajagopal for helping with some of the synthetic steps in this project.

I thank my committee members for agreeing to be a part of my thesis and for the impact each of you have had on my educational career.

I thank my classmates and colleagues from throughout my time at Emory for the opportunities, learning experiences, support, challenges, and insights they have provided me.

Finally, I thank my family for their endless love, encouragement, and wisdom. My parents have made me the man that I am today. I also thank my siblings, Penny, Peter, and Paul, for the opportunity to be their big brother. I hope that in some small way I have been a positive role model of what it means to be a Catholic.

Table of Contents

Introduction.....	1
Results and discussion	5
Chapter 1: Background, inspiration, and approach.....	5
Chapter 2: Synthesis of p-amino-m-ethynyl phenylalanine-containing peptides	8
Chapter 3: Converting linear peptides to cyclic triazenes.....	14
Chapter 4: Coarctate chemistry to convert cyclic triazenes to isoindazole 3-carbaldehyde peptides	17
Chapter 5: Derivatization of the isoindazole 3-carbaldehyde moiety	23
Conclusions and future directions.....	29
Acknowledgement of contributions	31
References.....	32
Supplemental Information	35
General.....	35
Materials	35
Purification.....	35
Instrumentation and sample analysis	36
Fmoc Solid-Phase Peptide Synthesis (Fmoc-SPPS)	36
Supplementary Figure 1: Synthesis of Fmoc-Phe(4-NH ₂ ,3-I)-OH	37
Supplementary Figure 2: Synthesis of Fmoc-Phe(4-NH ₂ ,3-(trimethylsilyl)ethyne)-OH.....	40
Supplementary Figure 3: Solid-phase Sonogashira coupling	43
Supplementary Figure 4: Triazene peptide synthesis.....	45
Supplementary Figure 5: Optimization of the coarctate reaction on peptides	48
Supplementary Figure 6: Synthesis of small molecule triazene 11	52
Supplementary Figure 7: Optimization of small molecule isoindazole 3-carbaldehyde 12 Synthesis ...	53
Supplementary Figure 8: Synthesis of Wittig, Horner-Wittig, and Henry Olefination Products	57

Supplementary Figure 9: Mechanistic considerations for formation of aryl diazonium and triazene	79
Supplementary Figure 10: Mechanisms for derivatization of aldehyde from Figure 14	81
Supplementary Figure 11: Amino acid coupling mechanism and discussion.....	82
References.....	83

Introduction

Peptide compounds (oligopeptides typically but not exclusively consisting of < 20 amino acids) are an important class of biomolecules that bridge the numerous gaps that exist between small molecule compounds and large protein (biologic) compounds (Fig. 1). There is currently significant research effort dedicated to developing peptide compounds into useful therapeutics and chemical tools for drugging, studying, and identifying diverse targets, particularly the “undruggable proteome” – proteins that lack well-defined and shapely active sites and that have resisted targeting efforts with conventional small molecule approaches.¹ In addition to their potential use for targeting the undruggable proteome, peptide compounds combine advantages of both small molecules and larger proteins. Small molecules and peptide compounds both exhibit oral bioavailability, whereas biologic drugs must be delivered either intravenously or subcutaneously (biologic drugs cannot withstand the harsh chemical and enzymatic environments of the digestive system; therefore, they are not orally bioavailable). Furthermore, peptides and small molecules exhibit lower immunogenicity than biologic compounds, reducing the likelihood of resistance or activation of the host immune system in response to the drug. Third, unlike biologics, which are expensive to produce owing to the need for cellular expression techniques,² peptides can be synthesized on a large scale using benchtop chemistry. This reduces development and production costs for peptide therapeutics. While compounds in each of these three categories serve as effective therapeutics, each category has its own benefits and limitations indicating a continued need for research that improves the properties and usefulness of these biologically useful compounds.

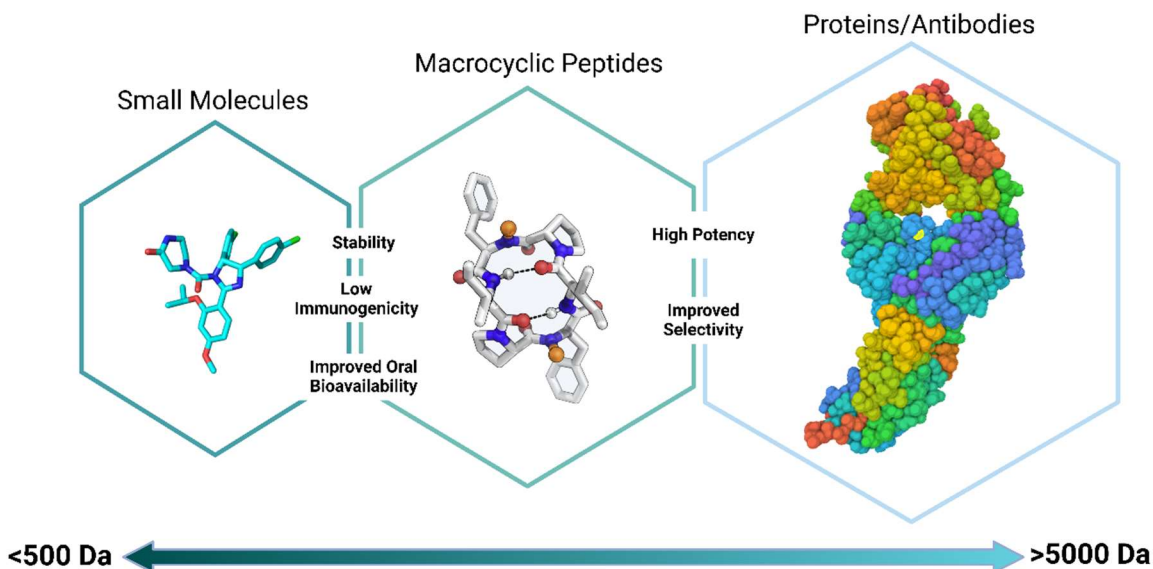


Figure 1. Comparison of the benefits and characteristics of small molecules, macrocyclic peptides, and biologic proteins as therapeutics. Figure re-printed with permission from Angele Bruce of the Raj Lab.

Peptide compounds have been used effectively as drugs for 101 years as of 2023; the first medical use of a peptide drug was that of insulin (an important drug for treatment of Type 1 Diabetes, containing two structurally critical disulfide bonds) in 1922.³ Today, there are over 80 peptide drugs on the market, including 18 cyclic peptide drugs approved between 2001 and 2021.^{3,4} Many peptide drugs are derivatives of natural products (such as the cyclic anti-tumor depsipeptide Romidepsin).⁵ With advances in library screening techniques, *de novo* acting inhibitor and bioactive peptide compounds such as Coagulation factor XII inhibitors have been discovered.⁶ Subsequent drug discovery for these inhibitors has followed a process that mirrors small molecule drug discovery using medicinal chemistry to modify and exchange amino acids for unnatural residues to improve the pharmacokinetic and pharmacodynamic characteristics of the compound.⁷

The two major hurdles to the use of peptide compounds as therapeutics are *in vivo* stability and cellular permeability. Linear peptides are flexible and have accessible termini; these peptides are quickly cleaved and degraded by abundant protease enzymes, leading to prohibitively short half-lives *in vivo*. The typical solution for this problem is to constrain the peptide through macrocyclization using either the termini or side chains.³ Constraining a peptide's structure limits its conformational flexibility, reducing the propensity for off-target binding and increasing proteolytic resistance as the peptide no longer fits easily into the protease binding site. Furthermore, head-to-tail cyclization makes it so that there are not free termini to undergo amide bond hydrolysis by C- or N-terminal proteases. Other methods for increasing proteolytic stability include the addition of unnatural or D-amino acids (most life forms evolved to use L-amino acids;⁸ D-amino acids are the mirror image of their L counterparts and thus do not fit well into proteases, which evolved to fit L amino acids in their active sites). Multiple methods exist to increase the stability of peptides to proteases, and this problem has been satisfactorily addressed. As for cellular permeability, this remains a largely unsolved problem because of the high polarity and H-bonding potential of peptides.⁹ Increasing hydrophobicity and intramolecular H-bonding, or the addition of multiple arginines (poly-Arg peptides) are two methods that increase cellular penetration,¹⁰ but this remains a continued challenge for researchers who wish to bind peptide compounds to intracellular targets. In fact, a 2018 review by Lau et al. reported that over 90 % of peptide compounds undergoing active clinical development were for extracellular targets.¹¹

An area of specialization within peptide compounds is the development of fluorescent peptides. Fluorescent peptides are used in screening, localization studies, cellular visualization experiments, target identification, cell permeability testing, and validation applications. While typically not therapeutics themselves, fluorescent peptides follow the same overarching rules and

require the same approaches as their therapeutic peptides because, like therapeutic peptides, fluorescent peptides are most often used for *in vivo* applications. Fluorescent peptides are thus thought of as an important part of the toolbox for diverse chemistry and biology-related fields.

Current methods to create fluorescent peptides include performing bioconjugation between a peptide and a Green Fluorescent Protein (GFP) derivative or a small molecule dye.¹² These methods require secondary derivatization of peptides with bulky fluorescent groups that can bias bioactivity, binding affinity, and cellular permeability. In contrast to these methods, in-built fluorescent moieties in peptides dispense with this problem of bias by directly incorporating the fluorescent group into the native structure of the constrained peptide. Only a few methods exist to create in-built fluorescent moieties upon peptide cyclization. These methods, reported simultaneously by Li and Perrin, utilize *ortho*-phthalaldehyde to react chemoselectively with an amine (lysine or N-terminus) and cysteine on peptides to create fluorescent isoindole cyclic peptides (Fig. 2).^{13,14} However, these methods exhibit limited tunability of the fluorescence excitation and emission wavelengths of the products (excitation wavelengths from 329 – 345 nm and emission wavelengths from 415 – 459) and are not tolerable of additional lysine and/or cysteine residues without protecting groups. The need for protecting groups complicates the synthesis of these products; if multiple reactive amines or thiols are present, a complex mixture of stapling products results. These are clear limitations of the current techniques and indicate a need for new methods to create cyclic peptides with in-built fluorescence that are tolerable of reactive amine and thiol residues.

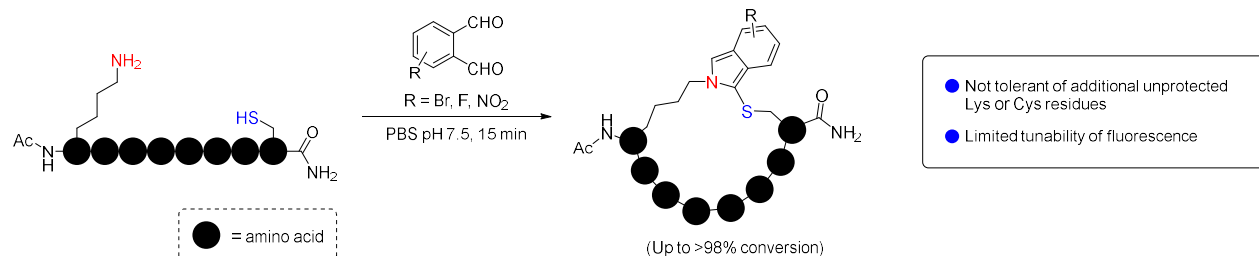


Figure 2. Existing method to create constrained peptides with in-built fluorescence using Fluorescent Isoindole Crosslink (FIICK) chemistry.

Presented herein, this work draws inspiration from a current project in our lab – developing a covalent chemical probe for monomethylated lysine posttranslational modifications (PTMs) – to create cyclic peptides with in-built fluorescence and an in-built aldehyde handle for derivatization with affinity tags, small molecules, or conjugated systems that enable the photophysical properties of the resulting peptide to be tuned over a range of excitation and emission wavelengths.

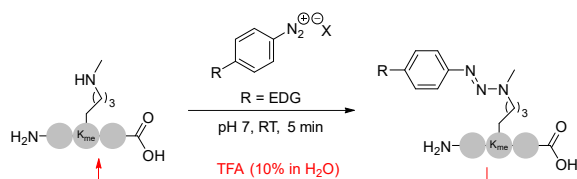
Results and discussion

Chapter 1: Background, inspiration, and approach

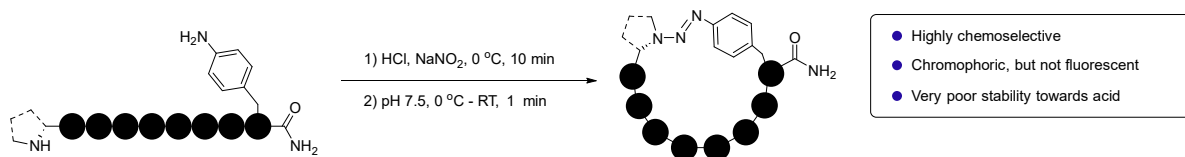
This work takes inspiration from a current project in our lab to target monomethylated lysine (K_{me}). Methylation is an abundant PTM with a host of biological roles, most notably in regulating gene expression through modification of histone proteins.¹⁵ Our lab has previously published on this method as a traceless enrichment technique for K_{me} residues in biocompatible conditions (Fig. 3a).¹⁶ Aryl diazonium salts were reacted with K_{me} under neutral or basic conditions to rapidly (<5 min) afford a covalent modification of the secondary amine, converting it into a triazene. The reaction between the aryl diazonium and secondary amine exhibits impressive kinetics (>99% conversion within 5 minutes) and chemoselectivity (no observed reaction with canonical amino acids at the end of the reaction). Further, the aryl triazene is dynamically responsive to pH: The triazene decomposes into the secondary amine and aryl diazonium ion

(traceless modification) under acidic conditions and rapidly re-forms when the solvent is brought back to pH 7 or above (see Fig. 9, Ch. 3, and Supplementary Fig. 9 for further discussion of the mechanism of this reaction). As an extension of the utility of this chemistry, our lab has also published a method to create dynamic cyclic peptides with triazene moieties (Figure 3b).¹⁷ This method works by installing *p*-amino phenylalanine on the C-terminal side of a peptide and cyclizing with various secondary amines in a side-to-tail (using N-terminal proline or an N-terminal methylated amino acid) or side-to-side (using methylated lysine) manner.

a. Existing method to target and enrich K_{me} -containing peptides using Selective Triazene Reaction (STaR) chemistry



b. Existing method to make triazene cyclic peptides



c. This work: Formation of isoindazole 3-carbaldehyde cyclic peptides and their late stage modification

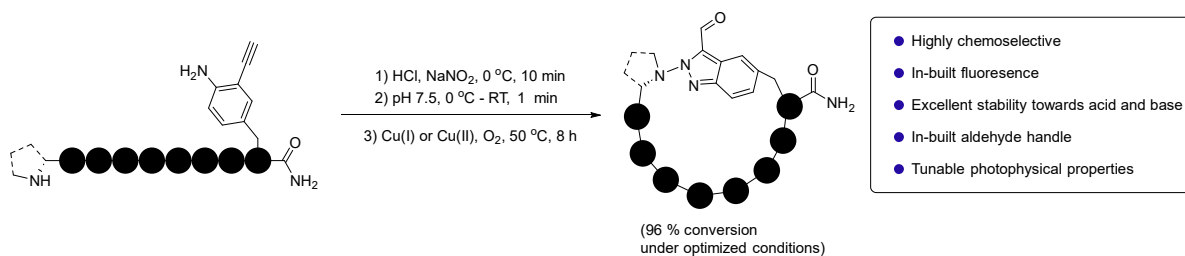


Figure 3. (a) Previous method developed by our lab to tracelessly tag and enrich monomethylated lysine (K_{me}) peptides under biocompatible conditions. (b) Previous method developed by our lab for creating dynamically responsive triazene cyclic peptides. (c) This work: formation of isoindazole 3-carbaldehyde cyclic peptides. The addition of an alkyne ortho to the aryl amine enables a copper-mediated thermal rearrangement to the fluorescent product, and the aldehyde handle may be reacted to increase the conjugation of the system.

The acid sensitivity of aryl triazenes led us to explore methods to increase the chemical stability of the structure. In the early 2000s, Haley et al. reported a novel rearrangement of *o*-ethynyl aryl triazenes to stable *2H*-indazoles (hereafter referred to as isoindazoles; the kinetic product) and cinnolines (the thermodynamic product). Their initial conditions required prohibitively high temperatures (170 – 200 °C) unsuitable for peptide chemistry and furnished a mixture of products. However, in the same paper, Haley et al. reported that the selective conversion of these *o*-ethynyl aryl triazenes to isoindazoles could be achieved at reasonable temperatures (RT up to 50 °C) using copper catalysts. The authors report that the critical intermediate in the formation of the isoindazole product is a carbene (Fig. 11, see Ch. 4 for a detailed discussion), a divalent carbon with a lone pair (in contrast to a carbanion, which is a trivalent carbon with a lone pair, bearing a negative formal charge). Copper salts are known to stabilize carbenes (resulting in a complex called a carbenoid), and the authors report high conversions to the isoindazole kinetic product with this method. The mechanism of this reaction is considered further in Chapter 4. We are currently preparing a manuscript that employs this isoindazole-forming chemistry as a bioconjugation technique to covalently modify and profile K_{me} PTMs.

This project focuses on developing isoindazole cyclic peptides and tuning the fluorescence characteristics of the resulting moiety. There are several challenges in this work:

- 1) Synthesizing peptides with the requisite unnatural amino acid *p*-amino-*m*-ethynyl phenylalanine (Chapter 2)
- 2) Converting these peptides to the cyclic triazene (Chapter 3)
- 3) Converting the cyclic triazene to the cyclic isoindazole (Chapter 4)
- 4) Derivatizing the isoindazole 3-carbaldehyde moiety to tune the fluorescence (Chapter 5)

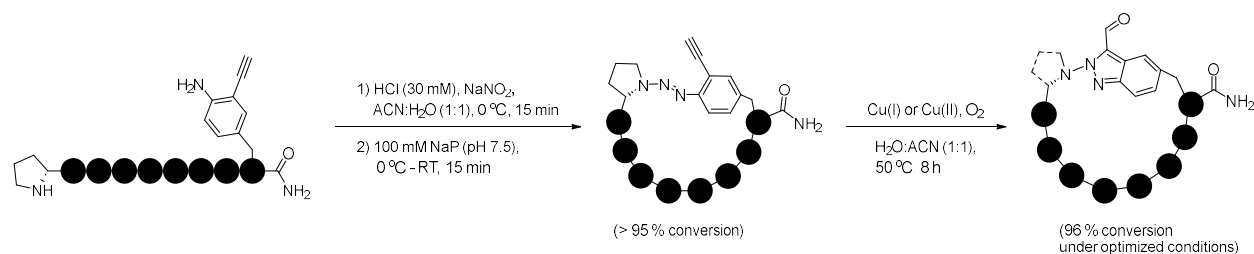


Figure 4. Generic scheme of this work to convert linear peptides to cyclic, fluorescent isoindazole 3-carbaldehyde peptides with an aldehyde handle for further conjugation or derivatization.

This work utilizes the chemically synthesized unnatural amino acid *p*-amino-*m*-ethynyl phenylalanine on the C-terminal position of the peptide. This aryl amine is converted to a reactive diazonium under facile conditions and then crosslinked with a secondary amine source on the other end of the peptide to form a triazene – any secondary amine can be used including N-terminal proline, N-methylated lysine, or N-methylated N-terminus. The reaction between the aryl diazonium and the secondary amine at neutral, buffered conditions yields a stable triazene which then undergoes a copper-mediated coarctate rearrangement to give an isoindazole 3-carbaldehyde fluorescent moiety (Fig. 4).

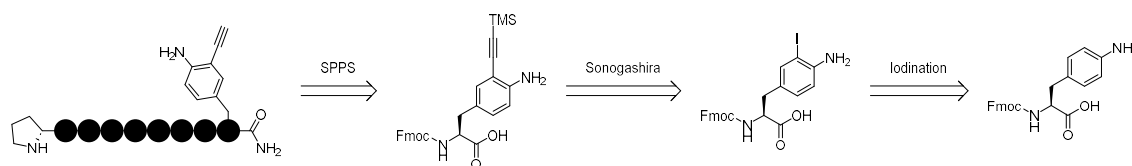
The following chapters describe the approaches taken to address each of the four challenges in this project listed above.

Chapter 2: Synthesis of *p*-amino-*m*-ethynyl phenylalanine-containing peptides

The first challenge in this project was to synthesize linear peptides with the unnatural amino acid *p*-amino-*m*-ethynyl phenylalanine at the C-terminus. Fmoc peptide synthesis is the method of choice for oligopeptide synthesis at high scale (0.1-0.6 mmol, or higher). Several retrosynthetic approaches were created in an attempt to obtain these linear peptides with the desired unnatural amino acid (Fig. 5). There were several concerns during the retrosynthetic analysis. First, it was considered that the aryl amine on *p*-amino phenylalanine might need to be protected to

prevent undesired peptide extension from that position (the free amine was hypothesized to react with the activated esters used in amino acid coupling steps, see Supplementary Figure 11). After some experiments, it was determined that the unprotected aryl amine did not interfere with SPPS and exhibited no peptide couplings off of this side chain. One explanation for this observation is the greatly reduced reactivity of the amine due to its conjugation with the attached benzyl ring, making the lone pair less available to serve as a nucleophile in the attack of an activated ester. Because the synthetic schemes were greatly simplified by using the free (unprotected) aromatic amine, the two approaches in Figure 5 were pursued using Fmoc-*p*-amino phenylalanine as the commercially available precursor.

Scheme 1: Employing Solution-phase Sonogashira Coupling



Scheme 2: Employing Solid-phase Sonogashira Coupling

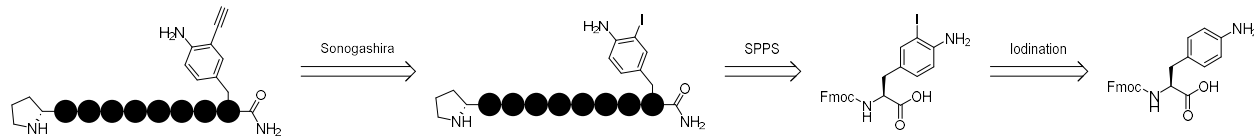


Figure 5. Two retrosynthetic approaches to obtain linear peptides with *p*-amino-*m*-ethynyl phenylalanine at the C terminus.

The first step of both **Scheme 1** and **Scheme 2** was to halogenate the commercially available Fmoc-Phe(4-NH₂)-OH (Fig. 6d). Iodination was hypothesized to afford the greatest polarity difference between the starting material and the product, given the large atomic radius of iodine as compared to chlorine and bromine, which would allow for the easiest separation of the starting material and product. Thus, iodine was chosen as the desired halogen for this step.

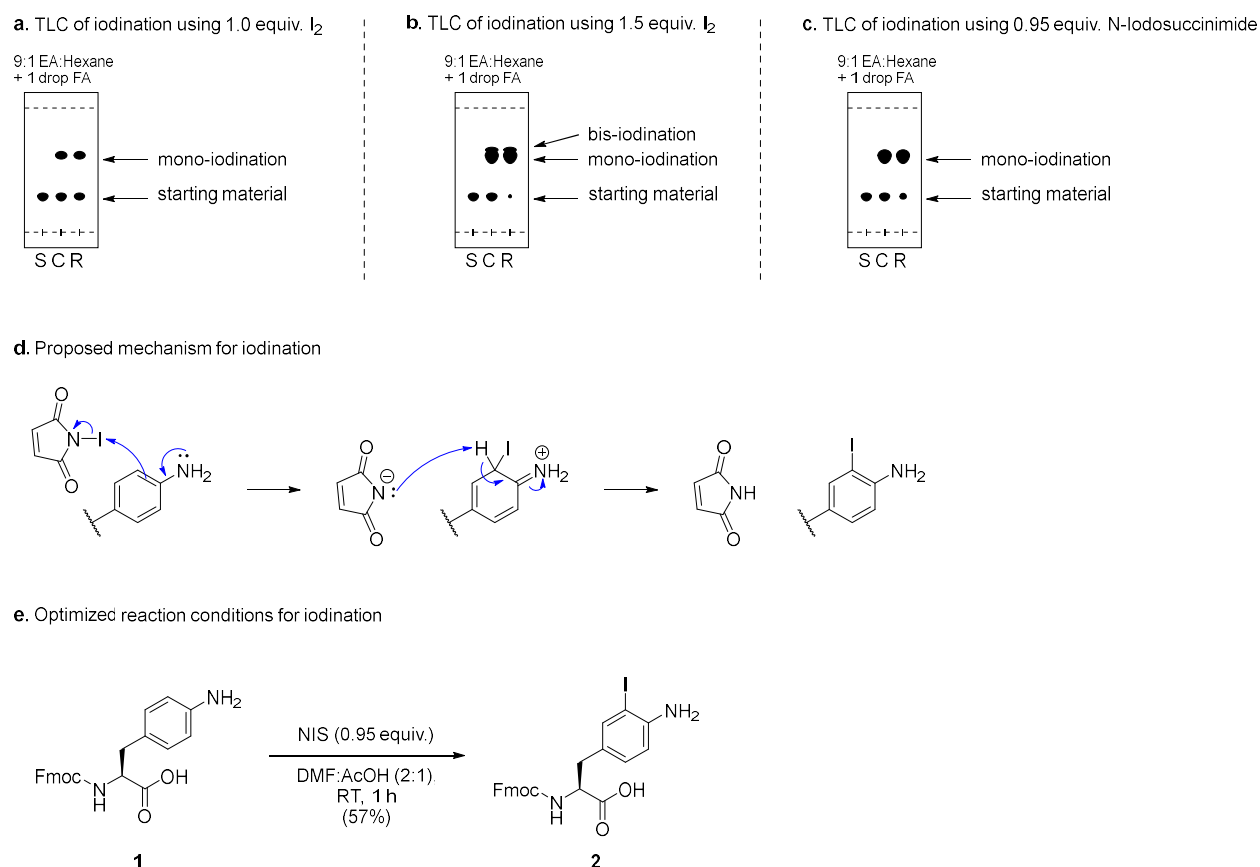


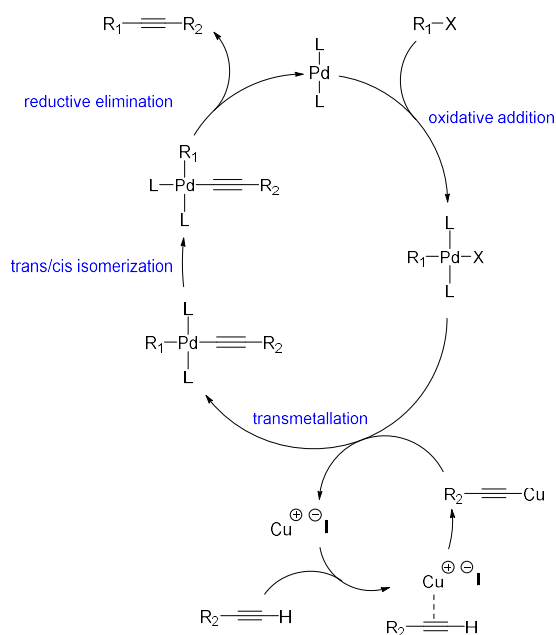
Figure 6. (a) molecular iodine as the halogenating agent afforded poor conversion to the desired mono-iodination product using 1 equiv. (< 40 % by visual TLC analysis). (b) TLC showing that 1.5 equiv. of I_2 furnished better conversion but an inseparable mixture of mono- and bis-iodination products. (c) TLC showing that 0.95 equivalents of N-Iodosuccinimide (NIS) gave higher conversions to the mono-iodination product. (d) Proposed mechanism for iodination of aryl amine using NIS. (e) Optimized reaction conditions for iodination using 0.95 equiv. of NIS. (a), (b) and (c) “S,” “C,” and “R” stand for starting material, co-spot, and reaction mixture lanes, respectively.

Iodination of aniline scaffolds is well-known in literature, but replicating known methods using I_2 did not afford the desired product **2** in pure form with good yields.¹⁸ Iodination was first attempted with molecular iodine (I_2) (Fig. 6a and Fig. 6b). 1 equiv. of I_2 resulted in less than 40 % conversion to the iodination product, but the product was exclusively mono-iodinated amino acid, as confirmed by TLC and NMR. When higher equivalents of iodine were used (1.5 equiv.), the TLC showed an inseparable mixture of mono- and bis-iodination products. The R_f of these two spots were so close that it was futile to separate them using silica gel column chromatography. Of

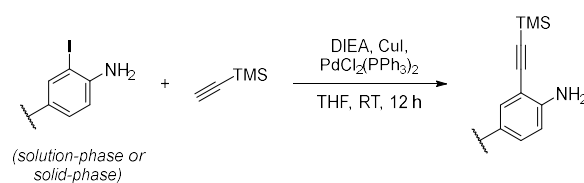
additional note, the free carboxylic acid of the compound required the addition of 1 % v/v acetic acid to the eluent during column chromatography to prevent dragging of the spots, but generally the presence of the carboxylic acid reduced the attainable resolution of spots during purification. A host of other conditions and halogenating agents were screened, and it was determined that 0.95 equiv. of N-iodosuccinimide afforded significantly improved conversion to the mono-iodination product **2** without creating the bis-iodination product. The electron-donating nature of the lone pair on the aryl amine enabled facile conditions to be used to obtain the iodination product **2** (Fig. 6d). On a 5 mmol scale, this reaction produced **2** in 57 % pure yield (Fig. 6e).

With multi-gram quantities of the iodination product **2** in hand, attention was turned to the replacement of the iodine for an alkyne via Sonogashira cross coupling. The Sonogashira coupling uses palladium and copper catalysts to cross couple an aryl iodide with terminal alkynes (Fig. 7).

a. Catalytic cycle of the Sonogashira cross coupling reaction



b. Generalized Sonogashira reaction for this work



c. Target products of the Sonogashira coupling

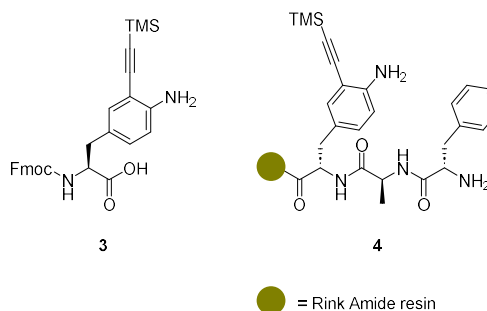


Figure 7. (a) The catalytic cycle for the Sonogashira cross coupling reaction involving palladium and copper co-catalysts. (b) A scheme demonstrating the application of the Sonogashira reaction to this work. (c) The targeted products of Sonogashira coupling from either solution-phase or solid-phase synthesis.

The Sonogashira coupling was first attempted according to **Scheme 1**, employing a solution-phase Sonogashira reaction. It was determined using TLC that while the starting material disappeared and some of the cross-coupling product **3** formed, there was an overwhelming amount of Fmoc deprotection that had occurred, in contrast to the literature reports.¹⁹ The mechanism of Fmoc deprotection occurs in base (Fig. 8) and can be slowed down by the use of sterically hindered amine bases such as diisopropylethylamine (DIEA) instead of less hindered bases such as triethylamine (TEA), which is a favorite among chemists who perform the Sonogashira reaction. In fact, many Sonogashira reactions are run in TEA as the solvent. However, even with the sterically hindered DIEA in lower amounts (5 equiv. instead of 1:1 with THF as the solvent), the Fmoc deprotection over the course of the reaction remained substantial. One possible explanation for this observation is that Fmoc deprotection reveals a primary amine, which can deprotect other Fmoc groups (this autocatalytic deprotection would not be prevented by lowering the equivalents of DIEA). After many attempts, product **3** was successfully made using 10 mol % of both the Bis(triphenylphosphine)palladium (II) dichloride and Copper (I) iodide, 10 equiv. of DIEA, and 5 equiv. of the alkyne stirred under N₂ in degassed THF for 12 h at RT. **3** was purified to > 90 % purity with 15 % yield, as analyzed by TLC and NMR. ESI (+) mass spectrometry also confirmed the Sonogashira reaction was successful (Supplementary Fig. 2). Deprotection of the trimethylsilyl (TMS) group to afford the free alkyne was not performed in the solution-phase; the basic conditions (K₂CO₃ in MeOH or tetrabutylammonium fluoride (TBAF) in THF) required for TMS deprotection also deprotect Fmoc group from the N-terminus, a protecting group which is essential

for SPPS. It was reasoned that the Sonogashira step could be performed on solid support during SPPS (discussed in next paragraph). TMS deprotection was effectuated on resin by shaking the synthesis vessel with 7 equiv. K_2CO_3 in MeOH for 12 h. Despite the low yields for solution-phase Sonogashira coupling, a linear peptide with *p*-amino-*m*-ethynyl phenylalanine obtained from SPPS following the synthesis of the unnatural amino acid **3** in the solution phase (Scheme 1) was successfully synthesized.

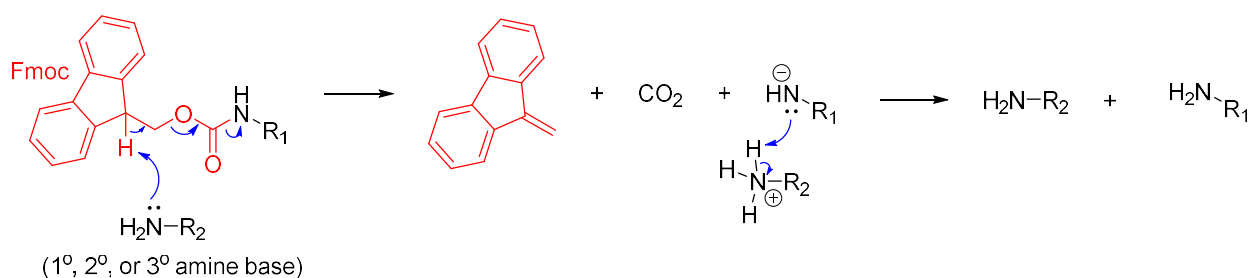


Figure 8. Mechanism of Fmoc deprotection in the presence of amine base.

Concurrently with the **Scheme 1** approach, efforts were made to develop the **Scheme 2** approach, employing the Sonogashira coupling chemistry on solid-support. There is literature precedent for the Sonogashira reaction on solid-support,^{20,19,21} and this approach was hypothesized to fix several of the issues with **Scheme 1**; namely that the Sonogashira product was not entirely pure (despite best efforts), the yields were poor, and the product was an oil which made weighing out an appropriate amount for SPPS coupling more difficult. For these reasons, **Scheme 2** was preferable. Successful performance of the on-resin Sonogashira coupling required over a month of trial-and-error, however after some failures the coupling began to work quantitatively with remarkable ease. Among the insights gained during the optimization of this reaction were that 1) degassed THF (bubbled with N_2 under Schlenk line conditions) was necessary to avoid catalyst poisoning by O_2 , 2) stirring of the resin in a round bottom flask with a stir bar resulted in high

shear stress that destroyed the solid support Rink resin (performing this reaction in a solid-phase synthesis vessel on a wrist-action shaker solved this problem),²² and 3) removal of the palladium after completion of the reaction using an appropriate chelating agent (0.2 M sodium dimethyldithiocarbamate in DMF, 2 x 15 minutes) was necessary to get metal-free crude peptides and cleaner HPLC spectra during purification. Palladium forms many adducts with peptide backbones, greatly complicating purification and analysis, so removal of palladium during SPPS was essential. After the Sonogashira coupling and removal of the excess palladium from the resin, the TMS group was cleanly deprotected on solid-support with 7 equiv. of K_2CO_3 in MeOH at RT for 12 h. After chain elongation and cleavage, ESI(+) mass spectrometry demonstrated quantitative conversion of the aryl halide to the free alkyne under optimized conditions (Supplementary Fig. 3).

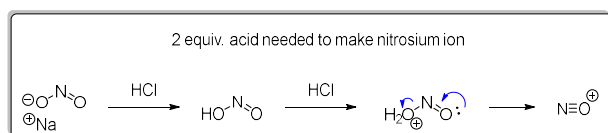
In conclusion, both **Scheme 1** and **Scheme 2** were successfully developed for the synthesis of linear peptides containing *p*-amino-*m*-ethynyl phenylalanine as the C-terminal residue. **Scheme 2**, employing Sonogashira coupling chemistry on solid support, was the clear favorite for the synthesis of these linear peptides. **Scheme 2** can be streamlined for the synthesis of multiple linear peptides by creating a stock of “prepared resin” by coupling 1-3 amino acids and performing the Sonogashira coupling chemistry before splitting the resin into smaller batches to make different linear peptides. This way, the two-day process of the Sonogashira coupling and the TMS deprotection does not need to be repeated for each peptide to be synthesized.

Chapter 3: Converting linear peptides to cyclic triazenes

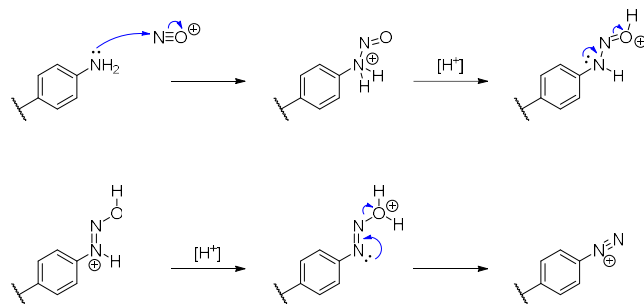
The arene triazene chemistry to make macrocyclic peptides used in this project has been previously published by our lab.¹⁷ Ideally, minimal optimization should be required to obtain the

triazene peptides. The reaction proceeds in one-pot through two steps: formation of the aryl diazonium, and the cyclization with secondary amine to give the cyclic triazene (Fig. 9, Fig. 10).

a. Formation of the aryl diazonium ion



Proposed mechanism:



b. Reaction of the aryl diazonium with secondary amine to give triazene

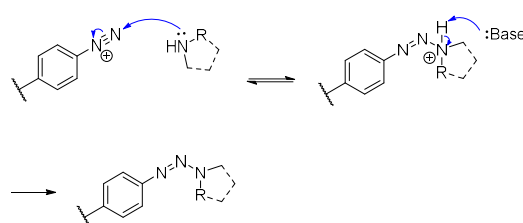


Figure 9. (a) mechanism for the formation of the reactive NO^+ ion from sodium nitrite under acidic conditions and its subsequent formation of the aryl diazonium. (b) Mechanism of the reaction of the aryl diazonium with a secondary amine to form a stable triazene.

mM peptide and 10 mM HCl for diazonium formation, we obtained just 10 % yield of the triazene peptide **6**. This represented a simple but significant mistake: Two equivalents of acid are required to make the reactive nitrosium cation, and the subsequent formation of the aryl diazonium is acid-catalyzed (Fig. 9a). Increasing peptide concentration without increasing the concentration of the acid led to the presence of an insufficient amount of HCl to form the aryl diazonium. We corrected this mistake by running the 10 mg scale reaction at an initial concentration of 3 mM peptide and 30 mM HCl, which immediately solved the problem of failed triazene synthesis while maintaining smaller reaction volumes. It was also determined that the reaction could be frozen, lyophilized, and dissolved in a lesser volume of solvent for purification. HPLC spectra showing poor conversion suddenly improved to > 95 % conversion to the cyclic triazene, with full consumption of the starting material. In this manner, tens of milligrams of our model cyclic triazene peptide (a relatively large amount for our work) were obtained in very pure form. Indeed, the problem was simply that there had not been enough acid in the reaction mixture to effectively convert the nitrite to the nitrosium ion and for that cation to react with the aryl amine to give the diazonium ion.

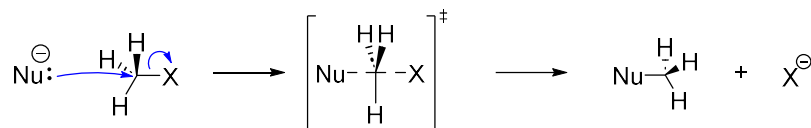
For further explanation of the chemoselectivity of this reaction, including the formation of the diazonium ion and selective formation of the triazene with secondary amines, see Supplementary Fig. 9.

Chapter 4: Coarctate chemistry to convert cyclic triazenes to isoindazole 3-carbaldehyde peptides

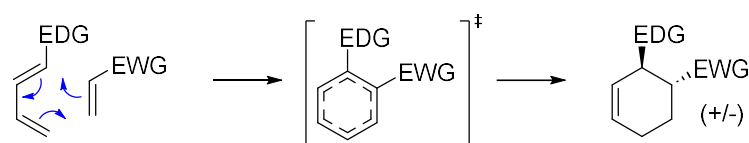
After successful synthesis of the triazene cyclic peptide **6**, the next step was to complete a coarctate rearrangement to the isoindazole 3-carbaldehyde product **7**. Coarctate reactions are defined as having bicyclic transition states wherein two bonds are made and broken to the same atom simultaneously. These are relatively rare reactions: the standard reaction topologies are linear

and pericyclic, but coarctate is a lesser-known third topology (Fig. 10).²³ The most well-known coarctate reactions are the epoxidation of alkenes by dimethyldioxirane (DMDO) or peracids.

a. Linear



b. Pericyclic



c. Coarctate

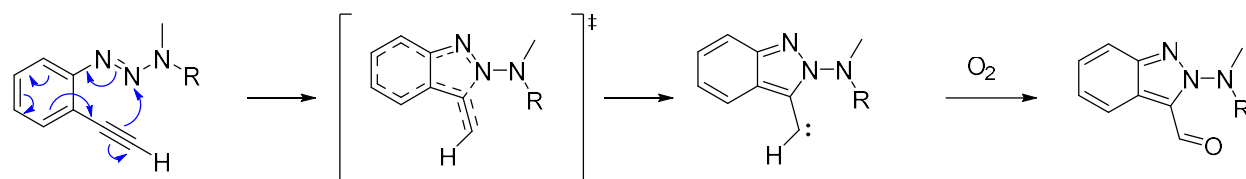


Figure 11. (a) Linear reaction topology. (b) Pericyclic reaction topology. (c) This work: Coarctate reaction topology showing formation and breakage of two bonds at the same atom. The aldehyde forming step involving the trapping of the carbene by O_2 is also shown.

It was at first desired to make the synthesis of the isoindazole 3-carbaldehyde peptides a one-pot reaction from the linear peptide to the final product. However, we encountered the issues of low solubility and precipitation of the copper salts in buffer and basic pH, which for now have prevented us from making this a one-pot reaction. So, triazene peptides were synthesized and then de-salted using HPLC purification and lyophilization. Peptides were re-dissolved in ACN:H₂O with the copper catalyst and heated in the presence of O_2 to form the isoindazole 3-carbaldehyde products. After some failures, initial success was obtained when 15 equivalents of Copper (II) acetate were incubated with the peptide in H₂O bubbled with O_2 at 50 °C for 16 h. When

considering the mechanistic pathway for this reaction, trapping of the carbene intermediate by O₂ is the final, critical step in forming the isoindazole 3-carbaldehyde (Fig. 11). Accordingly, the best results were obtained when both the solvent was bubbled with O₂ and the headspace of the vial was filled with O₂ before sealing off the vial for the reaction. The mechanism of the copper catalyst is to stabilize the kinetic carbene intermediate, giving time for the carbene to be trapped by O₂ to form the aldehyde. Fascinatingly, both Cu (I) and Cu (II) salts have been observed to catalyze this reaction, and our own results confirm that both appear to work equally well (Table 1).

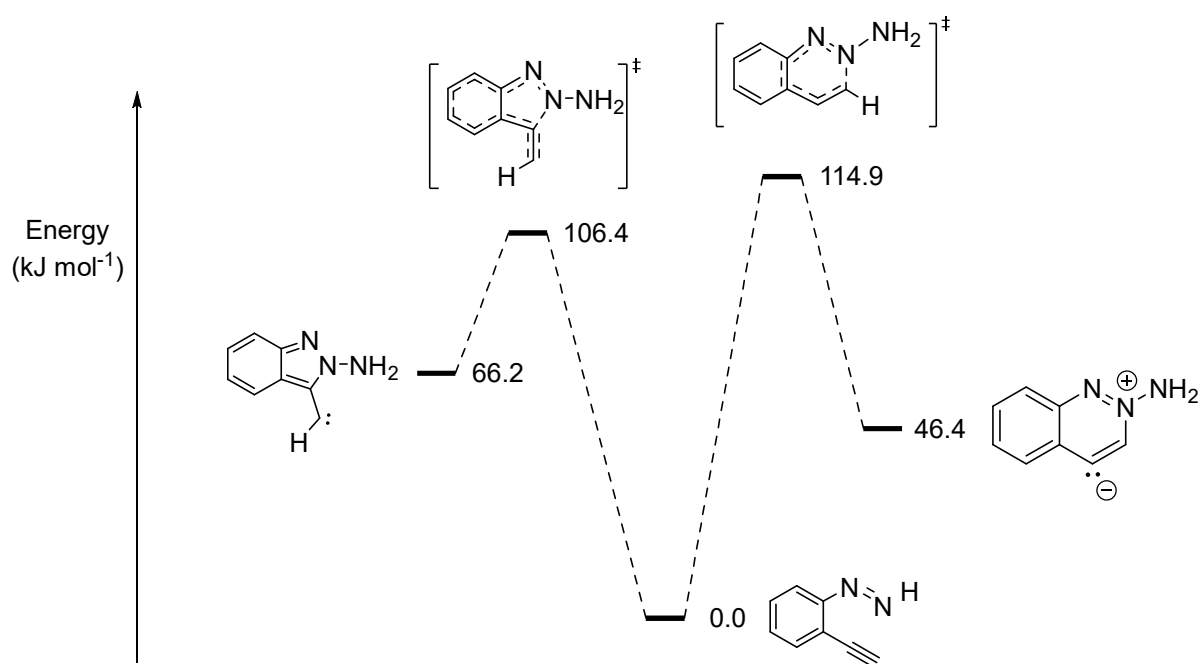
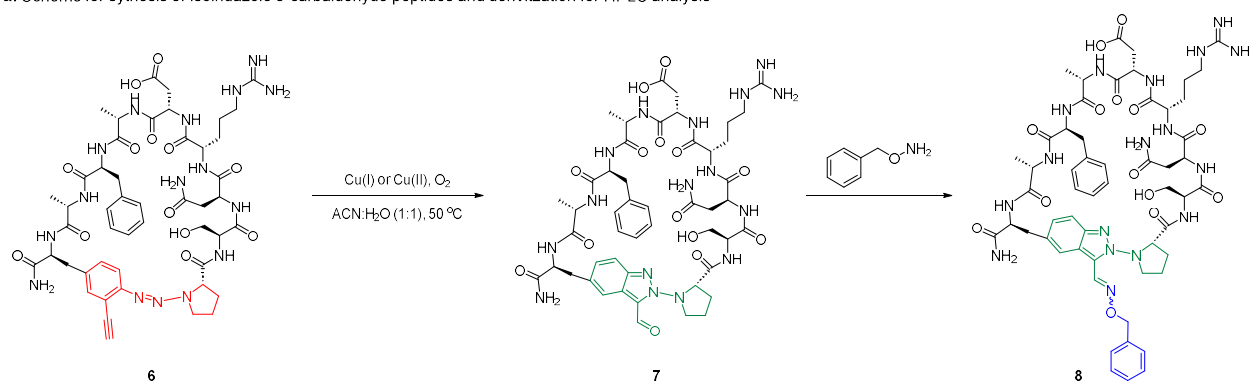


Figure 12. Mechanistic studies performed by Haley et. al using Density-functional theory (DFT) calculations.²⁴ The pathway to the isoindazole 3-carbaldehyde is considered to be the kinetic product. Addition of a copper catalyst stabilizes the carbene intermediate.

When optimizing this reaction, HPLC analysis at 220 nm (the standard wavelength used to monitor peptide reactions) was used to quantify conversion. A problem was encountered in that

both the triazene **6** and the isoindazole 3-carbaldehyde product **7** typically eluted together in the HPLC (the difference in retention time is approximately 1 minute, see Supplementary Figs. 4 and 5), preventing quantification of conversion. A simple solution to this problem was to react the aldehyde with benzyloxyamine to make an aldoxime that would be more nonpolar than the aldehyde, shifting the retention time of the product as compared to the triazene (Fig. 12). By mixing 5 equivalents of benzyloxyamine with the reaction aliquot, quantitative conversion of the aldehyde to the aldoxime **8** was observed, allowing for accurate HPLC analysis of conversion to the isoindazole.

a. Scheme for synthesis of isoindazole 3-carbaldehyde peptides and derivitization for HPLC analysis



b. HPLC spectra at 8 h for optimization of Coaracetate rearrangement reaction

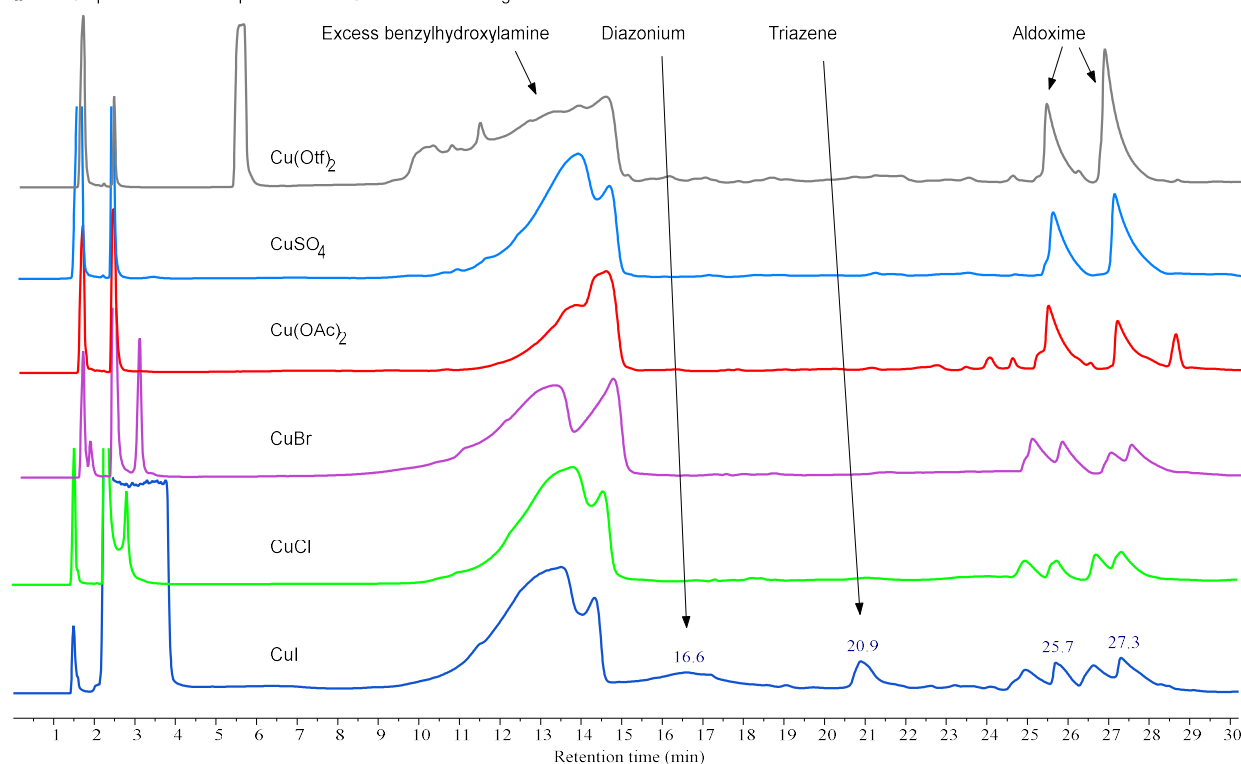
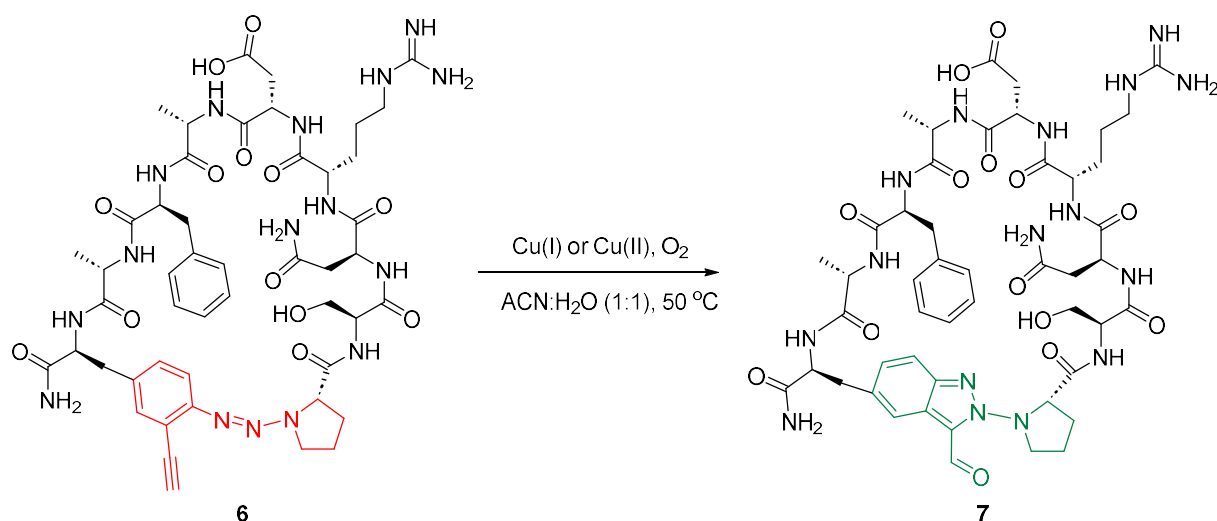


Figure 13 (a) Scheme showing the reaction with the model peptide converting from the triazene to the isoindazole 3-carbaldehyde, and subsequent reaction with benzylhydroxylamine to simplify HPLC analysis. (b) Overlaid HPLC absorbance (220 nm) of the optimization reactions at 8 h to form the isoindazole 3-carbaldehyde. The peak at 16.6 min is the linear diazonium ion (ring-opened triazene). The peak at 20.9 min is the cyclic triazene. The set of 2 or 4 peaks between 25 and 28 min are the isomers of the aldoxime peptide products. The conversions are quantified for these reactions in **Table 1**. The large, broad peak between 11 and 15 min is excess benzylhydroxylamine.

The initial round of optimization screened various copper catalysts available in our lab with otherwise identical conditions. All of the copper salts screened gave the isoindazole product in good yield, with the best being Copper (I) bromide (Fig. 12, Table 1).

Table 1. Table showing conversion to the isoindazole 3-carbaldehyde cyclic peptide, as analyzed by HPLC analysis at 220 nm.



<i>Catalyst (5 equiv.)</i>	<i>Conversion at 8 h</i>	<i>Conversion at 16 h</i>
CuI	58%	65%
CuCl	88%	88%
CuBr	96%	93%
Cu(OAc) ₂	81%	74%
CuSO ₄	91%	92%
Cu(Otf) ₂	82%	65%

The conversions generally decreased when the length of the reaction was extended from 8 h to 16 h (except for CuI, which increased from 58% to 65%). However, product **7** did not appear to significantly degrade during the reaction after 16 h at 50 °C. In the future, decreased reaction times will be explored to determine the optimal reaction duration.

The current status of this phase of the project is that isoindazole 3-carbaldehyde peptides are being created in good yield. More optimization studies will be completed in the future to include lower reaction times and lower catalyst loadings, as well as to further investigate the effect of temperature on the reaction. As for the purification of isoindazole 3-carbaldehyde peptides, preparative scale HPLC run with a slow gradient afforded separation between the triazene and product peaks, allowing for effective purification and characterization of **7** (Supplementary Fig. 5).

Chapter 5: Derivatization of the isoindazole 3-carbaldehyde moiety

It was envisioned that the in-built aldehyde after coarctate rearrangement would serve as an effective handle for simple attachment of additional dyes, affinity handles, or other species (Fig. 14.)

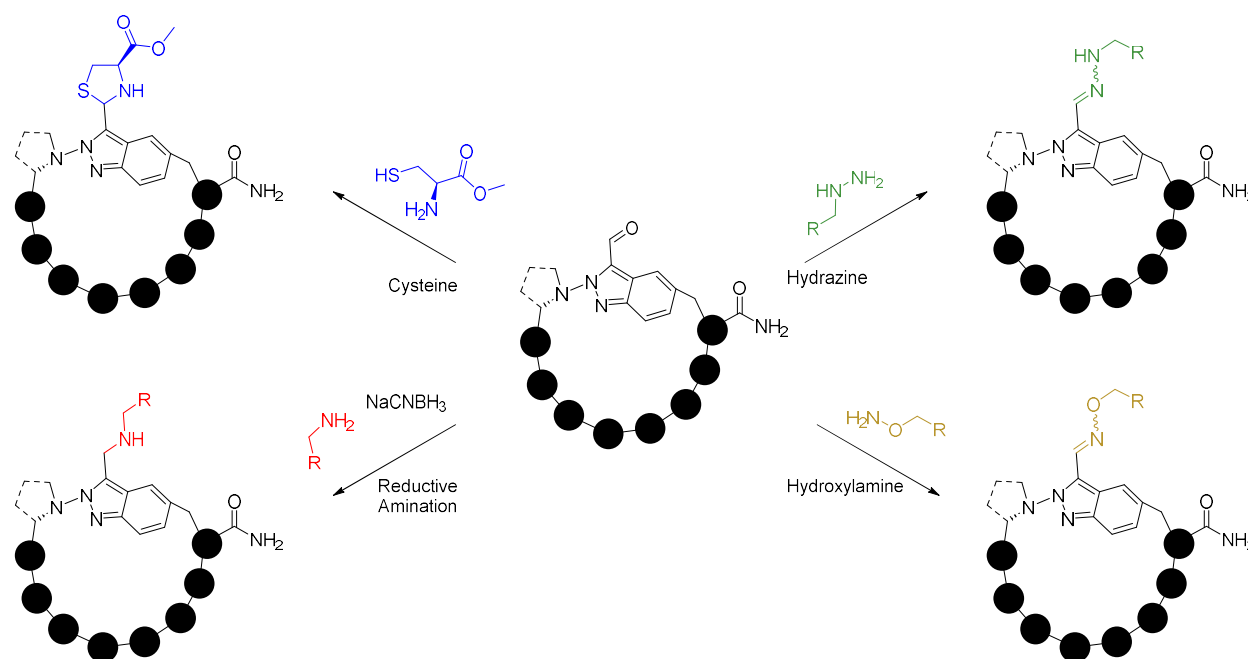


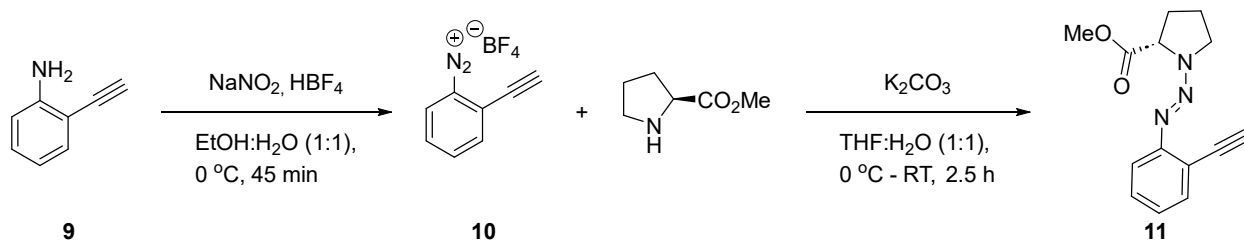
Figure 14. Simple reactions to derivatize isoindazole 3-carbaldehyde peptides using aldehyde-reactive molecules including cysteine (to thiazolidine), alkyl amine and sodium cyanoborohydride (to reductive amination), hydrazine (to hydrazone), and hydroxylamine (to aldoxime).

Each of these reactions are well-known and are commonly taught as part of a basic organic chemistry curriculum. These examples will be completed with the model peptide **7**. We turned our attention to a more scientifically interesting matter: Increasing the conjugation of the isoindazole 3-carbaldehyde peptides, thereby tuning the fluorescence characteristics of the resulting fluorophore. The isoindazole 3-carbaldehyde moiety exhibits excitation at 311 nm and emission at 410 nm (Supplementary Fig. 7). For cell-based applications, this wavelength is not ideal: the high energy photons of UV light can cause DNA damage and formation of destructive reactive oxygen species (ROS), leading to cell damage and death. Furthermore, there are a number of biomolecules that excite at these UV wavelengths, leading to cellular autofluorescence that complicates analysis of the exogenous fluorophore. Thus, red-shifted fluorophores are more ideal for cellular settings. We investigated methods to increase the conjugation of the system using the Wittig, Horner-Wittig, and Henry reactions (Fig. 15).

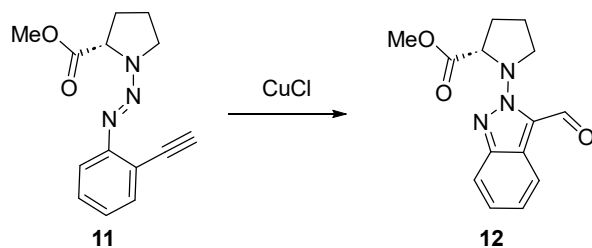
We began our investigation in this regard by synthesizing the small molecule isoindazole 3-carbaldehyde **12** as a small molecule formed from the reaction between 2-ethynylaniline and proline methyl ester (Fig. 15). The synthesis of triazene **11** and isoindazole 3-carbaldehyde **12** have been previously completed by our lab in an ongoing project. For the synthesis of the **12**, we opted to optimize this reaction for better yields, the highlights of which are detailed in Fig. 15b. An oxygen environment was found to be necessary to achieve good conversion. After determining that catalytic amounts of CuCl worked just as well as several stoichiometric equivalents of the catalyst (Fig. 16b, entries A-C), we investigated time, temperature, and solvent for this reaction.

The best yield was obtained when the reaction was run at RT for 24 h with 30 mol % loading of the copper catalyst (75 % yield, Fig. 15b, entry D). Adding water to the solvent decreased yield to < 5 % (Fig. 15b, entry E). This is notable as the peptide-based reactions were performed with good results in a mixture of ACN:H₂O (1:1). One potential explanation for this observation might be the poor solubility of the triazene or CuCl in aqueous conditions as compared to the model peptide.

a. Synthesis of small molecule triazene



b. Optimization of small molecule reaction to make isoindazole 3-carbaldehyde



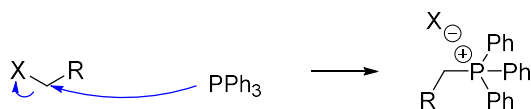
Condition	Yield
A) CuCl (15 equiv.), ACN, O ₂ , 60 °C, 1 h	52 %
B) CuCl (3 equiv.), ACN, O ₂ , 60 °C, 1 h	54 %
C) CuCl (30 mol %), ACN, O ₂ , 60 °C, 1 h	54 %
D) CuCl (30 mol %), ACN, O ₂ , RT, 24 h	75 %
E) CuCl (30 mol %), ACN:H ₂ O (1:1), O ₂ , RT, 4 h	< 5 %
F) CuCl (3 equiv.), ACN, air, 60 °C, 1 h	< 5 %

Figure 15. (a) Synthesis of triazene **11** over two steps. Both the diazonium salt and the triazene were used after workup without further purification. (b) Optimization of isoindazole 3-carbaldehyde **12** formation. Yields refer to product yield after silica gel chromatography.

Dr. Kuei Tang, Raj Lab graduate, evaluated the stability of **12** for an ongoing project in the Raj Lab. Dr. Tang demonstrated that isoindazole 3-carbaldehyde **12** was showed no signs of degradation (as analyzed by HPLC) after 6 h at RT in either 50 % Trifluoroacetic acid (TFA) in ACN or 50 % Piperidine in ACN, indicating that **12** is highly stable towards both acidic and basic conditions.

With several hundred milligrams of isoindazole 3-carbaldehyde **12** in-hand, we began performing Wittig reactions to increase the conjugation of the system. Based on the simple particle-in-a-box paradigm, a more conjugated systems represents a larger box size and thus the HOMO-LUMO gap should decrease, enabling for photons with longer wavelengths to excite the system, and for the subsequent fluorescence emission to also be of higher wavelength. The mechanism for the Wittig reaction is detailed in Fig. 15 below.

Step 1: Formation of Wittig salt



Step 2: Formation of ylide and reaction with aldehyde

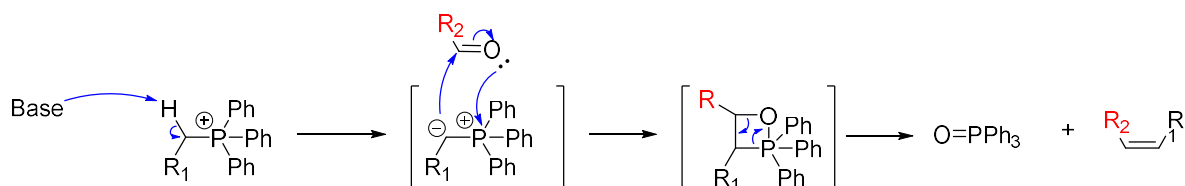


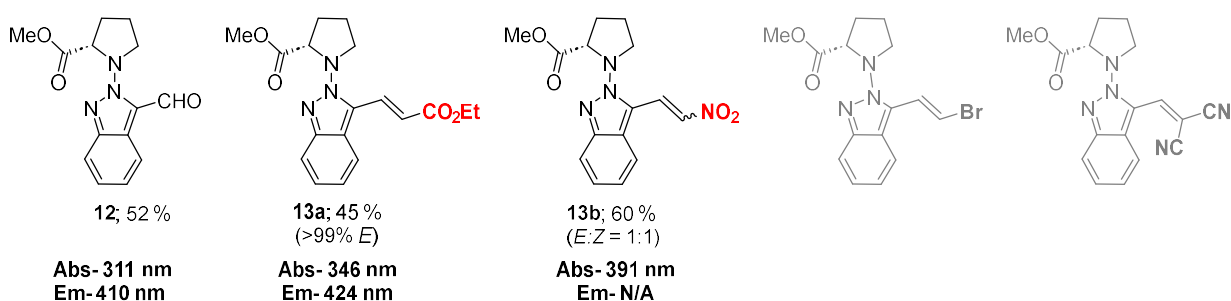
Figure 16. Mechanism of the Wittig reaction to convert an aldehyde into two conjugated R groups. Step 2 shows the deprotonation of the phosphonium salt followed by a [2+2] cycloaddition of the aldehyde with the ylide and subsequent elimination to form the olefin. The reaction is driven by the formation of the stable triphenylphosphine oxide.

The Wittig reaction replaces an aldehyde with a double bond attached to a new R group. The presence of this double bond allows the conjugation of the isoindazole system to extend into

withdrawing or aromatic groups. The Wittig reaction involves the deprotonation of the phosphonium salt using sodium hydride, whereupon the aldehyde is added to the reaction mixture and undergoes the [2+2] cycloaddition and elimination to give the olefin. After several attempts, the Wittig reaction was successful, and we were able to produce multiple examples of products with more conjugation than the isoindazole 3-carbaldehyde (substrate scope is ongoing). Absorbance and fluorescence were measured for these compounds (Fig. 17, Supplementary Fig. 8). By conjugating a double bond attached to an ethyl ester as in **13a** using the Horner-Wittig reaction, the excitation was shifted from 311 nm in isoindazole 3-carbaldehyde **12** to 346 nm in **13a**, and the emission shifted from 410 nm to 424 nm. Encouraged by this, we hoped that the addition of a phenyl ring instead of the ester would further red-shift the fluorophore. The 3-styryl product **13c** exhibited maximal absorbance at 351 nm, which gave fluorescence at 426 nm. Unfortunately, the addition of another double bond to the system as in 4-phenylbuta-1,3-dien-1-yl product **13d** only shifted the excitation wavelength by 1 nm further than **13c** to 352 nm (fluorescence emission at 434 nm). Likewise, the biphenyl system in **13e** did not significantly change the absorbance or fluorescence wavelengths (**13e** excited at 362 nm and fluoresced at 427 nm). Simply increasing the “box size” was not enough to shift the absorbance to the desired near-IR region. Based on a literature search of fluorophore designs, we came across a “push-pull” concept proposing, with evidence, that adding electron donating and withdrawing groups on opposite ends of an isoindole fluorophore can significantly red-shift the excitation and emission wavelengths.²⁵ Inspired by this, we synthesized the 2-nitrovinyl product **13b** using the Henry reaction and *p*-nitrobenzene product **13g** using the Wittig reaction, which both showed a larger red-shift than the products **13c** and **13d** to a maximal excitation at 391 nm (**13b**) and 392 nm (**13g**). However, neither **13b** nor **13g** exhibited fluorescence when excited at their respective absorption

wavelengths. The nitrogen atoms in our isoindazole ring do not sufficiently donate across the system, suggesting a better electron donating group should be attached on the opposite end of the isoindazole. Despite these setbacks, the red-shifted absorbance of **13b** and **13g** gives hope to our attempts to create red-shifted fluorophores. We are currently working to synthesize more small molecules that exhibit red-shifted fluorescence.

a. Effect of EWG in Absorption



b. Effect of Delocalization in Absorption

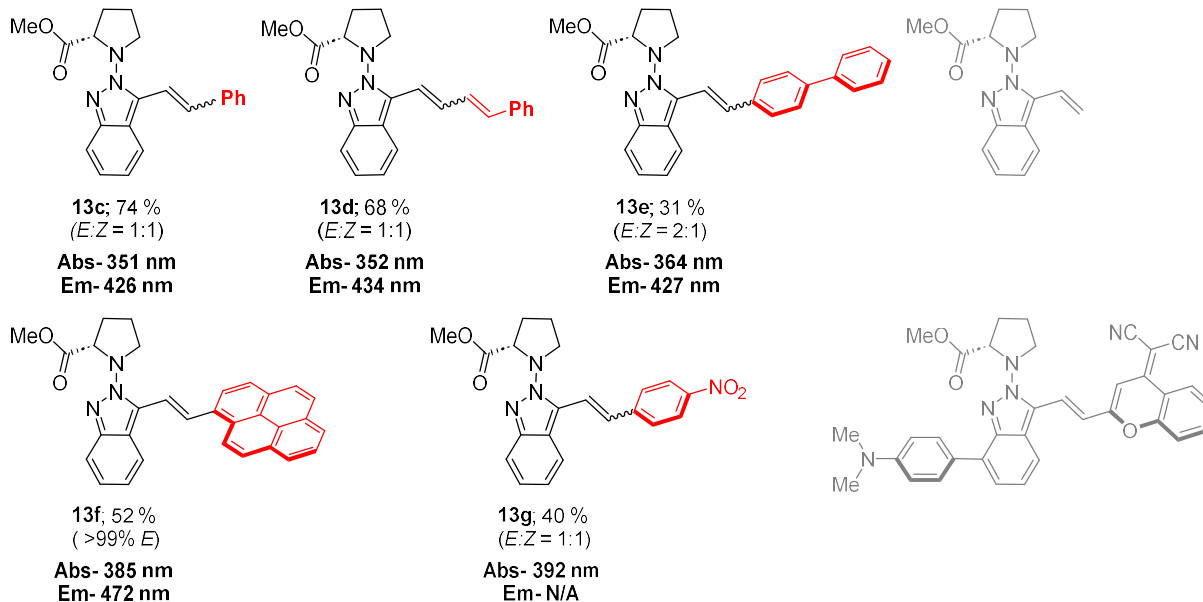


Figure 17. (a) determining the effect of electron withdrawing groups (EWG) on the photophysical properties of the fluorophore. (b) Determining the effect of electron delocalization through extended conjugation on the photophysical properties of the fluorophore. (a) and (b) The examples in grey are either in progress or yet to be completed. No fluorescence was observed for **13b** or **13g**.

The work for this part of the project remains unfinished. We will continue to synthesize new Wittig products in search of near-IR fluorophores. Determining quantum yield for each of these fluorophores will also be completed in due course, though the first priority is to create red-shifted fluorophores. Finally, the Wittig reaction still needs to be completed on peptides. There is literature precedent for Wittig reactions on peptides and in aqueous conditions, so we expect that this outstanding task will be possible.^{26,27} Alternatively, the Wittig reaction may be performed on peptides in solvents such as THF or DMF.

Conclusions and future directions

In summary, we have developed a robust and highly efficient triazene coarctate cyclization (TCC) for the synthesis of cyclic peptides with inbuilt fluorescence for cellular imaging for the first time. The reactivity of this protocol is unique because of the selectivity of the aryl diazonium ion to form a stable triazene with secondary amines only, followed by copper-catalyzed coarctate cyclization to generate isoindazole 3-carbaldehyde as a fluorophore at the site of cyclization. Our synthetic approach combines small molecule organic chemistry with on-resin cross-coupling, peptide cyclization, and late-stage peptide modification. We also demonstrated the use of the Wittig reaction to increase the conjugation of the fluorescent moiety. We found that adding highly withdrawing groups through this reaction red-shifted the fluorescence more than simply conjugating aromatic systems to increase the “box size”. Overall, this approach provides a toolbox for the synthesis of varying cyclic peptides with inbuilt fluorescence that will be applicable to many fields of chemistry.

As for the peptide side of the project, chemoselectivity and substrate scope still need to be demonstrated. We will complete chemoselectivity experiments for the peptide reactions within the

normal course of substrate scope by incorporating reactive amino acids in the sequences. Based on previously published work, the triazene cyclization is chemoselective. We have not observed and do not foresee any side reactions during the isoindazole cyclization or Wittig reaction. Additionally, we will complete substrate scope by varying ring sizes and secondary amines (N-terminal proline, methylated N-terminus, and monomethylated lysine (K_{me}), Fig. 18). The next phase of the project from there will be to visualize these peptides on/inside cells using fluorescence microscopy. Cell membrane visualization will be performed using a fluorescent peptide containing RGD (Arg-Gly-Asp) in the sequence, a known binding motif for integrin proteins expressed by many cell lines including CHO (Chinese hamster ovary),²⁸ A431 (human epidermoid carcinoma),²⁹ and OVCAR-4 (human ovarian cancer).³⁰ For visualization of fluorescent peptides inside the cell, we will synthesize cell-permeable peptides using either known cell-permeable sequences or using a polyArg sequence (the increased positive charge of the peptide likely increases association with the phospholipid heads at the outer edge of the cell membrane, ultimately leading to cellular penetration).

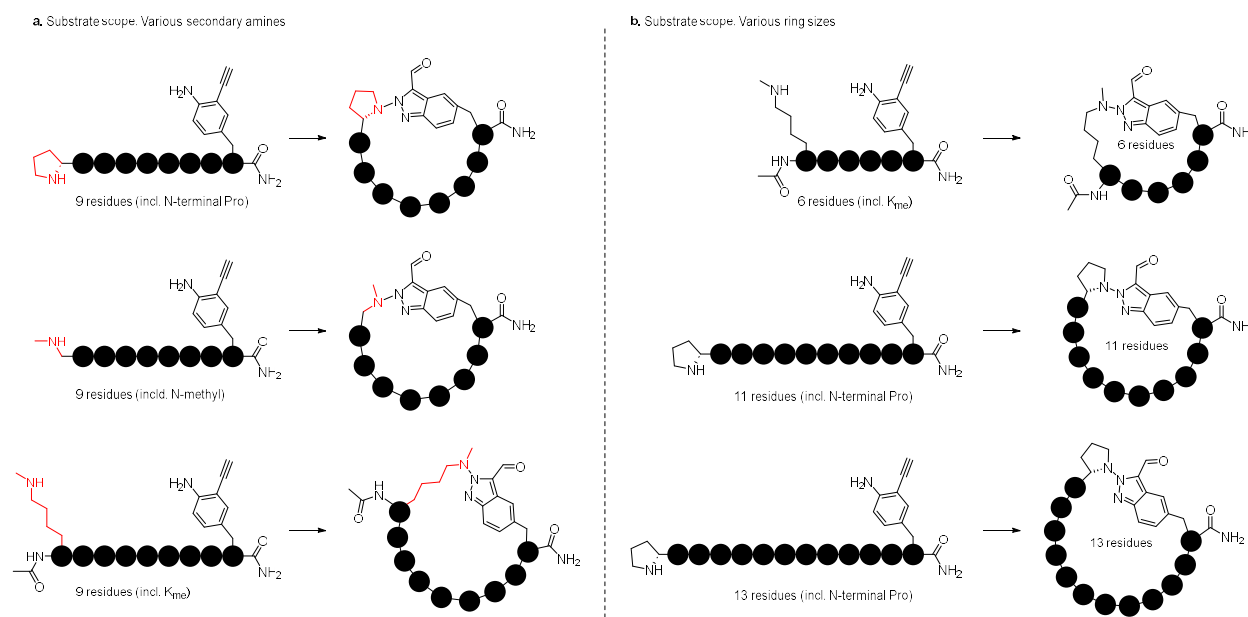


Figure 18. (a) Substrate scope using various secondary amines to form cyclic isoindazole 3-carbaldehydes. (b) Substrate scope making macrocycles of different sizes.

As an additional application of this work, we believe that our chemistry will work on solid-support resin. By using Merrifield resin, which is acid resistant (typically cleaved with HF or Triflic acid), the triazene, isoindazole, and Wittig product should all be accessible before global deprotection and peptide cleavage. This synthesis will demonstrate the applicability of TCC chemistry to generate pure libraries of fluorescent cyclic peptides on-resin in one batch using a split-and-pool synthesis method. Such libraries are frequently used for screening techniques; the presence of the in-built fluorophore reduces bias during target validation and later screening by removing the need to attach external fluorescent groups.

I am the first author on this project; second author Dr. Samrat Sahu and I expect to finish this project in Summer 2023 and submit it with Dr. Raj to an appropriate journal such as JACS or Angew. Chem.

In sum, TCC chemistry creates cyclic peptides with tunable, in-built fluorescence, and has applications in diverse fields of chemistry.

Acknowledgement of contributions

P.C and M.R designed the project. P.C. synthesized the unnatural Fmoc-amino acids and all peptides in this work, and analyzed the results and products using LCMS, HPLC, and NMR. S.R. helped with some of the synthetic steps. K.T. provided the procedure to synthesize **12** and data on the stability of **12**. S.S. optimized the synthesis of **12**. S.S. synthesized the derivatives **13a-g**. Absorbance and fluorescence data, ^1H and ^{13}C spectra, and the procedures for the synthesis of **13a-g** were collected, processed, and written by P.C., with S.S. assisting occasionally. P.C. made

peak assignments on NMR, where included. R.W. assisted in training P.C. to run the spectrophotometer. A.B. created Fig. 1 and gave permission for it to be re-printed in this thesis. Figs. 15 and 17 were made by P.C and S.S in collaboration. P.C. made all other figures and spectra. All mechanisms contained in this thesis were self-drawn using ChemDraw. P.C. wrote the manuscript and SI of this thesis. P.C and M.R wrote the abstract. J.T. offered edits on the manuscript and SI.

Patrick Czabala, Samrat Sahu, Monika Raj, Kuei-Chien Tang, Shreyas Rajagopal, Rachel Wills, Angele Bruce, John Talbott.

References

- (1) Zhang, G.; Zhang, J.; Gao, Y.; Li, Y.; Li, Y. Strategies for Targeting Undruggable Targets. *Expert Opin. Drug Discov.* **2022**, *17* (1), 55–69. <https://doi.org/10.1080/17460441.2021.1969359>.
- (2) Makurvet, F. D. Biologics vs. Small Molecules: Drug Costs and Patient Access. *Med. Drug Discov.* **2021**, *9*, 100075. <https://doi.org/10.1016/j.medidd.2020.100075>.
- (3) Muttenthaler, M.; King, G. F.; Adams, D. J.; Alewood, P. F. Trends in Peptide Drug Discovery. *Nat. Rev. Drug Discov.* **2021**, *20* (4), 309–325. <https://doi.org/10.1038/s41573-020-00135-8>.
- (4) Zhang, H.; Chen, S. Cyclic Peptide Drugs Approved in the Last Two Decades (2001–2021). *RSC Chem. Biol.* *3* (1), 18–31. <https://doi.org/10.1039/d1cb00154j>.
- (5) Smolewski, P.; Robak, T. The Discovery and Development of Romidepsin for the Treatment of T-Cell Lymphoma. *Expert Opin. Drug Discov.* **2017**, *12* (8), 859–873. <https://doi.org/10.1080/17460441.2017.1341487>.
- (6) Baeriswyl, V.; Calzavarini, S.; Chen, S.; Zorzi, A.; Bologna, L.; Angelillo-Scherrer, A.; Heinis, C. A Synthetic Factor XIIa Inhibitor Blocks Selectively Intrinsic Coagulation Initiation. *ACS Chem. Biol.* **2015**, *10* (8), 1861–1870. <https://doi.org/10.1021/acscchembio.5b00103>.
- (7) Middendorp, S. J.; Wilbs, J.; Quarroz, C.; Calzavarini, S.; Angelillo-Scherrer, A.; Heinis, C. Peptide Macrocyclic Inhibitor of Coagulation Factor XII with Subnanomolar Affinity and High Target Selectivity. *J. Med. Chem.* **2017**, *60* (3), 1151–1158. <https://doi.org/10.1021/acs.jmedchem.6b01548>.
- (8) Fujii, N. D-Amino Acids in Living Higher Organisms. *Orig. Life Evol. Biosphere J. Int. Soc. Study Orig. Life* **2002**, *32* (2), 103–127. <https://doi.org/10.1023/a:1016031014871>.
- (9) Wang, L.; Wang, N.; Zhang, W.; Cheng, X.; Yan, Z.; Shao, G.; Wang, X.; Wang, R.; Fu, C. Therapeutic Peptides: Current Applications and Future Directions. *Signal Transduct. Target. Ther.* **2022**, *7* (1), 1–27. <https://doi.org/10.1038/s41392-022-00904-4>.

- (10) Futaki, S.; Goto, S.; Sugiura, Y. Membrane Permeability Commonly Shared among Arginine-Rich Peptides. *J. Mol. Recognit.* **2003**, *16* (5), 260–264. <https://doi.org/10.1002/jmr.635>.
- (11) Lau, J. L.; Dunn, M. K. Therapeutic Peptides: Historical Perspectives, Current Development Trends, and Future Directions. *Bioorg. Med. Chem.* **2018**, *26* (10), 2700–2707. <https://doi.org/10.1016/j.bmc.2017.06.052>.
- (12) Mendive-Tapia, L.; Wang, J.; Vendrell, M. Fluorescent Cyclic Peptides for Cell Imaging. *Pept. Sci.* **2021**, *113* (1), e24181. <https://doi.org/10.1002/pep2.24181>.
- (13) Todorovic, M.; Schwab, K. D.; Zeisler, J.; Zhang, C.; Bénard, F.; Perrin, D. M. Fluorescent Isoindole Crosslink (FLiCK) Chemistry: A Rapid, User-Friendly Stapling Reaction. *Angew. Chem. Int. Ed.* **2019**, *58* (40), 14120–14124. <https://doi.org/10.1002/anie.201906514>.
- (14) Zhang, Y.; Zhang, Q.; Wong, C. T. T.; Li, X. Chemoselective Peptide Cyclization and Bicyclization Directly on Unprotected Peptides. *J. Am. Chem. Soc.* **2019**, *141* (31), 12274–12279. <https://doi.org/10.1021/jacs.9b03623>.
- (15) Hyun, K.; Jeon, J.; Park, K.; Kim, J. Writing, Erasing and Reading Histone Lysine Methylations. *Exp. Mol. Med.* **2017**, *49* (4), e324–e324. <https://doi.org/10.1038/emm.2017.11>.
- (16) Nwajiobi, O.; Mahesh, S.; Streety, X.; Raj, M. Selective Triazene Reaction (STaR) of Secondary Amines for Tagging Monomethyl Lysine Post-Translational Modifications. *Angew. Chem. Int. Ed.* **2021**, *60* (13), 7344–7352. <https://doi.org/10.1002/anie.202013997>.
- (17) Nwajiobi, O.; Verma, A. K.; Raj, M. Rapid Arene Triazene Chemistry for Macrocyclization. *J. Am. Chem. Soc.* **2022**, *144* (10), 4633–4641. <https://doi.org/10.1021/jacs.2c00464>.
- (18) Roman, D. S.; Takahashi, Y.; Charette, A. B. Potassium Tert-Butoxide Promoted Intramolecular Arylation via a Radical Pathway. *Org. Lett.* **2011**, *13* (12), 3242–3245. <https://doi.org/10.1021/ol201160s>.
- (19) Le Qument, S. T.; Nielsen, T. E.; Meldal, M. Divergent Pathway for the Solid-Phase Conversion of Aromatic Acetylenes to Carboxylic Acids, α -Ketocarboxylic Acids, and Methyl Ketones. *J. Comb. Chem.* **2008**, *10* (4), 546–556. <https://doi.org/10.1021/cc8000037>.
- (20) Doan, N.-D.; Poujol de Molliens, M.; Létourneau, M.; Fournier, A.; Chatenet, D. Optimization of On-Resin Palladium-Catalyzed Sonogashira Cross-Coupling Reaction for Peptides and Its Use in a Structure–Activity Relationship Study of a Class B GPCR Ligand. *Eur. J. Med. Chem.* **2015**, *104*, 106–114. <https://doi.org/10.1016/j.ejmech.2015.09.017>.
- (21) Cohrt, A. E. O.; Le Qument, S. T.; Nielsen, T. E. Solid-Phase Synthesis of NH-1,2,3-Triazoles Using 4,4'-Bismethoxybenzhydryl Azide. *SYNLETT Acc. Rapid Commun. Chem. Synth.* **2014**, *25* (13), 1891–1895. <https://doi.org/10.1055/s-0034-1378228>.
- (22) Alshanski, I.; Bentolila, M.; Gitlin-Domagalska, A.; Zamir, D.; Zorsky, S.; Joubran, S.; Hurevich, M.; Gilon, C. Enhancing the Efficiency of the Solid Phase Peptide Synthesis (SPPS) Process by High Shear Mixing. *Org. Process Res. Dev.* **2018**, *22* (9), 1318–1322. <https://doi.org/10.1021/acs.oprd.8b00225>.
- (23) Herges, R. Coarctate Transition States: The Discovery of a Reaction Principle. *J. Chem. Inf. Comput. Sci.* **1994**, *34* (1), 91–102. <https://doi.org/10.1021/ci00017a011>.
- (24) Kimball, D. B.; Herges, R.; Haley, M. M. Two Unusual, Competitive Mechanisms for (2-Ethynylphenyl)Triazene Cyclization: Pseudocoarctate versus Pericyclic Reactivity. *J. Am. Chem. Soc.* **2002**, *124* (8), 1572–1573. <https://doi.org/10.1021/ja017227u>.

- (25) Yu, C.; Fang, X.; Wu, Q.; Guo, X.; Chen, N.; Cheng, C.; Hao, E.; Jiao, L. Synthesis and Spectral Properties of Aggregation-Induced Emission-Active Push–Pull Chromophores Based On Isoindole Scaffolds. *Org. Lett.* **2022**, *24* (25), 4557–4562. <https://doi.org/10.1021/acs.orglett.2c01659>.
- (26) El-Batta, A.; Jiang, C.; Zhao, W.; Anness, R.; Cooksy, A. L.; Bergdahl, M. Wittig Reactions in Water Media Employing Stabilized Ylides with Aldehydes. Synthesis of α,β -Unsaturated Esters from Mixing Aldehydes, α -Bromoesters, and Ph₃P in Aqueous NaHCO₃. *J. Org. Chem.* **2007**, *72* (14), 5244–5259. <https://doi.org/10.1021/jo070665k>.
- (27) Han, M.-J.; Xiong, D.-C.; Ye, X.-S. Enabling Wittig Reaction on Site-Specific Protein Modification. *Chem. Commun. Camb. Engl.* **2012**, *48* (90), 11079–11081. <https://doi.org/10.1039/c2cc35738k>.
- (28) Bunch, T. A. Integrin AIIb β 3 Activation in Chinese Hamster Ovary Cells and Platelets Increases Clustering Rather than Affinity. *J. Biol. Chem.* **2010**, *285* (3), 1841–1849. <https://doi.org/10.1074/jbc.M109.057349>.
- (29) Kato, T.; Enomoto, A.; Watanabe, T.; Haga, H.; Ishida, S.; Kondo, Y.; Furukawa, K.; Urano, T.; Mii, S.; Weng, L.; Ishida-Takagishi, M.; Asai, M.; Asai, N.; Kaibuchi, K.; Murakumo, Y.; Takahashi, M. TRIM27/MRTF-B-Dependent Integrin B1 Expression Defines Leading Cells in Cancer Cell Collectives. *Cell Rep.* **2014**, *7* (4), 1156–1167. <https://doi.org/10.1016/j.celrep.2014.03.068>.
- (30) Shaw, S. K.; Schreiber, C. L.; Roland, F. M.; Battles, P. M.; Brennan, S. P.; Padanilam, S. J.; Smith, B. D. High Expression of Integrin Av β 3 Enables Uptake of Targeted Fluorescent Probes into Ovarian Cancer Cells and Tumors. *Bioorg. Med. Chem.* **2018**, *26* (8), 2085–2091. <https://doi.org/10.1016/j.bmc.2018.03.007>.

Supplemental Information

General

All commercial materials were used without further purification. All solvents were reagent or HPLC grade. Yields refer to chromatographically pure compounds; percent conversions were obtained by comparing HPLC peak areas of products and starting materials. TLC, HPLC, and MS were used to monitor reaction progress, and product characterization was done using MS and NMR.

Materials

Fmoc-amino acids, Rink amide resin, Hydroxybenzotriazole (HOBT), N,N'-diisopropylcarbodiimide (DIC), and triisopropylsilane (TIS) were obtained from CreoSalus. Piperidine and trifluoroacetic acid (TFA) were obtained from Alfa Aesar. N,N-dimethylformamide (DMF), dichloromethane (DCM), methanol (MeOH), and acetonitrile (ACN) were obtained from VWR. All other small molecules were obtained from Sigma-Aldrich, AmBeed, or VWR.

Purification

HPLC. Purification of peptides was performed using preparatory high performance liquid chromatography (HPLC) on a Teledyne ISCO ACCQPrep 150 equipped with a C-18 reverse phase column with a particle size of 5 μm and column size 20 x 150 mm. Separations involved a mobile phase of 0.1 % formic acid in water (solvent A) and 0.1 % formic acid in acetonitrile (solvent B). For acid-sensitive triazene purification, HPLC was run without formic acid in the eluent. The eluent was monitored by absorbance at 220 nm. Gradients are shown overlaid on spectral data.

Silica Gel Column Chromatography. 230-400 mesh, SiliaFlash P60 was used in glass column, normal phase chromatography. Increasing gradients of EA in Hexane were used to purify small molecule compounds. To reduce dragging, 1 % v/v AcOH was added to the mobile phase during purification of Fmoc-amino acid compounds.

Instrumentation and sample analysis

NMR. ^1H and ^{13}C spectra were acquired at 25 °C in DMSO- d_6 , MeOD, or CDCl_3 using a Bruker NEO 400 MHz spectrometer. All ^1H NMR chemical shifts (δ) were referenced relative to the residual DMSO- d_6 peak at 2.50 ppm, MeOD peak at 3.29 ppm, CDCl_3 peak at 7.28 ppm, or internal tetramethylsilane (TMS) at 0.00 ppm. ^{13}C NMR chemical shifts were referenced to DMSO- d_6 at 39.52 ppm and CDCl_3 at 77.2 ppm. ^{13}C NMR spectra were proton decoupled. NMR spectral data are reported as chemical shift (multiplicity, coupling constants (J), integration). Multiplicity is reported as follows: singlet (s), doublet (d), doublet of doublets (dd), doublet of doublet of doublets (ddd), doublet of triplets (td), triplet (t), and multiplet (m). Coupling constants (J) are reported in hertz (Hz).

Analytical HPLC. Analytical HPLC chromatography (HPLC) was performed on an Agilent 1200 series HPLC equipped with a 5 μm pore size C-18 reversed-phase column (4.6 x 150 nm). All separations involved mobile phase of H_2O (solvent A) and ACN (solvent B) run in linear gradients with a constant flow rate of 1 mL min^{-1} . The eluent was monitored with a detection wavelength of 220 nm. For analysis and characterization of acid-sensitive triazene reactions and pure compounds, formic acid was not added to the eluent. Spectra were analyzed and processed using Mestrenova.

HPLC METHOD A: Gradient 2-40 % B over 30 min.

HRMS. High resolution MS data were acquired on Thermo Exactive Plus using a heated electrospray source. The solution was infused at a rate of 10-25 $\mu\text{L min}^{-1}$ electrospray using 3.3 kV. Spectra were analyzed with Freestyle software (ThermoFisher) or MassHunter (Agilent).

Absorbance and Fluorescence. Fluorescence spectroscopy was performed with an Agilent Cary Eclipse Fluorescence Spectrophotometer. The excitation and emission slits were set to 5 nm. The photomultiplier tube (PMT) detector voltage was set at 600 V. Spectra were analyzed and generated using Excel.

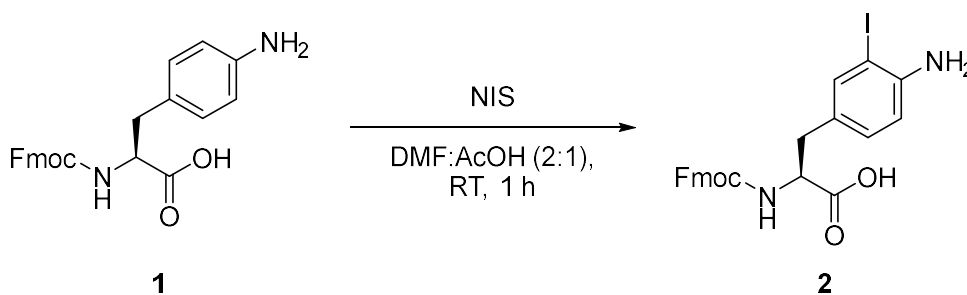
Fmoc Solid-Phase Peptide Synthesis (Fmoc-SPPS)¹

Peptides were synthesized using standard protocols. Peptides were synthesized manually on 0.1475 mmol, 0.295 mmol, or 0.59 mmol scale using Rink amide resin (resin loading: 0.59 mmol g^{-1}). Resin was swollen with DCM for 30 min at RT. Fmoc was deprotected using 20 % piperidine in DMF for 15 min to obtain deprotected resin. Fmoc protected amino acid (5 equiv.) was coupled using HOBT (5 equiv.) and DIC (5 equiv.) in DMF for 15 min at RT, followed by Fmoc

deprotection using 20 % piperidine in DMF for 15 min. Fmoc-protected amino acids (5 equiv.) were sequentially coupled on the resin using HOBt (5 equiv.) and DIC (5 equiv.) in DMF for 15 min at RT. After each deprotection and coupling step, the resin was washed with DMF, MeOH, and DCM (successively in 2 cycles). Peptides were cleaved from the resin using 4 mL of a cleavage cocktail consisting of 95 % TFA, 2.5 % H₂O, and 2.5 % TIS for 2 h. The resin was removed by filtration and the resulting solution was concentrated under air. Peptides were precipitated, centrifugated, and the supernatant decanted using cold diethyl ether (3 x 10 mL) to obtain the crude product. Crude peptides were dissolved in ACN:H₂O and purified by preparative HPLC.

Supplementary Figure 1: Synthesis of Fmoc-Phe(4-NH₂,3-I)-OH

(S)-2-((((9H-fluoren-9-yl)methoxy)carbonyl)amino)-3-(4-aminophenyl)propanoic acid



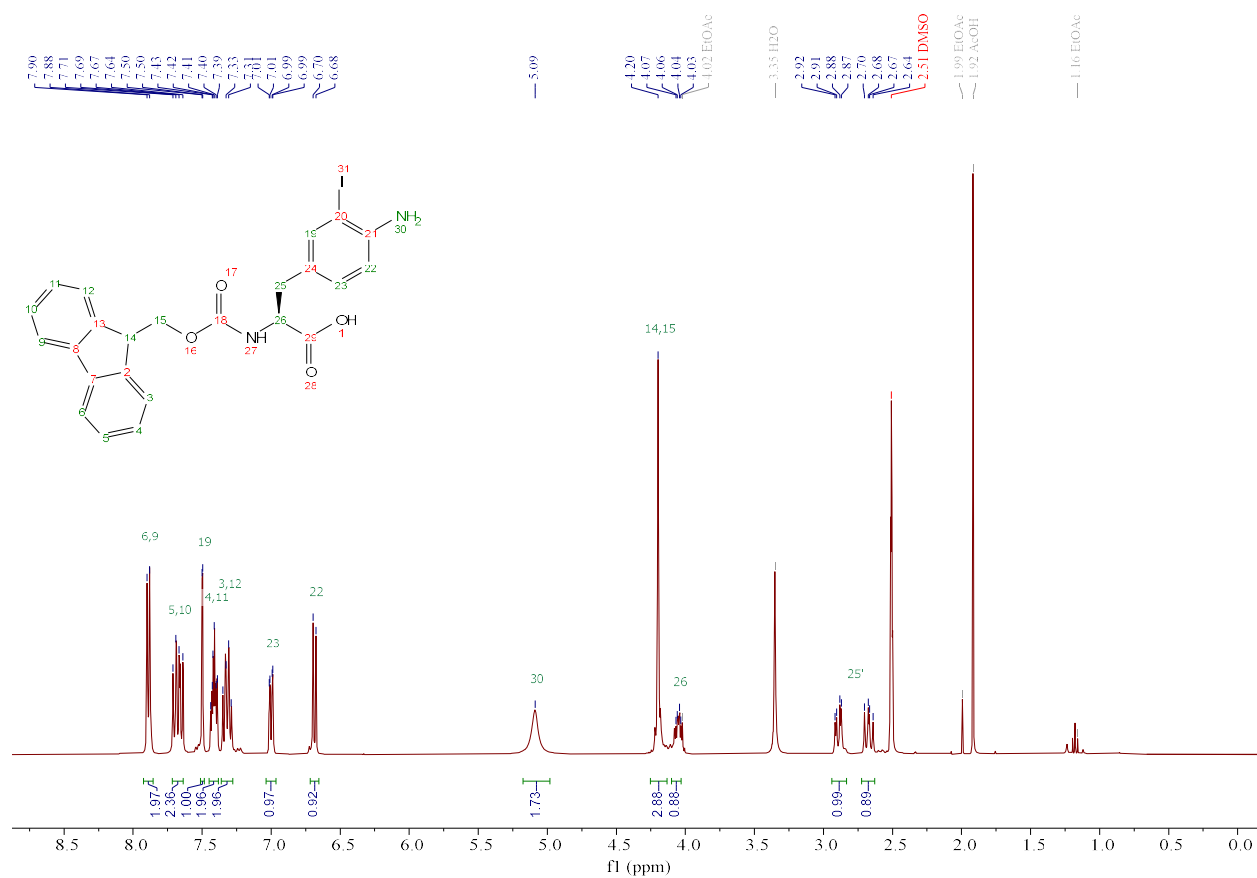
Procedure: 2.00 g (4.97 mmol) of Fmoc-Phe(4-NH₂)-OH **1** was dissolved in 30 mL DMF:AcOH (2:1) in a 250 mL RBF with a teflon stir bar. Following this, 1062 mg (4.72 mmol, 0.95 equiv.) of N-iodosuccinimide (NIS) was added in one portion and the round bottom flask was stoppered with a rubber septum. A needle was pierced through the septum to prevent pressure buildup. Reaction progress was monitored via TLC (90 % EA in Hexane (2 mL) with 10 μ L AcOH). After 1 h, the remaining NIS was quenched with saturated aqueous sodium thiosulfate (75 mL). Most of the acetic acid was removed under reduced pressure. The reaction was diluted with H₂O and the aqueous layer was extracted three times with EA. The organic layers were combined, dried with Na₂SO₄, and the solvent was removed under reduced pressure to afford the crude product. The product was purified with silica gel chromatography (30-50 % EA in Hexane, with 1% v/v AcOH added to the eluent). The product fractions were combined and extracted three times with brine to remove the

acetic acid, and the organic layers were dried with Na₂SO₄ before concentrating under reduced pressure to afford 1490 mg of an off-white powder (57 % yield).

NMR Data for Compound 2

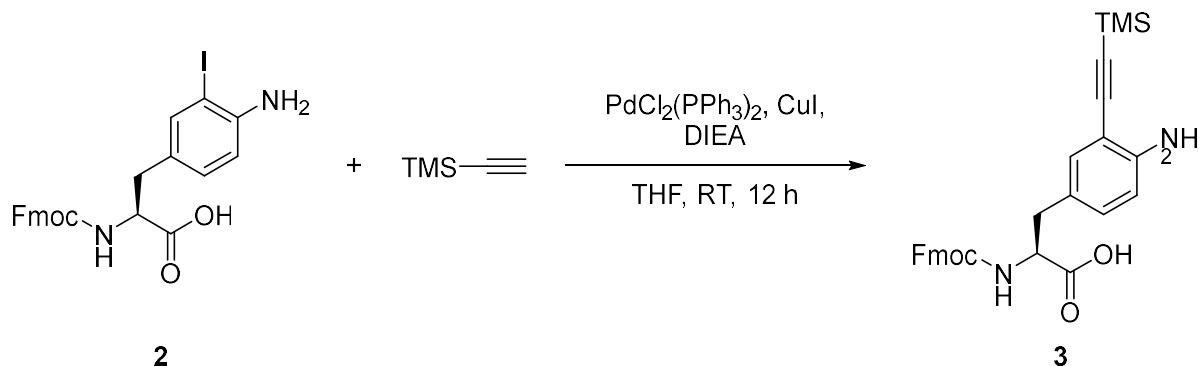
(S)-2-(((9H-fluoren-9-yl)methoxy)carbonyl)amino)-3-(4-aminophenyl)propanoic acid. ¹H NMR (400 MHz, DMSO) δ 7.89 (d, *J* = 7.1 Hz, 2H), 7.73 – 7.62 (m, 2H), 7.50 (d, *J* = 2.0 Hz, 1H), 7.46 – 7.37 (m, 2H), 7.37 – 7.27 (m, 2H), 7.00 (dd, *J* = 8.2, 2.0 Hz, 1H), 6.69 (d, *J* = 8.2 Hz, 1H), 5.09 (s, 2H), 4.24 – 4.18 (m, 3H), 4.10 – 3.98 (m, 1H), 2.98 – 2.62 (m, 2H).

¹H NMR spectrum of 2



Supplementary Figure 2: Synthesis of Fmoc-Phe(4-NH₂,3-(trimethylsilyl)ethyne)-OH

(S)-2-(((9H-fluoren-9-yl)methoxy)carbonyl)amino)-3-(4-amino-3-((trimethylsilyl)ethynyl)phenyl)propanoic acid



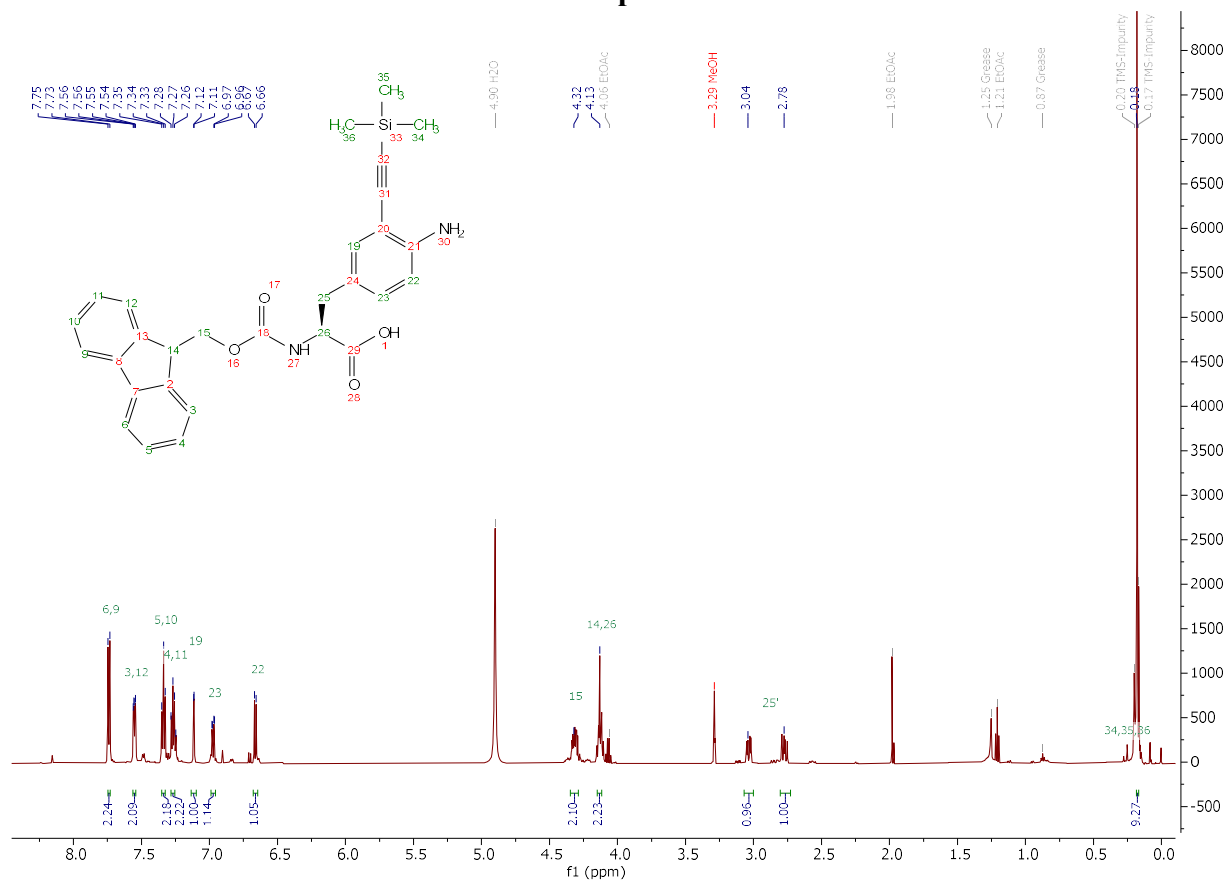
Procedure: A flame-dried 100 mL RBF was charged with 1670 mg (3.16 mmol, 1 equiv.) of Fmoc-Phe(4-NH₂,3-I)-OH **2**, 222 mg Bis(triphenylphosphine)palladium(II) dichloride (0.316 mmol, 0.1 equiv.), and 60 mg Copper (I) iodide (0.316 mmol, 0.1 equiv.). Under Schlenk line conditions, the RBF was purged with 3 x alternating cycles of vacuum and N₂. Then, 30 mL of degassed THF was added to the RBF. 5.5 mL of DIEA (31.6 mmol, 10 equiv.) and 1.55 mL of TMS-alkyne (15.8 mmol, 5 equiv.) were added to the RBF. The reaction was stoppered with a rubber septum, and a nitrogen balloon was added to maintain the inert environment. The reaction was allowed to stir at RT for 12 h, then the THF was removed under reduced pressure. The reaction mixture was suspended in brine and extracted with EA (3 x 50 mL). The organic layers were combined, dried with Na₂SO₄, and the solvent was removed under reduced pressure to afford the crude product. The product was purified with silica gel chromatography (0-20 % EA in Hexane, with 1% v/v AcOH added to the eluent). The product fractions were combined and extracted three times with brine to remove the acetic acid, and the organic layers were dried with Na₂SO₄ before concentrating under reduced pressure to afford 230 mg of an oily residue (15 % yield).

NOTE: During purification, small spots with R_f's slightly higher than the product were observed on TLC, even with very slow gradients, indicating the product was not entirely pure. This was confirmed by the poor quality of the NMR spectrum. Furthermore, the addition of the TMS group turned the product into an oily residue which was not ideal for weighing the product for peptide synthesis. The shown NMR spectrum is from the best of many attempts at this synthetic step. As such, the solid-phase Sonogashira approach (Scheme 2) was pursued with better results.

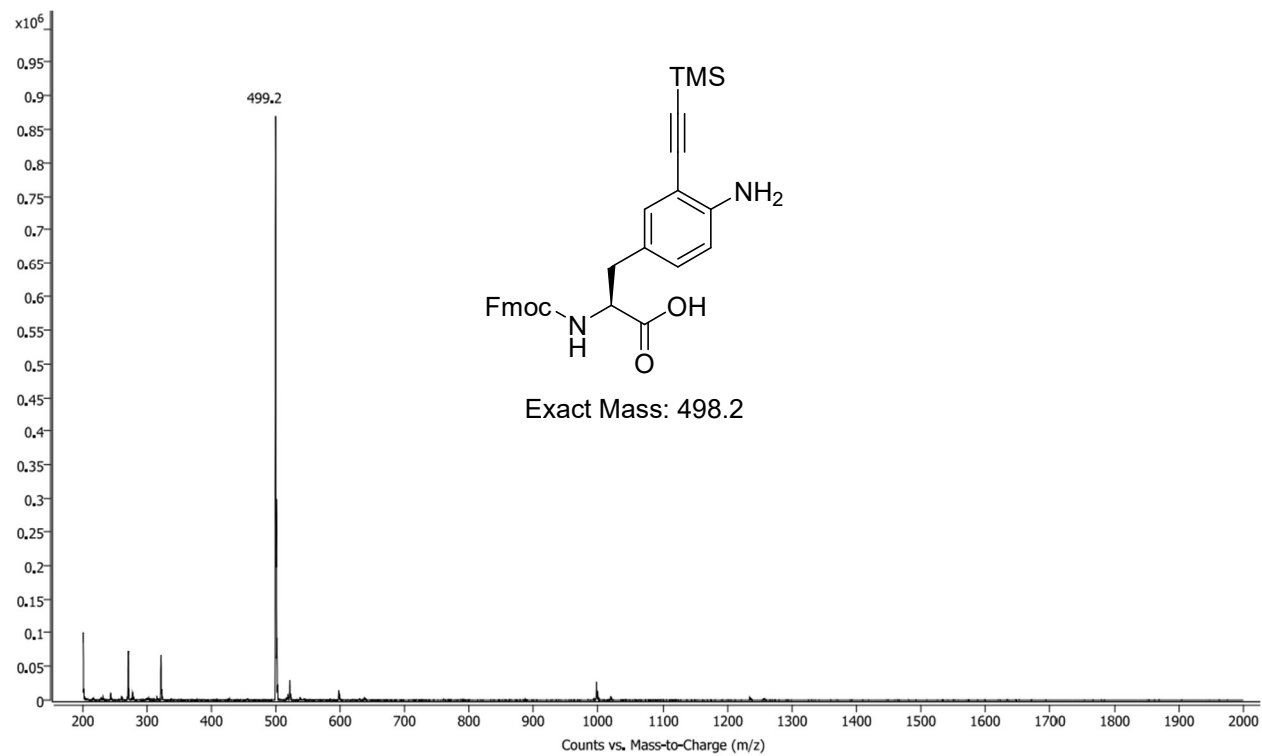
Spectral Data for Compound 3

(S)-2-(((9H-fluoren-9-yl)methoxy)carbonyl)amino)-3-(4-amino-3-((trimethylsilyl)ethynyl)phenyl)propanoic acid. $^1\text{H NMR}$ (600 MHz, MeOH- d_4) δ 7.74 (d, $J = 7.5$ Hz, 2H), 7.55 (dd, $J = 7.5, 3.4$ Hz, 2H), 7.34 (t, $J = 7.5$ Hz, 2H), 7.31 – 7.22 (m, 2H), 7.11 (d, $J = 2.3$ Hz, 1H), 6.97 (dd, $J = 8.3, 2.2$ Hz, 1H), 6.66 (d, $J = 8.2$ Hz, 1H), 4.34 – 4.25 (m, 2H), 4.20 – 4.09 (m, 2H), 3.10 – 2.64 (m, 2H), 0.18 (s, 9H). **LCMS** m/z 499.2 (calcd. $[M+H]^+ = 499.2$).

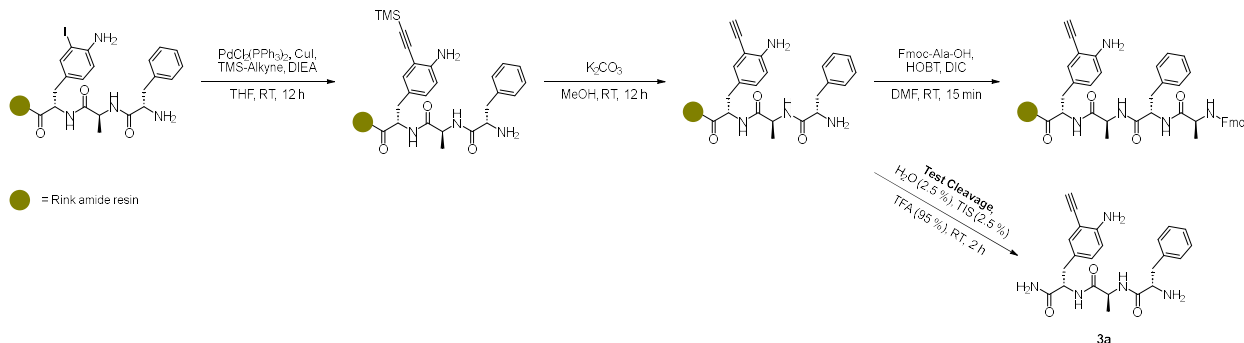
$^1\text{H NMR}$ spectrum of 3



Mass Spectrum of 3

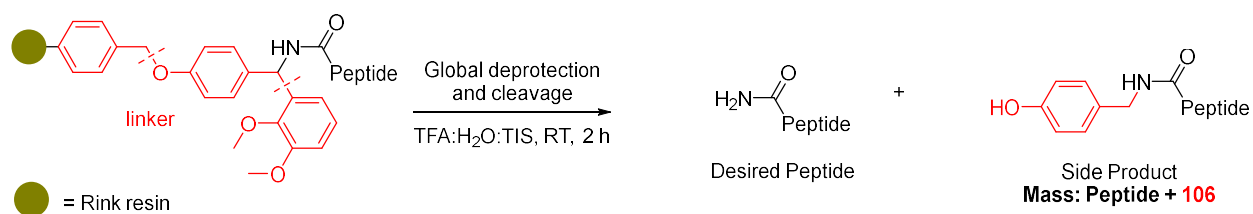


Supplementary Figure 3: Solid-phase Sonogashira coupling



Representative Procedure: The tripeptide Phe(4-NH₂,3-I)-Ala-Phe-NH₂ was synthesized on Rink resin (0.59 mmol scale). The resin was dried thoroughly on vacuum. The solid-phase synthesis vessel was charged with 41.4 mg Bis(triphenylphosphine)palladium (II) dichloride (59 μmol, 0.1 equiv.) and 11.2 mg Copper (I) iodide (59 μmol, 0.1 equiv.). N₂ was flushed through the solid-phase synthesis vessel. To the 25 mL solid-phase synthesis vessel was then added 13 mL degassed THF, 390 μL TMS-alkyne (2.95 mmol, 5 equiv.), and 1.105 mL DIEA (5.9 mmol, 10 equiv.). The reaction vessel was sealed tightly and agitated on a wrist action shaker for 12 h. Following this, the solvent was drained from the vessel using vacuum filtration, and the resin was washed with DMF, MeOH, and DCM (10 mL, successively in 2 cycles). To remove any remaining metal from the palladium, the resin was washed twice with 0.2 M sodium dimethyldithiocarbamate in DMF for 15 min. Then, 570.7 mg of potassium carbonate (4.13 mmol, 7 equiv.) was added with 15 mL MeOH to the solid-phase synthesis vessel, and the vessel was sealed tightly. The mixture was agitated on the wrist action shaker for 12 h. After washing the K₂CO₃ out of the vessel, 5 mg of resin was test-cleaved using 95:5:5 TFA:H₂O:TIS for 30 minutes. HRMS confirmed essentially quantitative conversion of the iodo-arene to the alkyne. To enhance the long-term stability of this stock of prepared resin, Fmoc-Ala-OH was coupled to the N-terminus of the growing chain. We have observed that our peptides last longer in the desiccator when the N-terminus is protected.

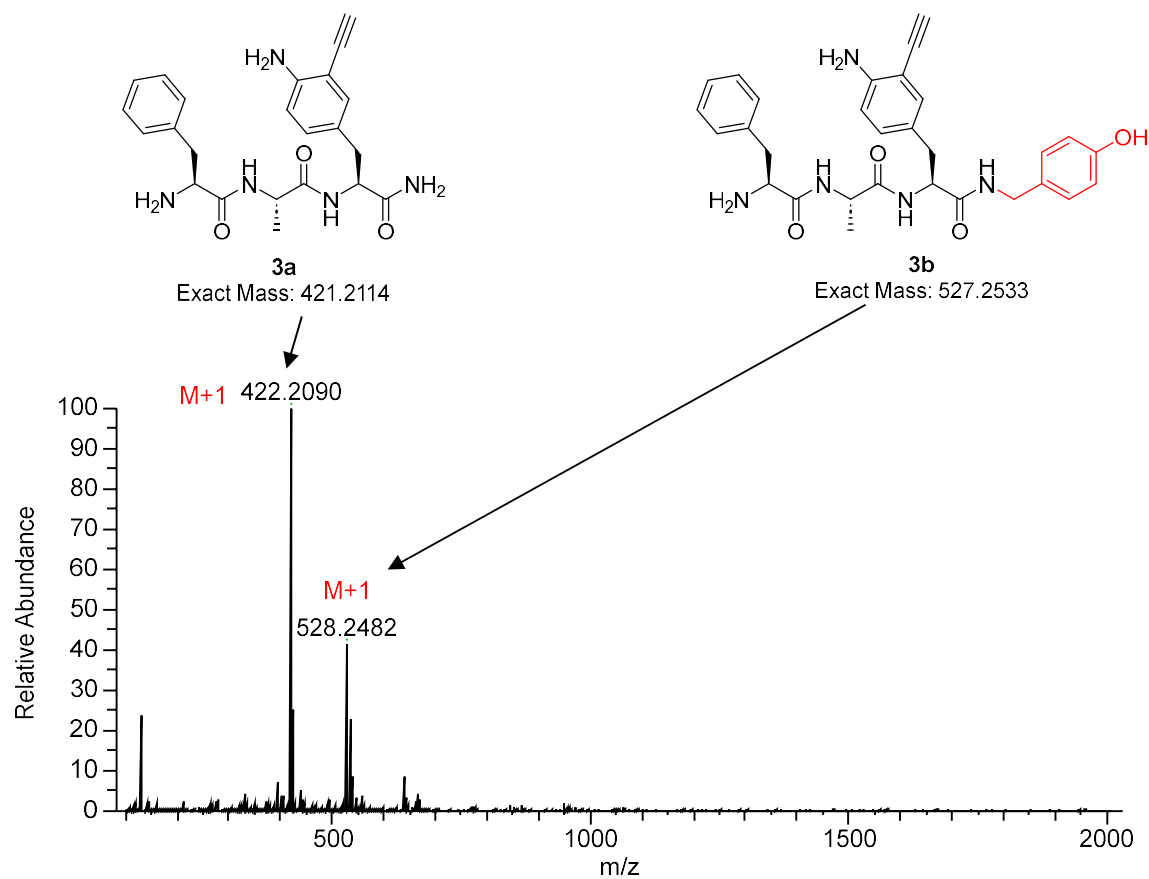
NOTE: During global deprotection and cleavage, a C-terminal N-alkylated peptide is sometimes observed, particularly at lower scale cleavage. This alkylated peptides exhibits a mass of +106 amu from the desired C-terminal amide. The origin of this alkylated peptide is improper cleavage of the Rink amide resin linker.² Simply, this side-product is not concerning and is typically seen in low abundance during purification.



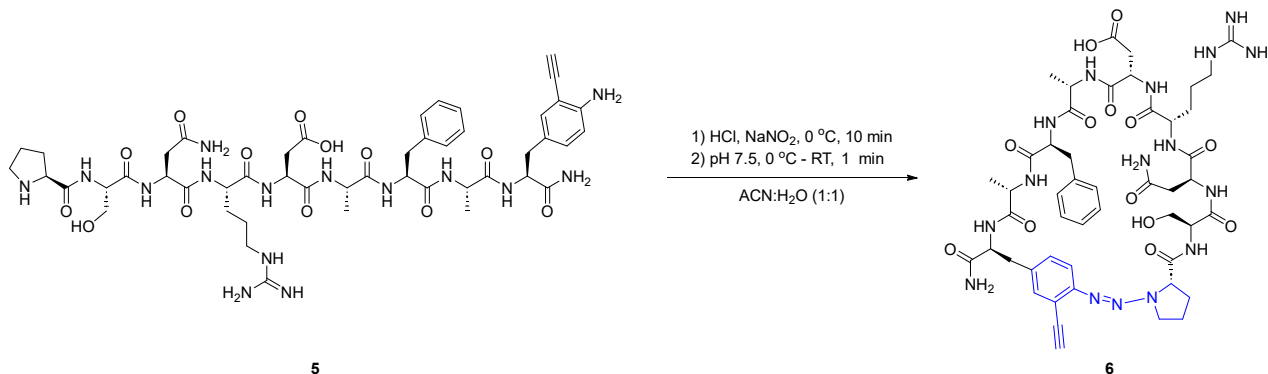
Test cleaved FAX 3a. LCMS m/z 422.2090 (calcd. $[M+H^+] = 422.2187$).

Test cleaved C-terminal N-alkylated resin fragment FAX 3b. LCMS m/z 528.2482 (calcd. $[M+H^+] = 528.2605$).

HRMS Spectrum of 3a and 3b



Supplementary Figure 4: Triazene peptide synthesis

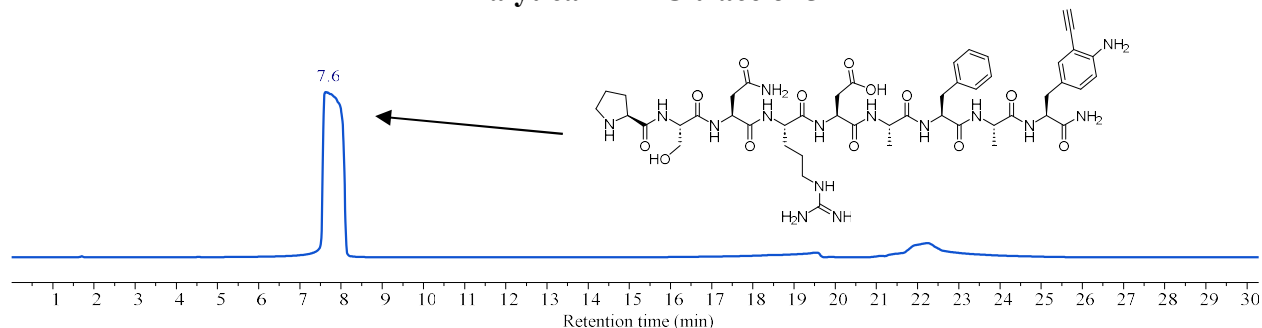


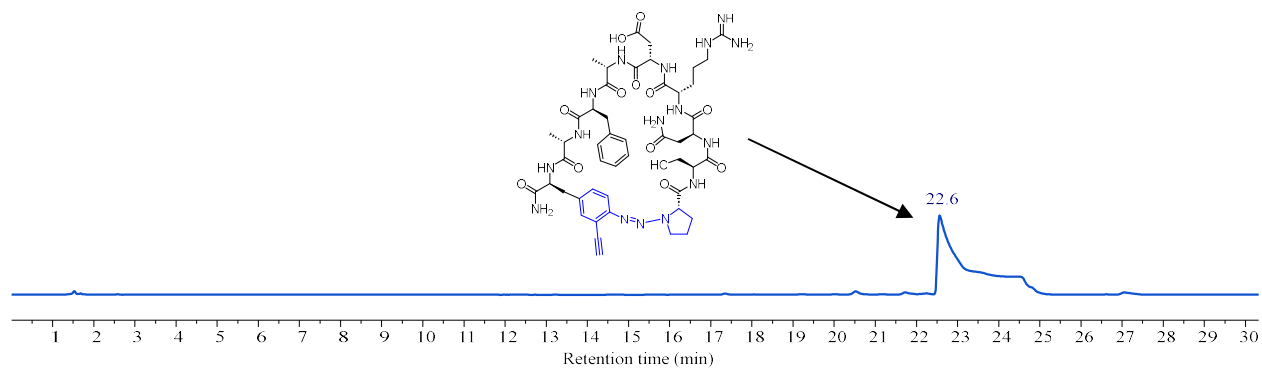
Procedure: 10 mg of linear peptide **5** (9.4 μmol, 1 equiv.) was dissolved in 3 mL 30 mM HCl in ACN:H₂O (1:1). A stir bar was added, and the vial was placed in an ice bath until the temperature of the reaction mixture reached 0 °C. Then, 3.25 mg NaNO₂ (47 μmol, 5 equiv.) was added from a prepared stock solution in DI H₂O to the reaction mixture, which was allowed to stir for 15 minutes at 0 °C. Following this, 2 mL of 100 mM NaP buffer at pH 7.5 was added and the reaction mixture was removed from the ice bath and allowed to warm to RT, whereupon the reaction mixture was directly injected into preparatory HPLC for purification. The triazene peptide eluted at 35 % B in > 95 % conversion based on analysis of eluent absorbance at 220 nm. The SM was observed to be entirely consumed. Pure fractions were collected together, frozen, and lyophilized to afford triazene **6** as a white powder (6.3 mg, 63 % yield).

PSNRDAFAX Linear peptide 5. LCMS m/z 1062.4929 (calcd. $[M+H]^+$ = 1062.5116), m/z 531.7502 (calcd. $[M+H]^+$ = 531.7594), Purity: > 95 % (HPLC analysis at 220 nm). Retention time in HPLC: 7.6 min (Method A).

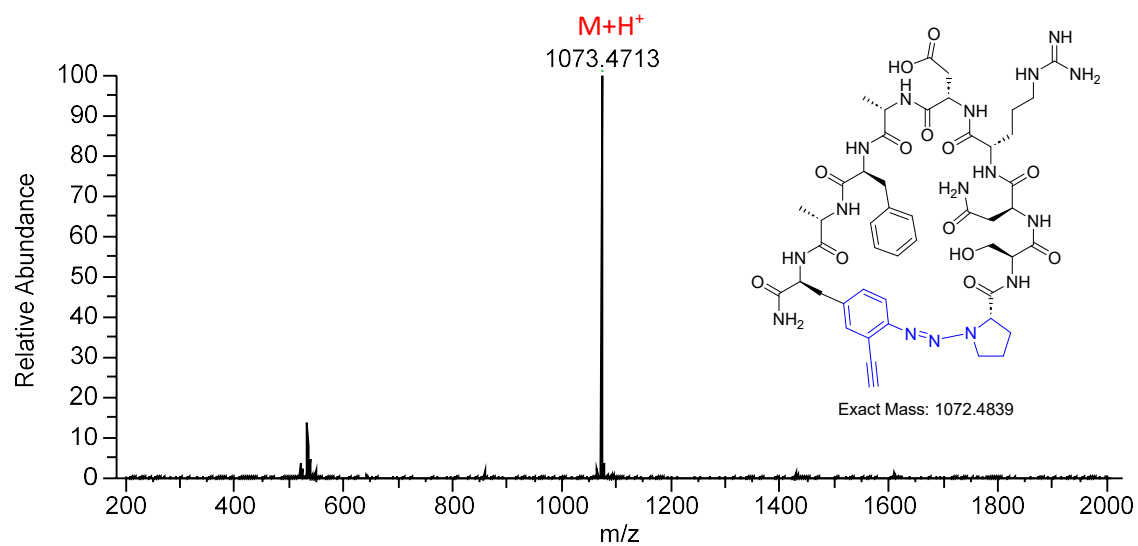
PSNRDAFAX Triazene peptide 6. LCMS m/z 1073.4713 (calcd. $[M+H]^+$ = 1073.4912), Purity: > 95 % (HPLC analysis at 220 nm). Retention time in HPLC: 22.6 min (Method A).

Analytical HPLC trace of 5

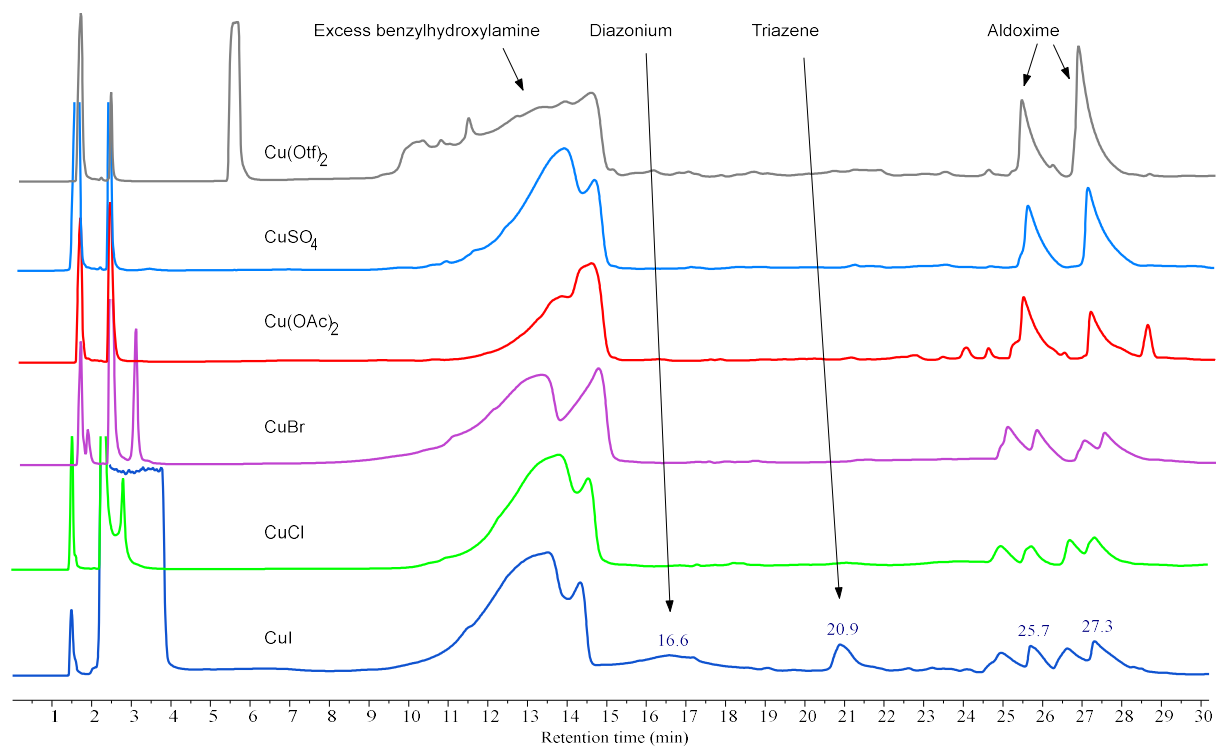




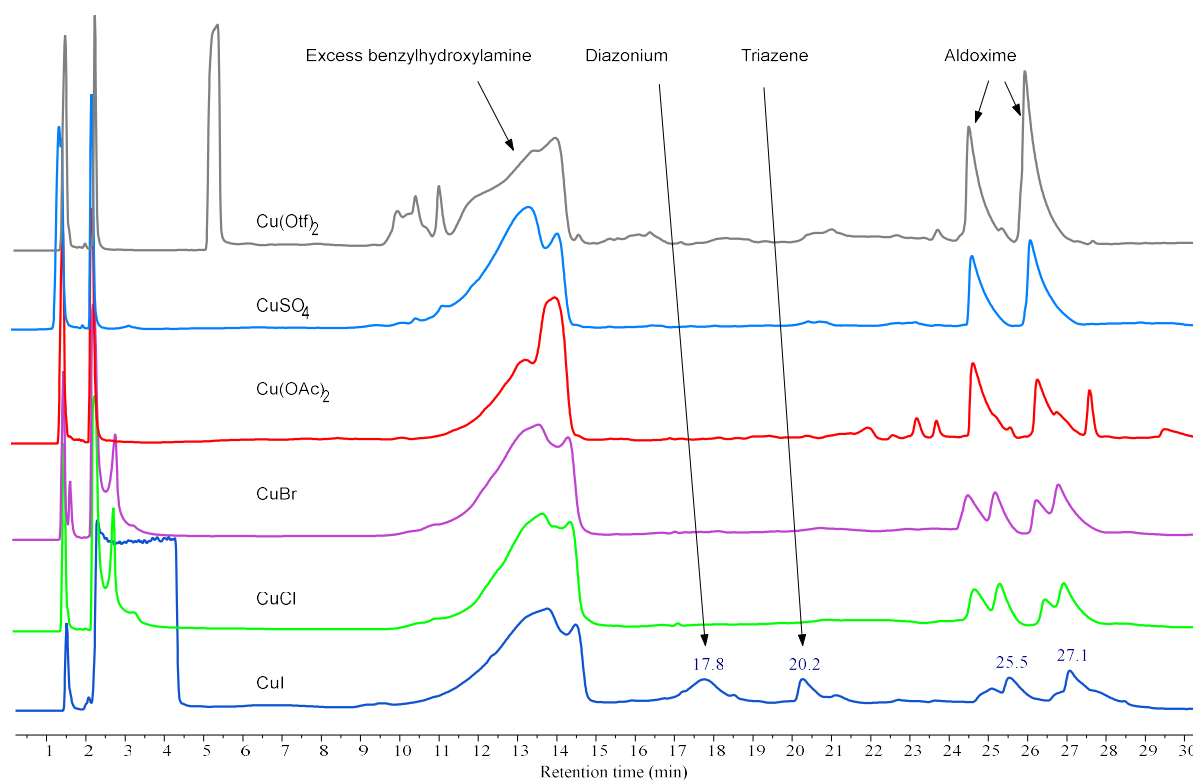
HRMS spectrum of 6



Analytical HPLC Spectra at 8 h



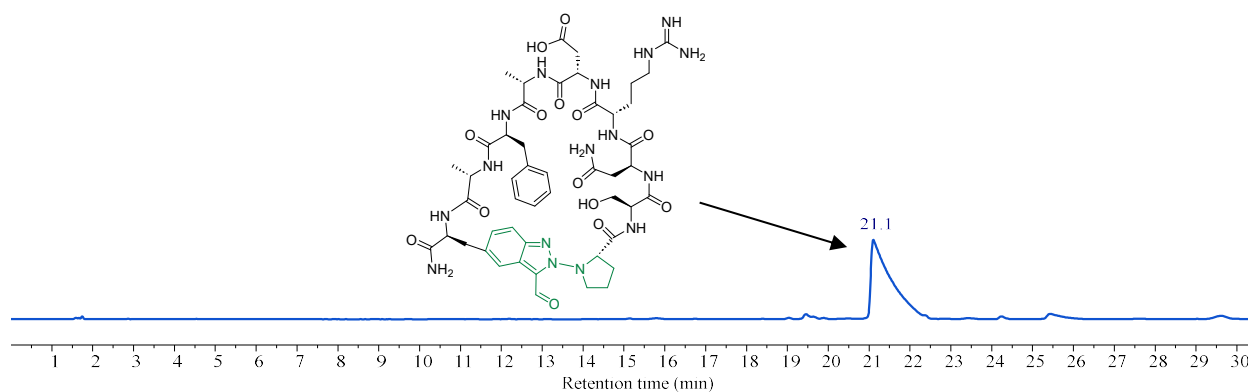
Analytical HPLC Spectra at 16 h



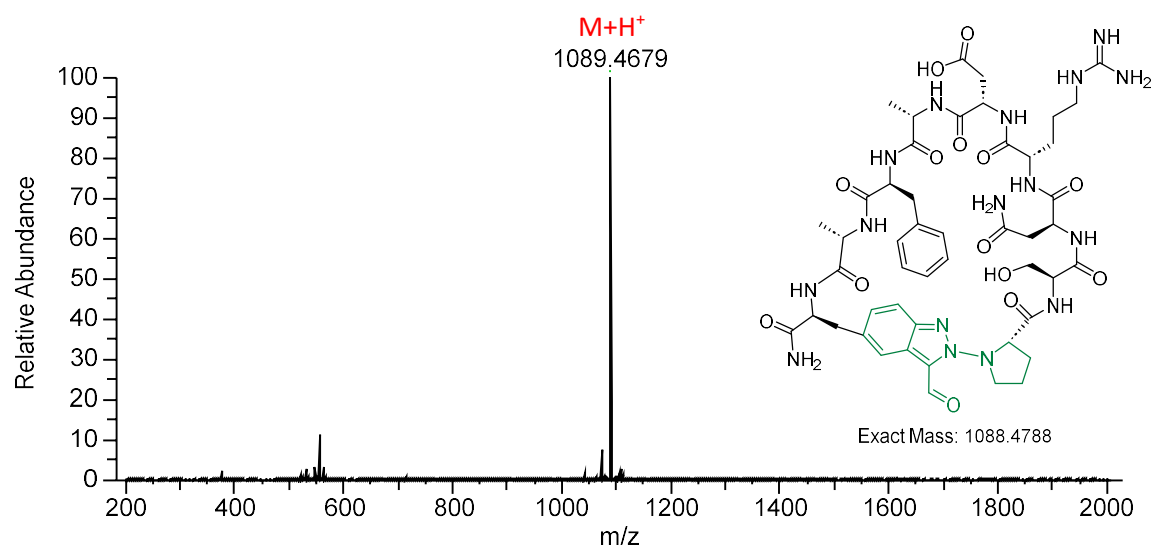
PSNRDAFAX Isoindazole 3-carbaldehyde peptide 7. LCMS m/z 1089.4679 (calcd. $[M+H]^+ = 1089.4861$), Purity: > 95 % (HPLC analysis at 220 nm). Retention time in HPLC: 21.1 min (Method A).

PSNRDAFAX Isoindazole 3-carbaldehyde O-benzyl oxime peptide 8. LCMS m/z 1194.5237 (calcd. $[M+H]^+ = 1194.5439$), Purity: > 95 % (HPLC analysis at 220 nm). Retention time in HPLC: 28.8 min; 30.4 min (Method A).

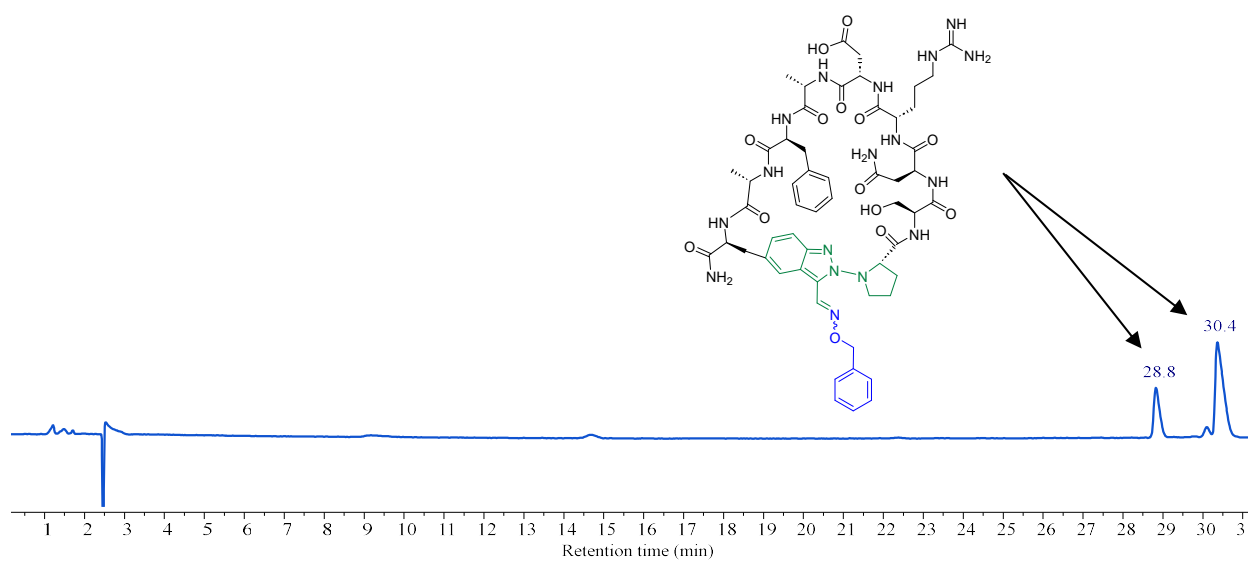
Analytical HPLC trace of 7



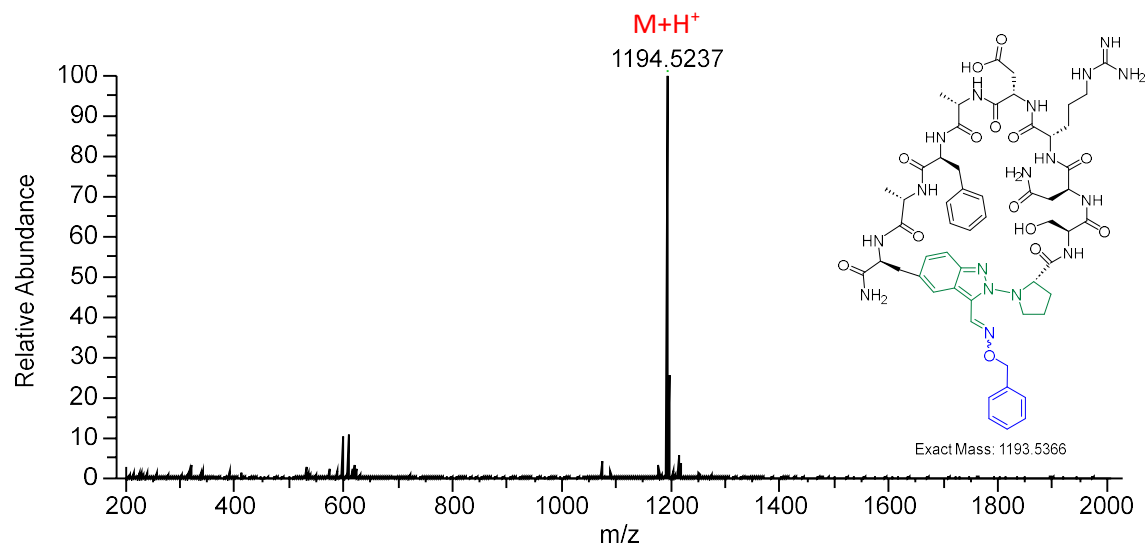
HRMS spectrum of 7



Analytical HPLC trace of 8

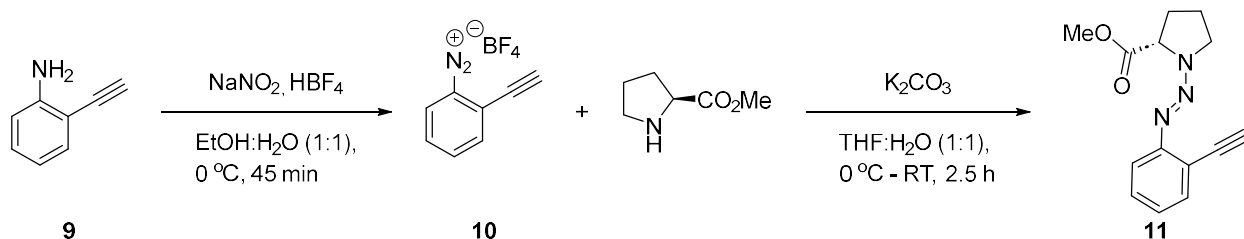


HRMS spectrum of 8



Supplementary Figure 6: Synthesis of small molecule triazene 11

methyl (*E*)-((2-ethynylphenyl)diazenyl)-*L*-prolinate

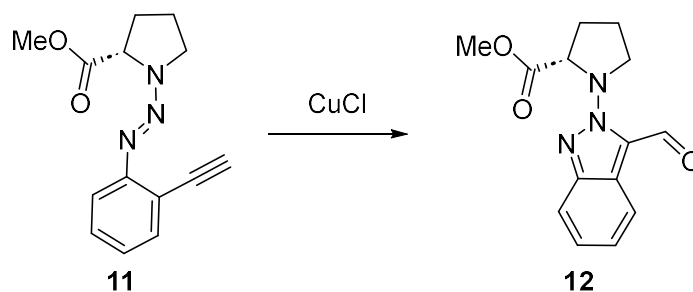


Synthesis of diazonium salt 10: 500 mg of 2-ethynylaniline **9** (4.27 mmol, 1 equiv.) was dissolved in a mixture of 48 % HBF₄ (1.5 mL), EtOH (5 mL), and H₂O (5 mL). The reaction mixture was cooled to 0 °C, and 353 mg of NaNO₂ (5.12 mmol, 1.2 equiv.) in DI H₂O (2 mL) were added dropwise to the mixture over a period of 5 min. The reaction was allowed to stir at 0 °C for 45 min. The precipitate was collected, washed with cold Et₂O, and dried under vacuum to afford 830 mg of diazonium salt **10** as brown powder (90 %). The crude product was used directly for the next reaction without further purification.

Synthesis of triazene 11: To a solution containing 5.75 g (*L*)-proline methyl ester hydrochloride (34.7 mmol, 3.0 equiv.) and 4.8 g of K₂CO₃ (34.7 mmol, 3.0 equiv.) in 80 mL THF:H₂O (1:1) at 0 °C was added 2.5 g of diazonium salt **10** (11.57 mmol, 1.0 equiv.) in five batches over 15 min. The reaction mixture was stirred at 0 °C for 30 min followed by 2 h at RT. After that, it was quenched with H₂O and extracted with EA (3 × 30 mL). The organic layers were combined, dried over Na₂SO₄, concentrated, and the crude triazene product **11** was used for the next step without further purification.

Supplementary Figure 7: Optimization of small molecule isoindazole 3-carbaldehyde 12 Synthesis

Methyl (3-formyl-2H-indazol-2-yl)-L-prolinate



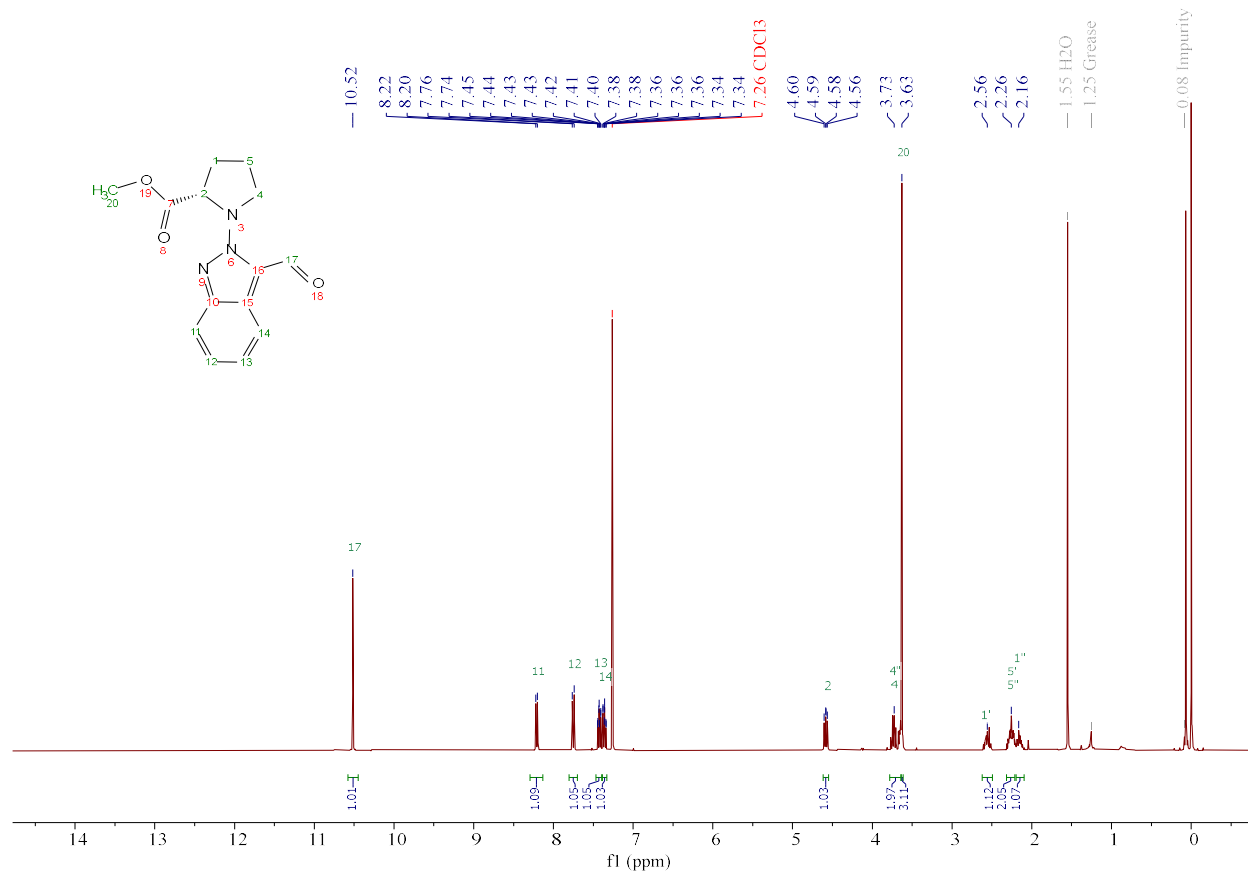
Condition	Yield
A) CuCl (15 equiv.), ACN, O ₂ , 60 °C, 1 h	52 %
B) CuCl (3 equiv.), ACN, O ₂ , 60 °C, 1 h	54 %
C) CuCl (30 mol %), ACN, O ₂ , 60 °C, 1 h	54 %
D) CuCl (30 mol %), ACN, O ₂ , RT, 24 h	75 %
E) CuCl (30 mol %), ACN:H ₂ O (1:1), O ₂ , RT, 4 h	< 5 %
F) CuCl (3 equiv.), ACN, air, 60 °C, 1 h	< 5 %

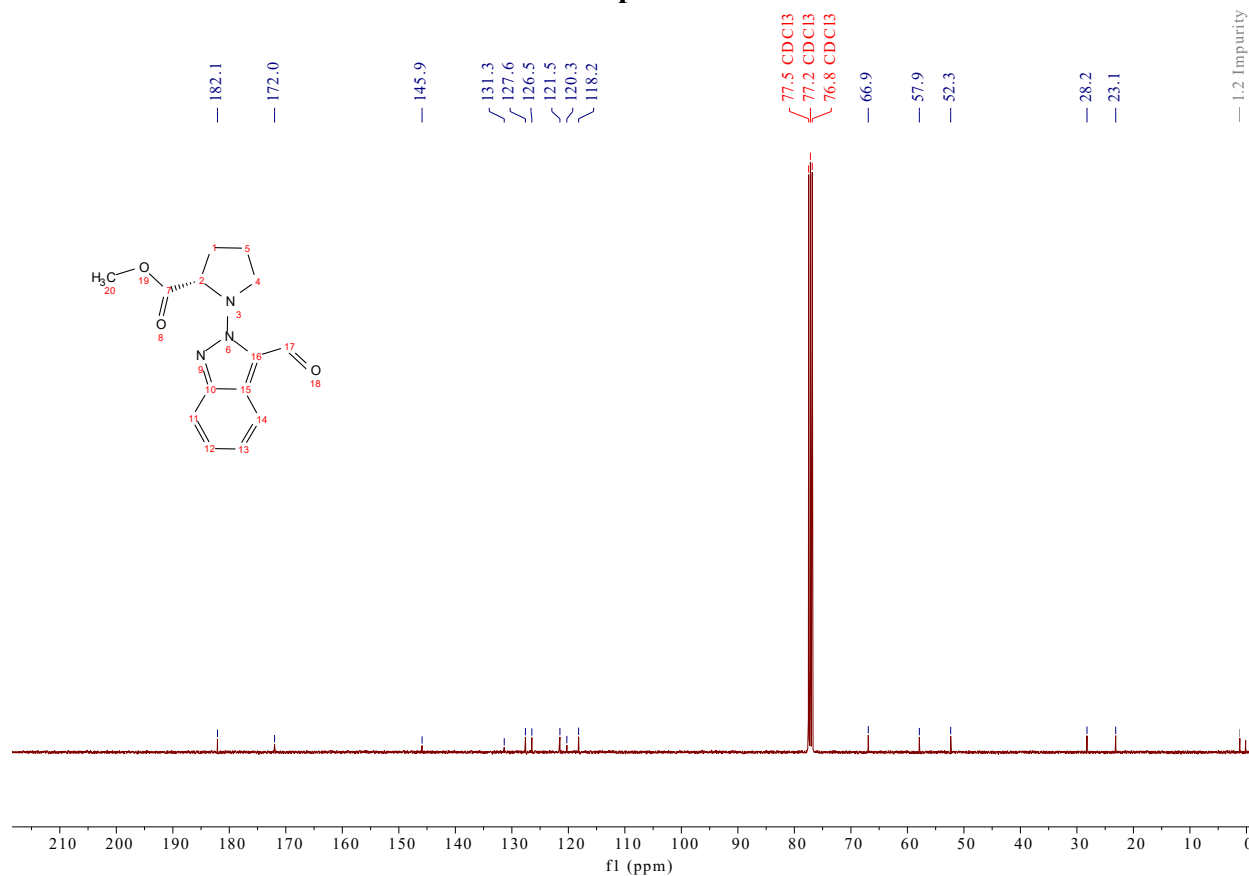
Representative Procedure (A): To a solution of 50 mg of methyl (*E*)-((2-ethynylphenyl)diazenyl)-*L*-prolinate **11** (0.19 mmol, 1.0 equiv.) in dry ACN was added CuCl (177 mg, 1.8 mmol, 15.0 equiv.) under oxygen atmosphere. The resulting solution was heated at 60 °C for 1 h. The reaction was then cooled to RT, diluted with EA, and washed with dilute NH₄OH to remove extra copper. The combined organic layers were dried using Na₂SO₄, concentrated, and purified on silica gel column chromatography using 0-15 % EA in Hexane to give the titled compound **12** as white solid (27 mg, 52 %).

Spectral data for compound 12

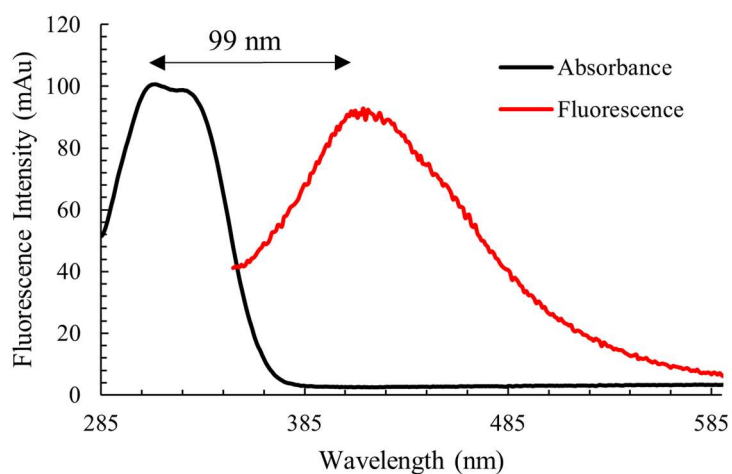
Methyl (3-formyl-2H-indazol-2-yl)-*L*-prolinate. ¹H NMR (400 MHz, CDCl₃) δ 10.52 (s, 1H), 8.21 (d, *J* = 8.2 Hz, 1H), 7.75 (d, *J* = 8.5 Hz, 1H), 7.43 (ddd, *J* = 8.5, 6.8, 1.3 Hz, 1H), 7.36 (ddd, *J* = 7.9, 6.8, 1.0 Hz, 1H), 4.58 (dd, *J* = 9.4, 7.0 Hz, 1H), 3.74 (td, *J* = 8.9, 7.5 Hz, 1H), 3.67 – 3.63 (m, 4H), 2.61 – 2.51 (m, 1H), 2.31 – 2.20 (m, 2H), 2.19 – 2.11 (m, 1H) ppm. ¹³C NMR (101 MHz, CDCl₃) δ 182.10, 171.99, 145.89, 131.35, 127.60, 126.46, 121.49, 120.27, 118.18, 66.93, 57.88, 52.34, 28.22, 23.14, 1.17.

¹H NMR Spectrum of 12



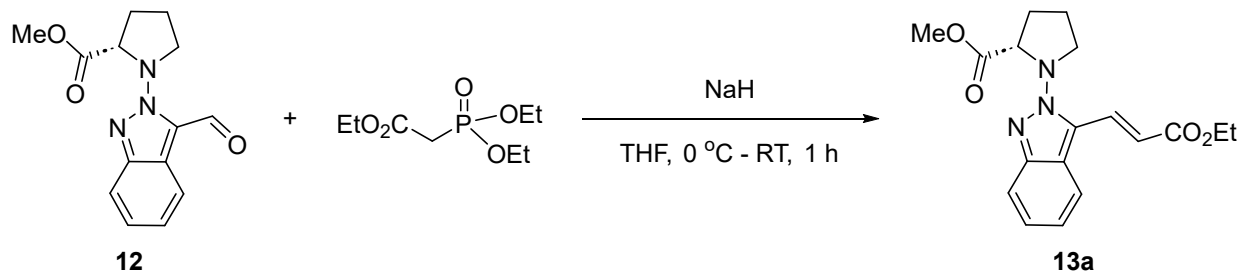
¹³C NMR Spectrum of 12

Absorbance maximum: 311 nm; Fluorescence emission maximum (excitation at 311 nm): 410 nm. Absorbance normalized to baseline and zoomed for comparative viewing of excitation and emission spectra.

Fluorescence Spectrum of 12

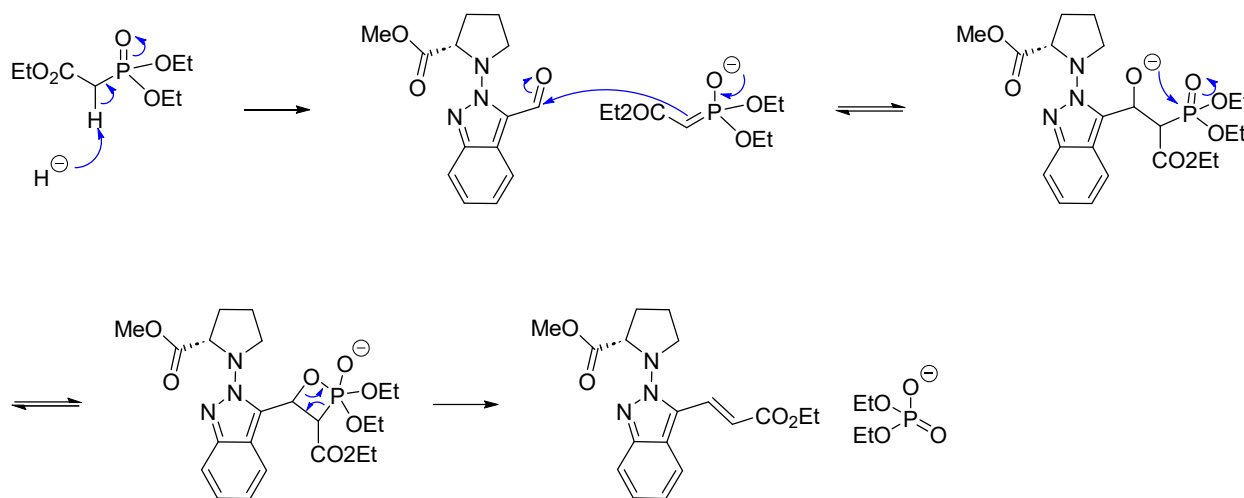
Supplementary Figure 8: Synthesis of Wittig, Horner-Wittig, and Henry Olefination Products

Methyl (E)-(3-(3-ethoxy-3-oxoprop-1-en-1-yl)-2H-indazol-2-yl)-L-prolinate



Procedure: The Horner-Wittig reaction was used to synthesize **13a**. A 15 mL Schlenk tube was charged with NaH (24 mg, 0.6 mmol, 2.0 equiv., 60 % in mineral oil) and was backfilled with N₂ three times. Then, 2 mL of anhydrous THF was added and the tube was cooled to 0 °C. To this slurry, triethylphosphonoacetate (136 mg, 0.6 mmol, 2.0 equiv.) was added dropwise. After stirring at 0 °C for 15 min, a solution of isoindazole 3-carbaldehyde **12** (54 mg, 0.3 mmol, 1.0 equiv.) in 1 mL anhydrous THF was added dropwise at 0 °C. After 15 min, the reaction was brought to rt and stirred for 1 h. After completion, the reaction was quenched with H₂O and extracted with EA (3 × 3 mL). The combined organic layers were dried using Na₂SO₄, concentrated, and purified on silica gel column chromatography using 0-12% EA in Hexane to get 46 mg of the olefination product **13a** as yellowish liquid (45 %).

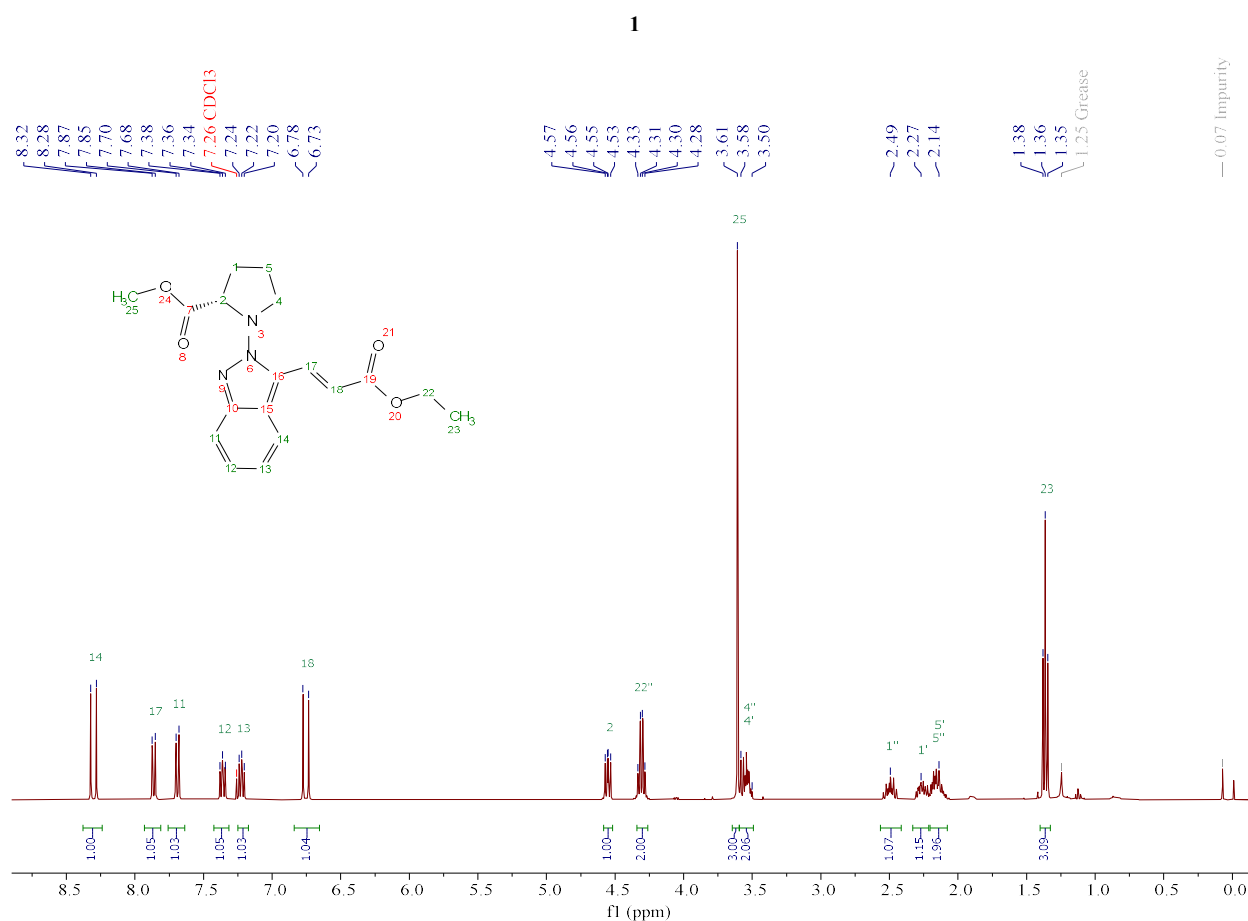
Proposed mechanism for Wittig-Horner reaction:

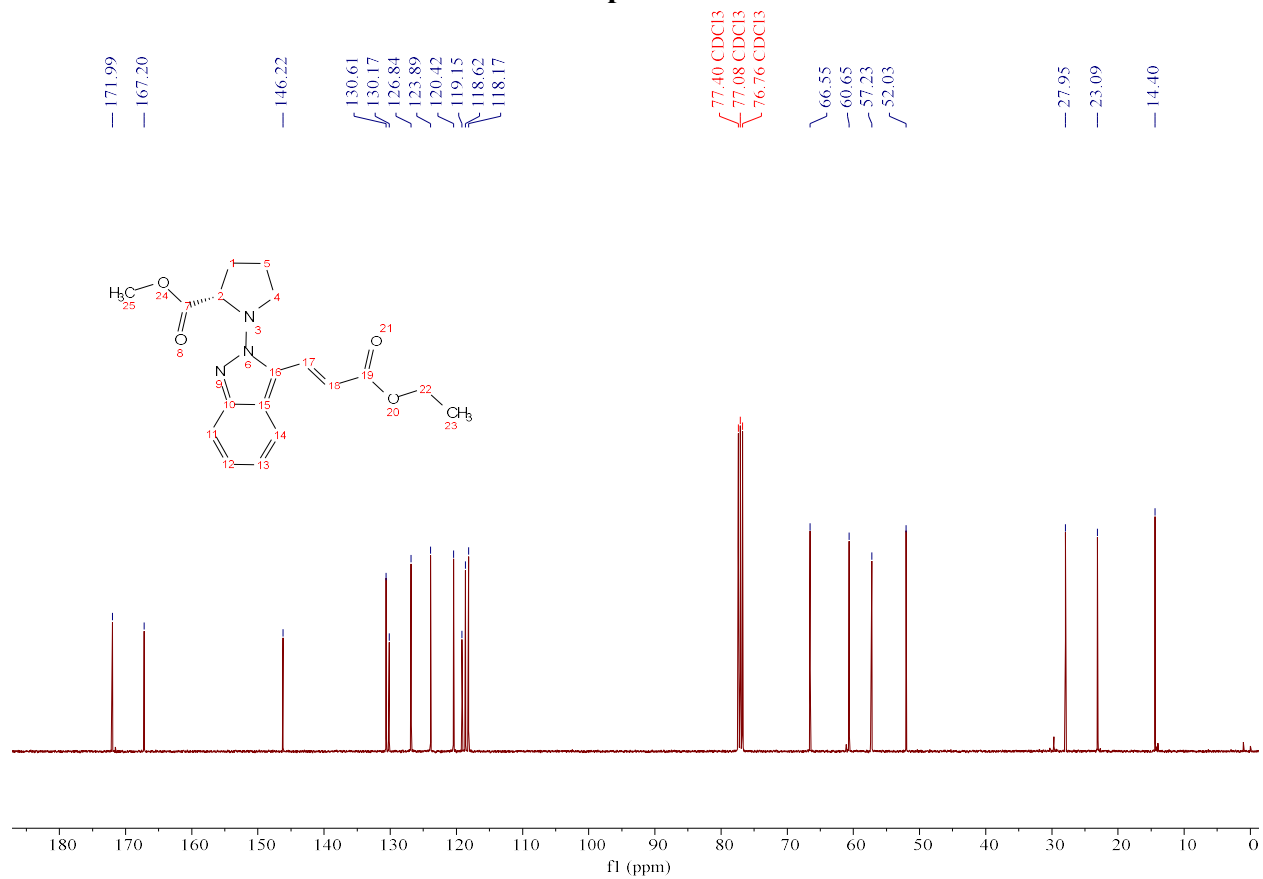


*Antiperiplanar approach during the nucleophilic attack of the aldehyde gives this reaction a strong preference for *E* product. In our example, **13a** was isolated with the *E* isomer as the sole product.

Spectral data for compound 13a

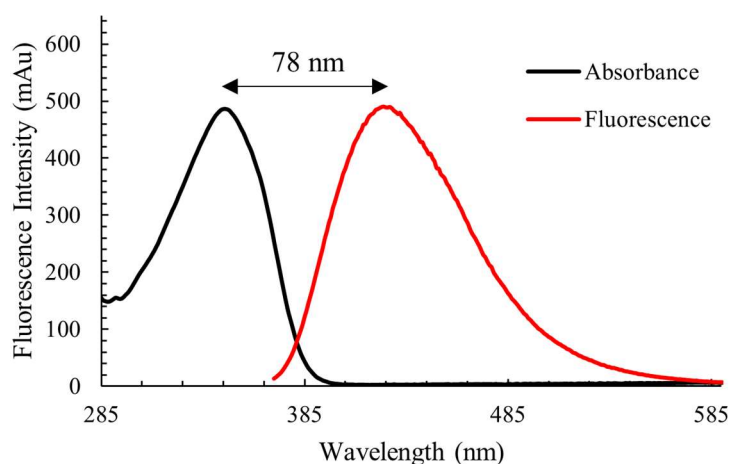
Methyl (E)-(3-(3-ethoxy-3-oxoprop-1-en-1-yl)-2H-indazol-2-yl)-L-prolinate. ^1H NMR (400 MHz, CDCl_3) δ 8.30 (d, $J = 16.5$ Hz, 1H), 7.86 (d, $J = 8.5$ Hz, 1H), 7.69 (d, $J = 8.7$ Hz, 1H), 7.36 (t, $J = 7.7$ Hz, 1H), 7.22 (d, $J = 7.7$ Hz, 1H), 6.75 (d, $J = 16.5$ Hz, 1H), 4.55 (dd, $J = 9.3, 6.8$ Hz, 1H), 4.31 (q, $J = 7.2$ Hz, 2H), 3.61 (s, 3H), 3.59 – 3.46 (m, 2H), 2.49 (s, 1H), 2.32 – 2.22 (m, 1H), 2.14 (s, 2H), 1.36 (t, $J = 7.1$ Hz, 3H). ^{13}C NMR (101 MHz, CDCl_3) δ 171.99, 167.20, 146.22, 130.61, 130.17, 126.84, 123.89, 120.42, 119.15, 118.62, 118.17, 66.55, 60.65, 57.23, 52.03, 27.95, 23.09, 14.40.



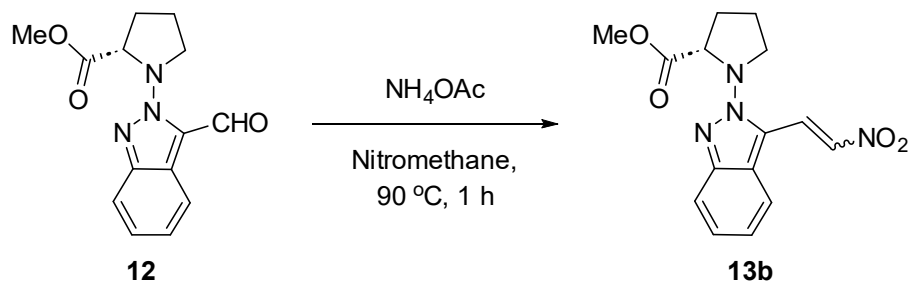
^{13}C NMR spectrum of 13a

Absorbance maximum: 346 nm; Fluorescence emission maximum (excitation at 346 nm): 424 nm. Absorbance normalized to baseline and zoomed for comparative viewing of excitation and emission spectra.

Fluorescence Spectrum of **13a**

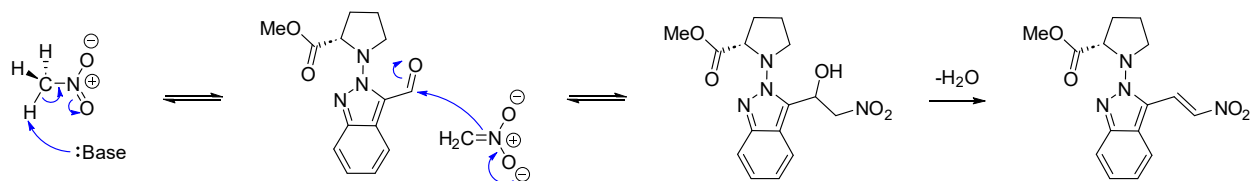


Methyl (E)-(3-(2-nitrovinyl)-2H-indazol-2-yl)-L-prolinate



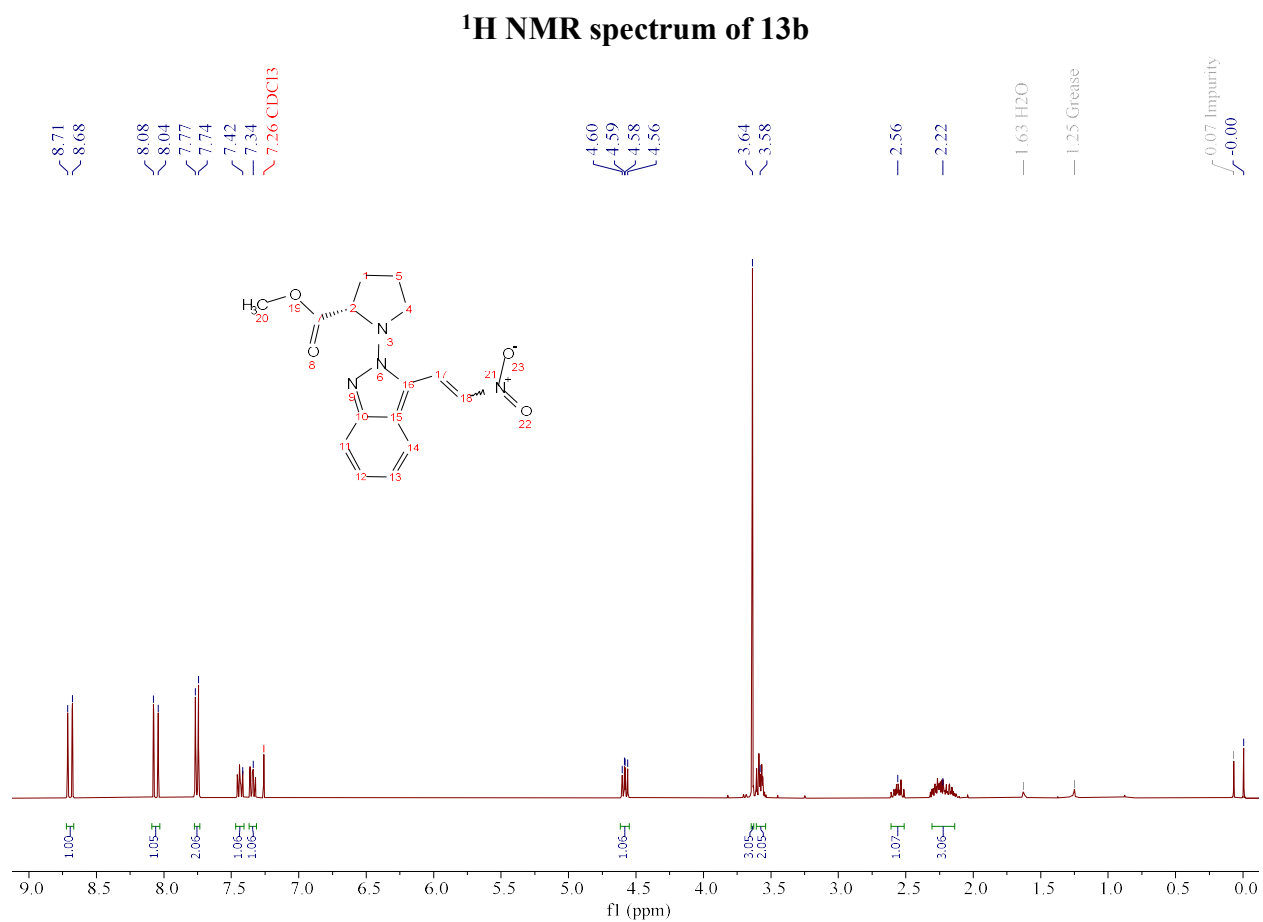
Procedure: The Henry reaction was used to obtain **13b**. 27 mg (0.1 mmol, 1 equiv.) of isoindazole 3-carbaldehyde **12** was dissolved in 1 mL of Nitromethane. 14.4 mg (0.2 mmol, 2 equiv.) of Ammonium acetate was added to the round bottom flask. The reaction was heated at $90\text{ }^\circ\text{C}$ for 1 h, upon which TLC showed consumption of the starting material. The reaction mixture was diluted with H_2O (5 mL) and extracted with EA (3 x 5 mL). The organic layers were combined, dried over Na_2SO_4 , and concentrated. The crude product was purified using silica gel chromatography with 0-10 % EA in Hexane as the eluent. 19 mg of **13b** was obtained as a yellow solid (60 %).

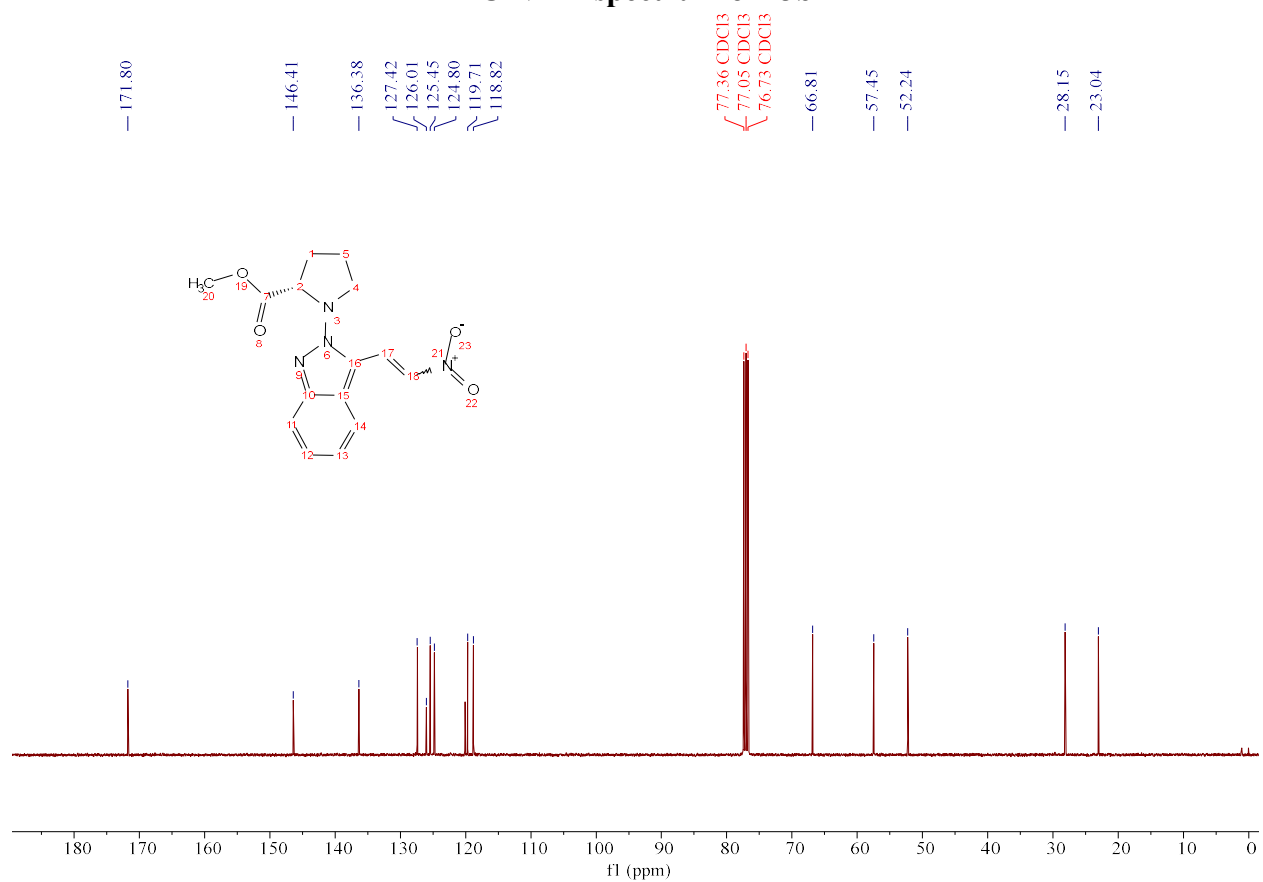
Proposed mechanism for Henry reaction:



Spectral data for **13b**

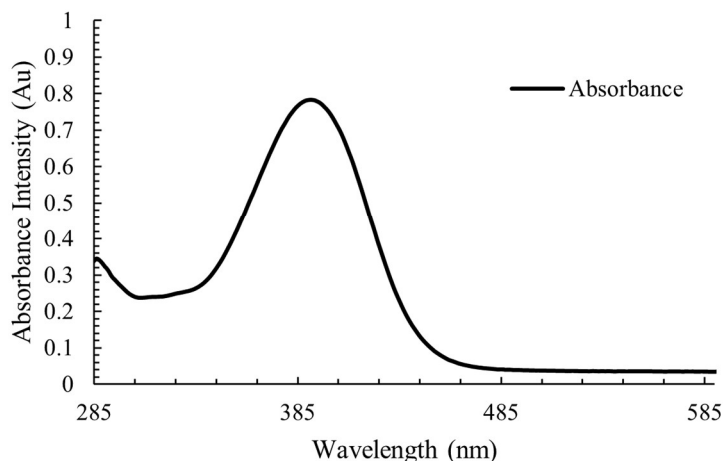
^1H NMR (400 MHz, CDCl_3) δ 8.70 (d, $J = 13.8$ Hz, 1H), 8.06 (d, $J = 13.9$ Hz, 1H), 7.79 – 7.72 (m, 2H), 7.48 – 7.39 (m, 1H), 7.38 – 7.30 (m, 1H), 4.58 (dd, $J = 9.3, 6.9$ Hz, 1H), 3.64 (s, 3H), 3.61 (s, 2H), 2.63 – 2.49 (m, 1H), 2.35 – 2.10 (m, 3H). **^{13}C NMR** (101 MHz, CDCl_3) δ 171.8, 146.4, 136.4, 127.4, 126.0, 125.5, 124.8, 119.7, 118.8, 66.8, 57.5, 52.2, 28.1, 23.0.



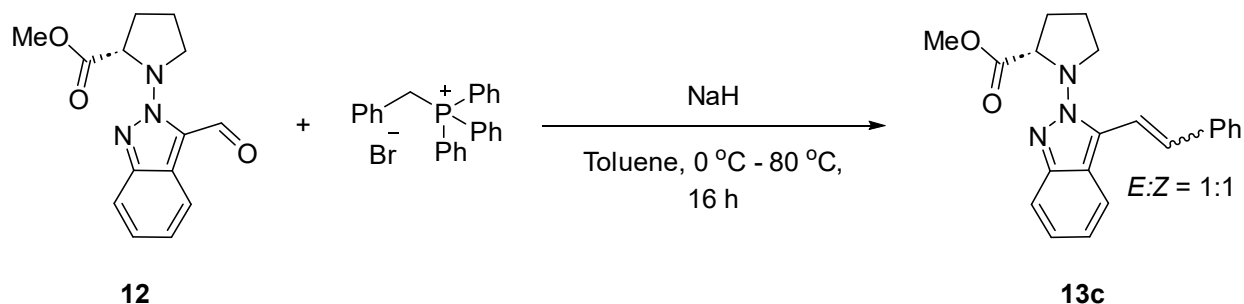
¹³C NMR spectrum of 13b

Absorbance maximum: 391 nm; No fluorescence was observed for 13b at the excitation wavelength of 391 nm.

Absorbance Spectrum of 13b



Methyl (3-styryl-2H-indazol-2-yl)-L-prolinate

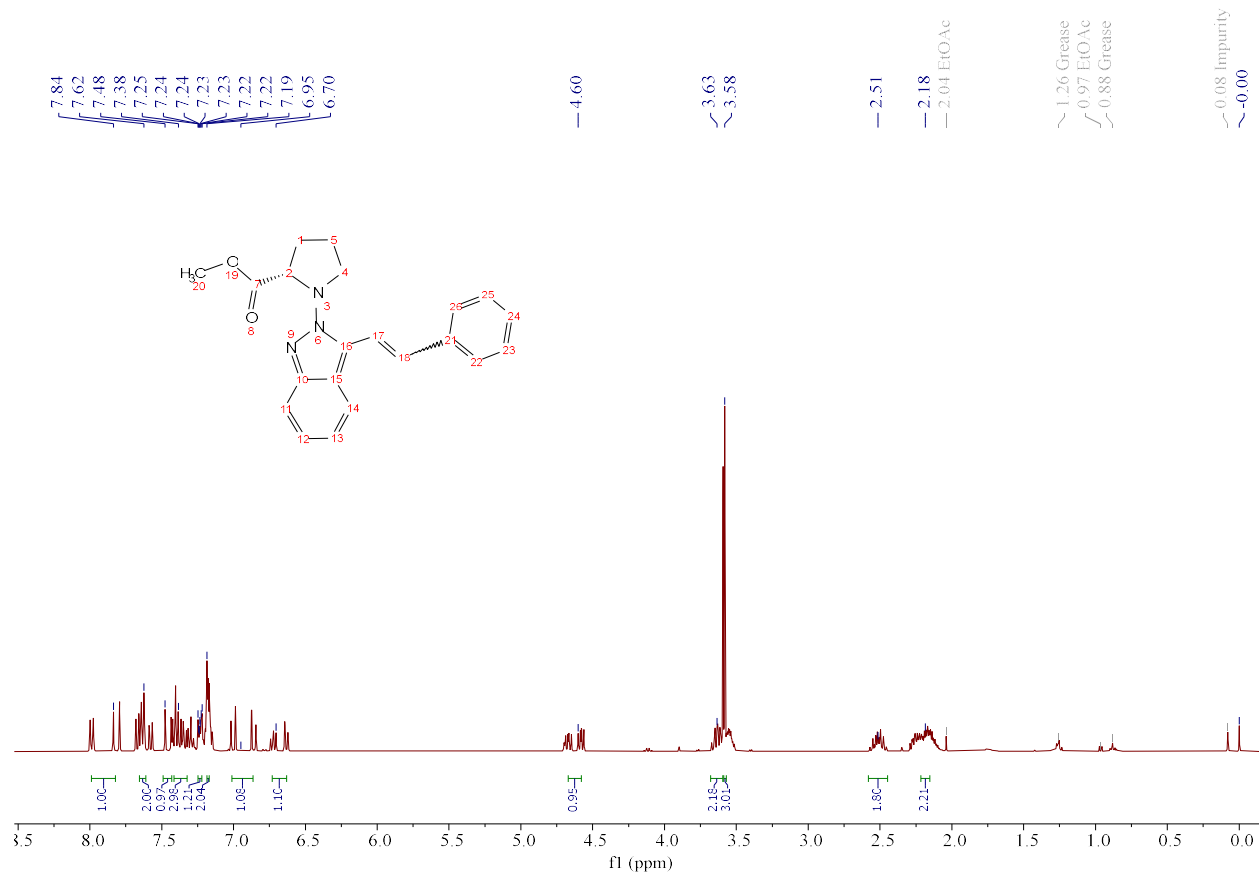


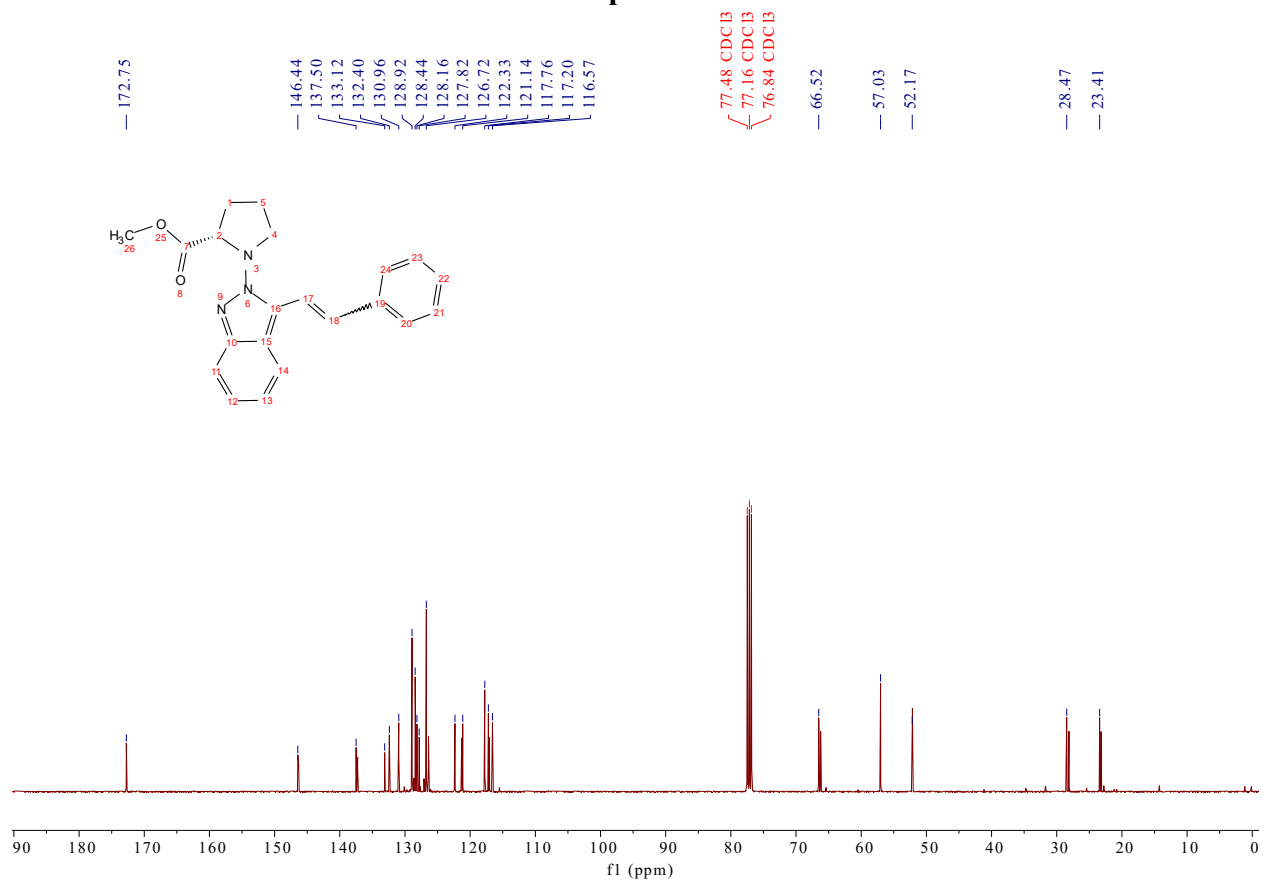
Procedure: A 25 mL Schlenk tube was charged with Benzyl triphenylphosphonium bromide (259 mg, 0.6 mmol, 3.0 equiv.) and backfilled with N₂ three times. Then, 2 mL of anhydrous toluene was added under N₂. The resulting mixture was cooled to 0 °C. To this cooled solution was added 24 mg of NaH (0.6 mmol, 3.0 equiv., 60% in mineral oil). The resulting mixture was stirred for 15 min, and then brought to room temperature and stirred for 1 h. Following this, 54 mg of isoindazole 3-carbaldehyde **12** (0.2 mmol, 1.0 equiv.) was added in one portion and the resulting mixture was heated at 80 °C for 16 h. Upon completion of the reaction, as indicated by TLC, the reaction was quenched with H₂O and extracted with EA (3 × 5 mL). The combined organic fractions were dried under Na₂SO₄, concentrated, and purified on silica using 0-10 % EA in Hexane as the eluent to give 51 mg of the titled product **13c** as a gummy liquid (74 %, *E:Z* = 1:1).

Spectral data for compound 13c

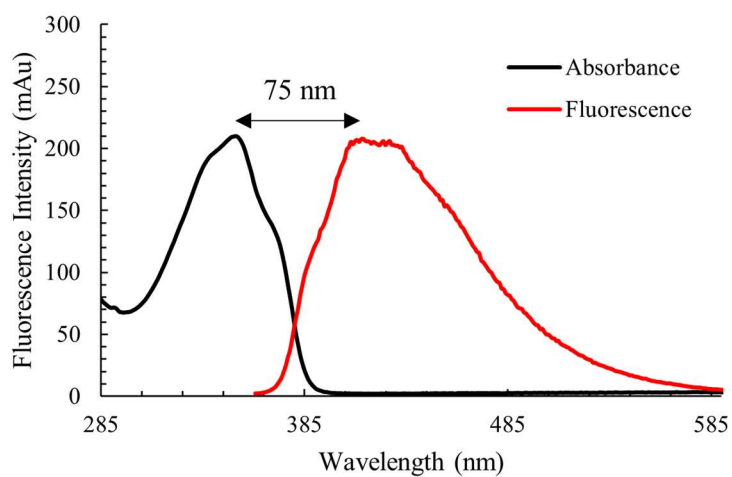
Methyl (3-styryl-2H-indazol-2-yl)-L-prolinate. ^1H NMR (400 MHz, CDCl_3) δ 8.01 – 7.77 (m, 1H), 7.69 – 7.56 (m, 2H), 7.50 – 7.42 (m, 1H), 7.41 – 7.28 (m, 3H), 7.25 – 7.21 (m, 1H), 7.20 – 7.14 (m, 2H), 6.75 – 6.61 (m, 1H), 4.60 (s, 1H), 3.68 – 3.61 (m, 2H), 3.60 – 3.57 (m, 3H), 2.58 – 2.45 (m, 2H), 2.30 – 2.09 (m, 2H). ^{13}C NMR (101 MHz, CDCl_3) δ 172.75, 146.44, 137.50, 133.12, 132.40, 130.96, 128.92, 128.44, 128.16, 127.82, 126.72, 122.33, 121.14, 117.76, 117.20, 116.57, 66.52, 57.03, 52.17, 28.47, 23.41.

^1H NMR spectrum of 13c

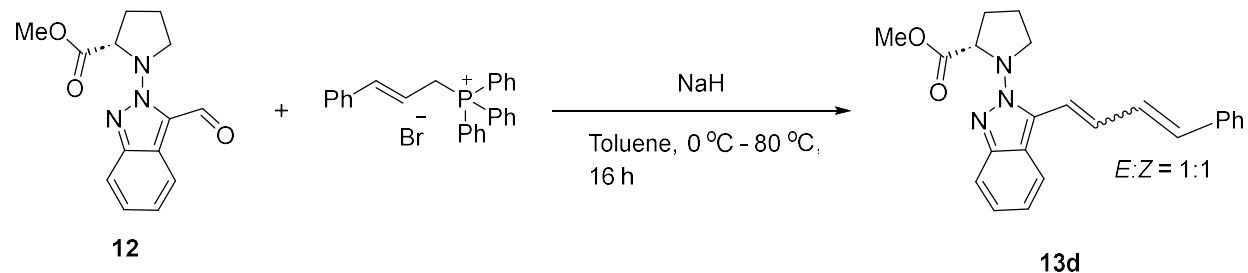


^{13}C NMR spectrum of 13c

Absorbance maximum: 351 nm; Fluorescence emission maximum (excitation at 351 nm): 426 nm. Absorbance normalized to baseline and zoomed for comparative viewing of excitation and emission spectra.

Fluorescence Spectrum of 13c

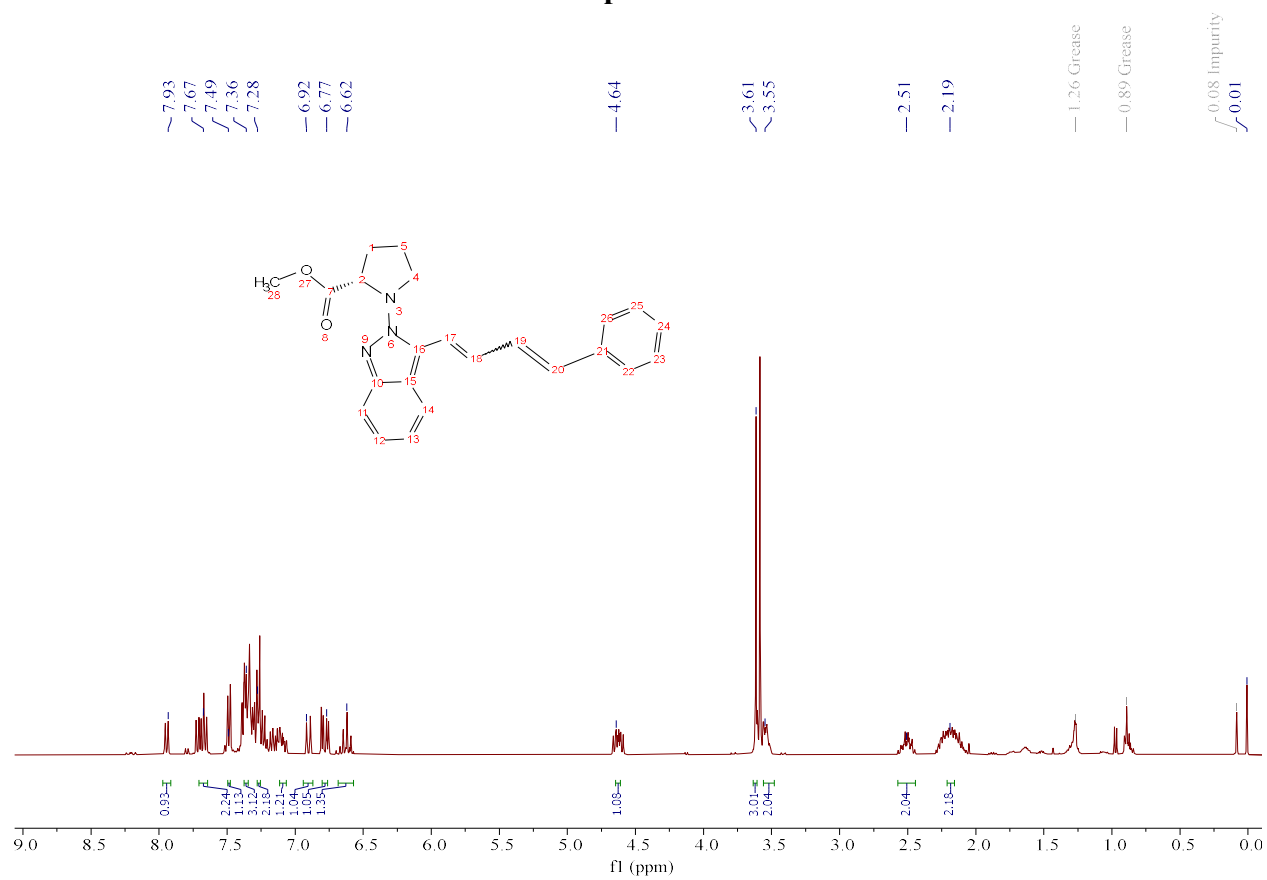
Methyl (3-(4-phenylbuta-1,3-dien-1-yl)-2H-indazol-2-yl)-L-prolinate

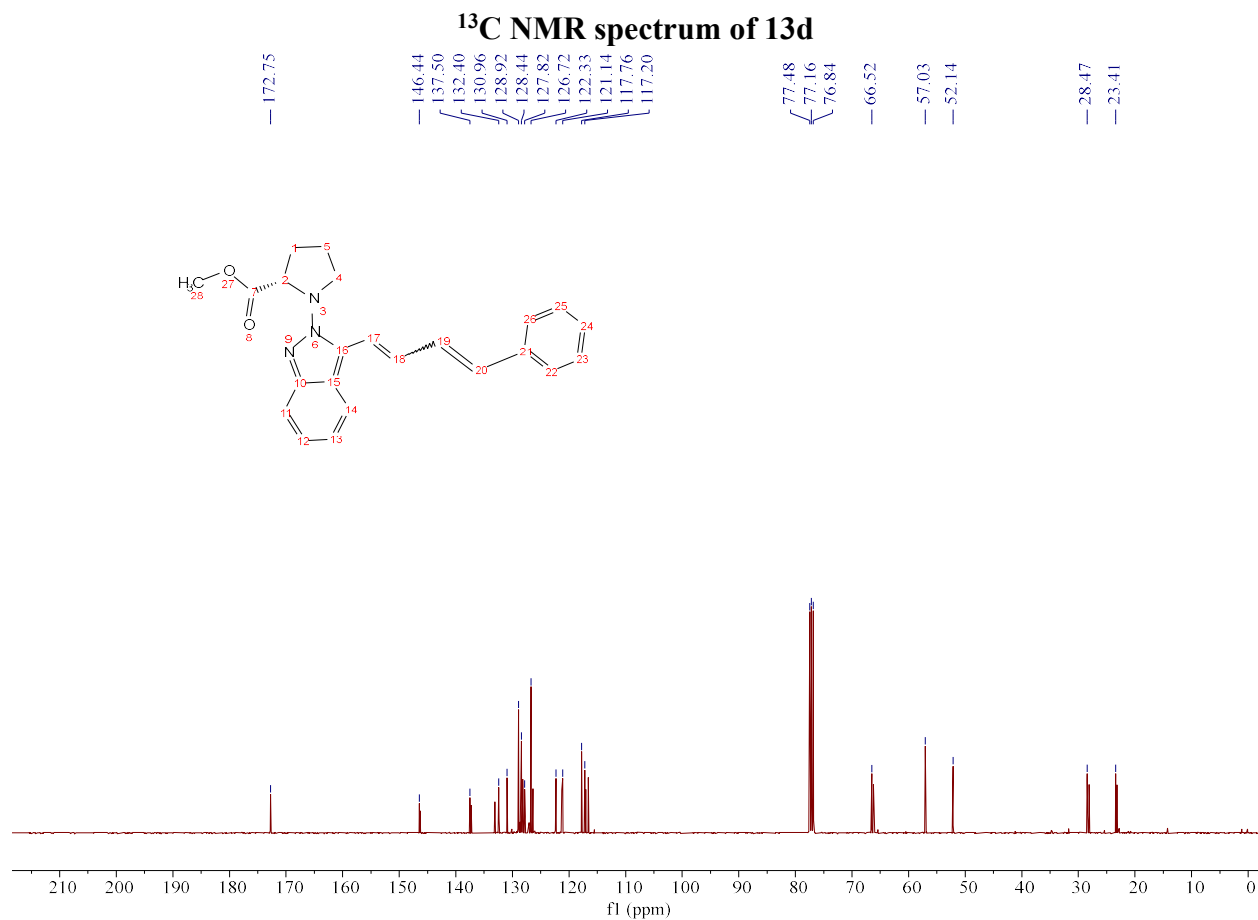


Procedure: A 25 mL Schlenk tube was charged with 275 mg of Cinnamyltriphenylphosphonium bromide salt (0.6 mmol, 3.0 equiv.) and was backfilled with N₂ three times. Then, 2 mL of anhydrous toluene was added under N₂. The resulting mixture was cooled to 0 °C. To this cooled solution, 24 mg of NaH (0.6 mmol, 3.0 equiv., 60 % dispersion in mineral oil) was added. The resulting mixture was stirred for 15 min, and then brought to room temperature and stirred for 1 h. 54 mg of Isoindazole 3-carbaldehyde **12** (0.2 mmol, 1.0 equiv.) was added in one portion, and the resulting mixture was heated at 80 °C for 16 h. Upon completion of the reaction, as indicated by TLC, the reaction was quenched with water and extracted with EA (3 × 5 mL). The combined organic fractions were dried under Na₂SO₄, concentrated, and purified on silica using 0-10 % EA in Hexane as the eluent to give 48 mg of the titled product **13d** as a gummy liquid (68 %, *E*:*Z* = 1:1).

NMR data for compound 13d

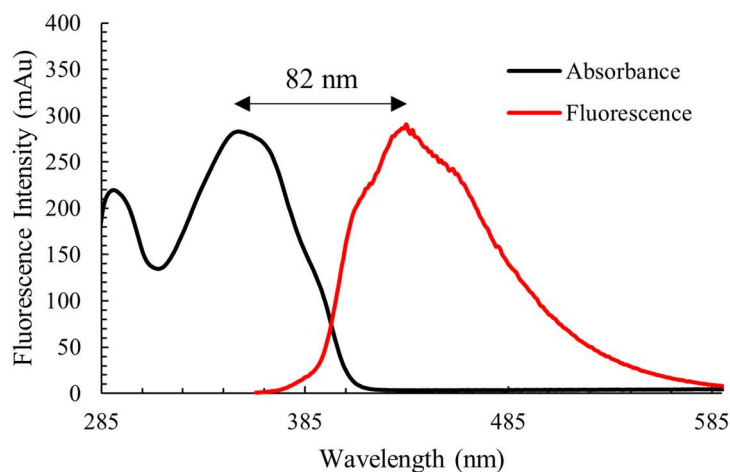
Methyl (3-(4-phenylbuta-1,3-dien-1-yl)-2H-indazol-2-yl)-L-prolinate. ¹H NMR (400 MHz, CDCl₃) δ 7.97 – 7.91 (m, 1H), 7.74 – 7.62 (m, 2H), 7.52 – 7.45 (m, 1H), 7.40 – 7.30 (m, 3H), 7.29 – 7.20 (m, 2H), 7.18 – 7.04 (m, 1H), 6.94 – 6.87 (m, 1H), 6.82 – 6.73 (m, 1H), 6.69 – 6.58 (m, 1H), 4.69 – 4.58 (m, 1H), 3.64 – 3.60 (m, 3H), 3.58 – 3.49 (m, 2H), 2.58 – 2.44 (m, 2H), 2.30 – 2.06 (m, 2H). ¹³C NMR (101 MHz, CDCl₃) δ 172.7, 146.4, 137.5, 132.4, 131.0, 128.9, 128.4, 127.8, 126.7, 122.3, 121.1, 117.8, 117.2, 66.5, 57.0, 52.1, 28.5, 23.4.

¹H NMR spectrum of 13d

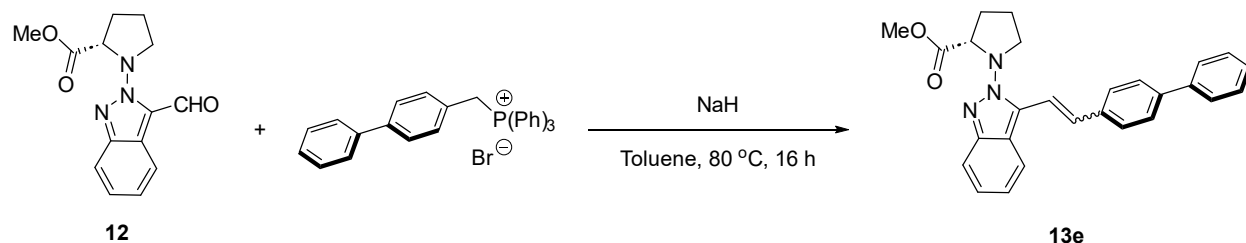


Absorbance maximum: 352 nm; Fluorescence emission maximum (excitation at 352 nm): 434 nm. Absorbance normalized to baseline and zoomed for comparative viewing of excitation and emission spectra.

Fluorescence Spectrum of **13d**



Methyl (3-(2-([1,1'-biphenyl]-4-yl)vinyl)-2H-indazol-2-yl)-L-prolinate



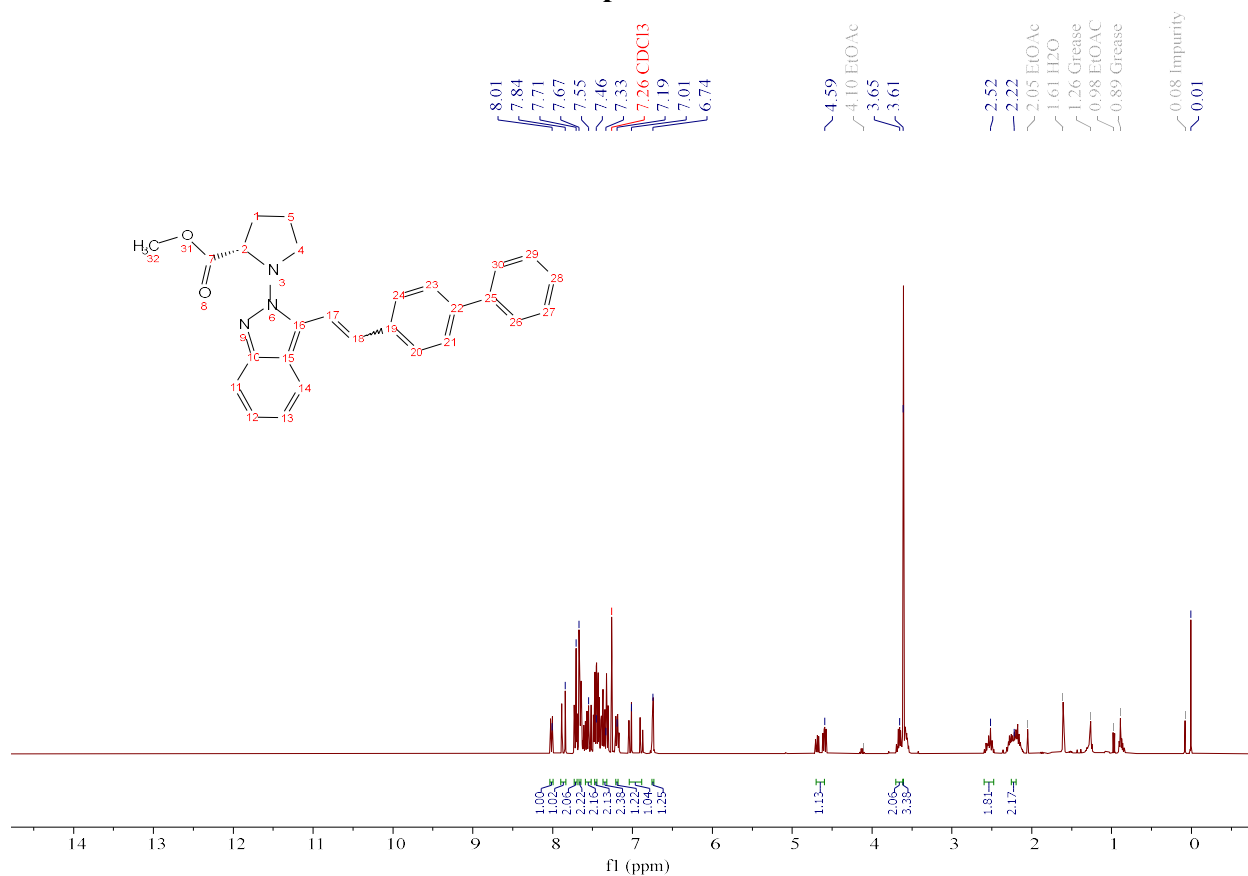
Procedure: A 25 mL Schlenk tube was charged with 305 mg of ([1,1'-biphenyl]-4-ylmethyl)triphenylphosphonium bromide salt (0.6 mmol, 3.0 equiv.) and was backfilled with N₂ three times. Then, 2 mL of anhydrous toluene was added under N₂. The resulting mixture was cooled to 0 °C. To this cooled solution, 24 mg of NaH (0.6 mmol, 3.0 equiv., 60 % dispersion in mineral oil) was added. The resulting mixture was stirred for 15 min, and then brought to room temperature and stirred for 1 h. 54 mg of isoindazole 3-carbaldehyde **12** (0.2 mmol, 1.0 equiv.) was added in one portion, and the resulting mixture was heated at 80 °C for 16 h. Upon completion of the reaction, as indicated by TLC, the reaction was quenched with water and extracted with EA (3 × 5 mL). The combined organic fractions were dried under Na₂SO₄, concentrated, and purified on silica using 0-10 % EA in Hexane as the eluent to give 13 mg of the titled product **13e** as a gummy liquid (31 %, *E:Z* = 2:1).

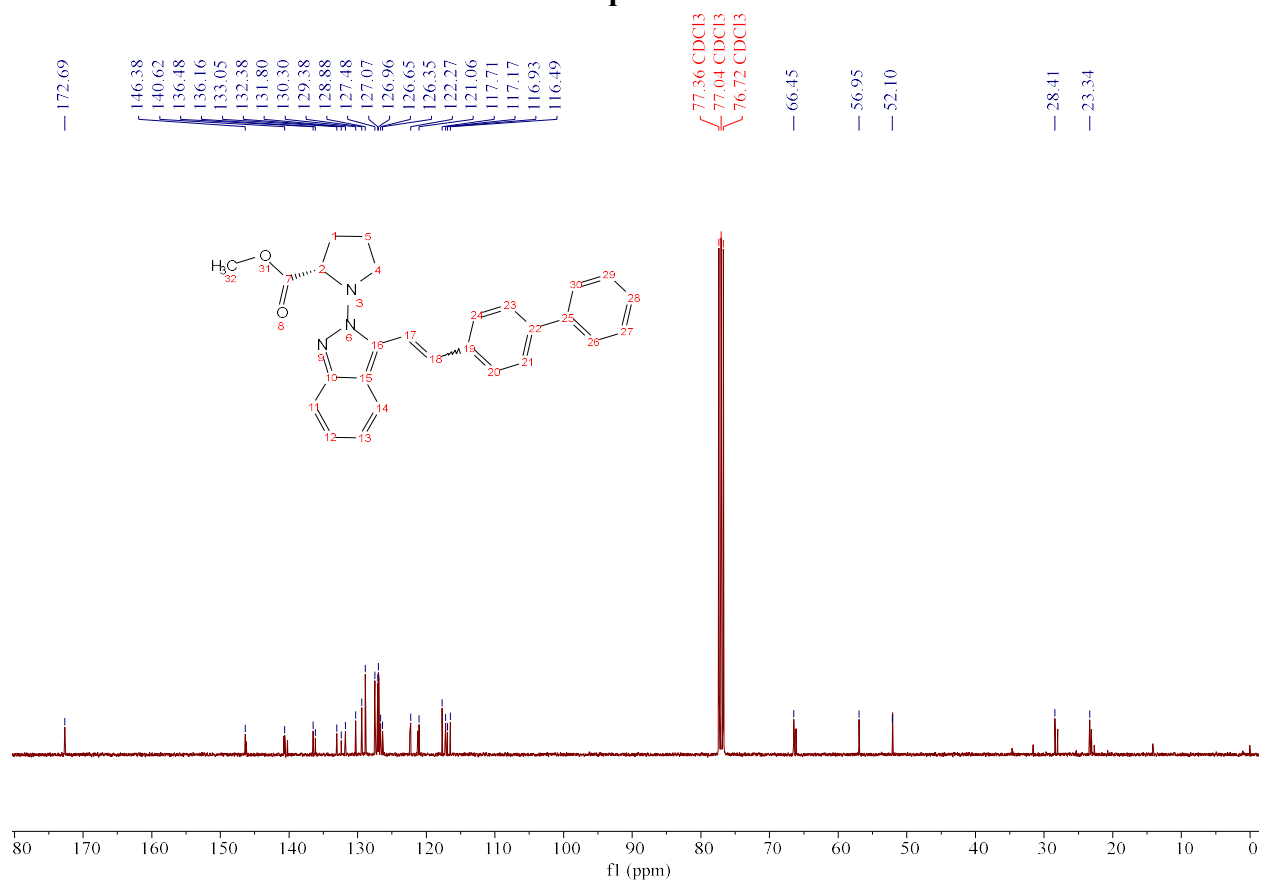
Spectral data for **13e**

Methyl (3-(2-([1,1'-biphenyl]-4-yl)vinyl)-2H-indazol-2-yl)-L-prolinate. ¹H NMR (400 MHz, CDCl₃) δ 8.06 – 8.01 (m, 1H), 7.92 – 7.85 (m, 1H), 7.77 – 7.71 (m, 2H), 7.70 – 7.64 (m, 2H), 7.62 – 7.54 (m, 2H), 7.52 – 7.44 (m, 2H), 7.42 – 7.32 (m, 2H), 7.25 – 7.19 (m, 1H), 7.08 – 6.89 (m,

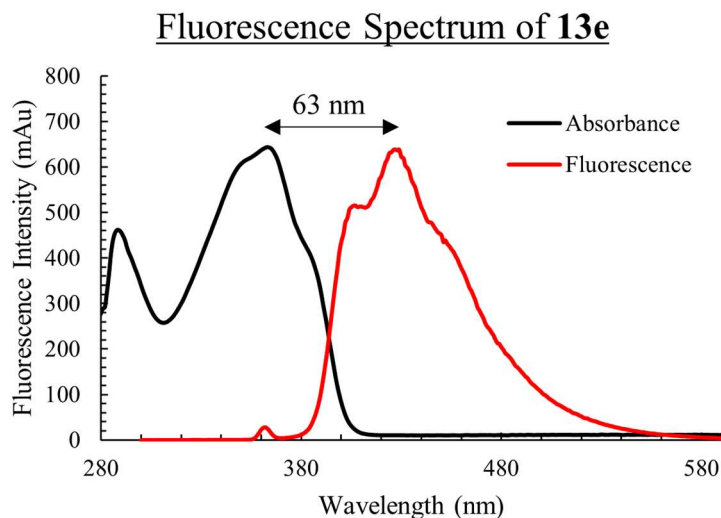
1H), 6.82 – 6.73 (m, 1H), 4.75 – 4.58 (m, 1H), 3.74 – 3.66 (m, 2H), 3.65 – 3.58 (m, 2H), 2.64 – 2.48 (m, 2H), 2.36 – 2.11 (m, 3H). ¹³C NMR (101 MHz, CDCl₃) δ 172.7, 146.4, 140.6, 136.5, 136.2, 133.1, 132.4, 131.8, 130.3, 129.4, 128.9, 127.5, 127.1, 127.0, 126.7, 126.4, 122.3, 121.1, 117.7, 117.2, 116.9, 116.5, 66.4, 57.0, 52.1, 28.4, 23.3.

¹H NMR spectrum of 13e

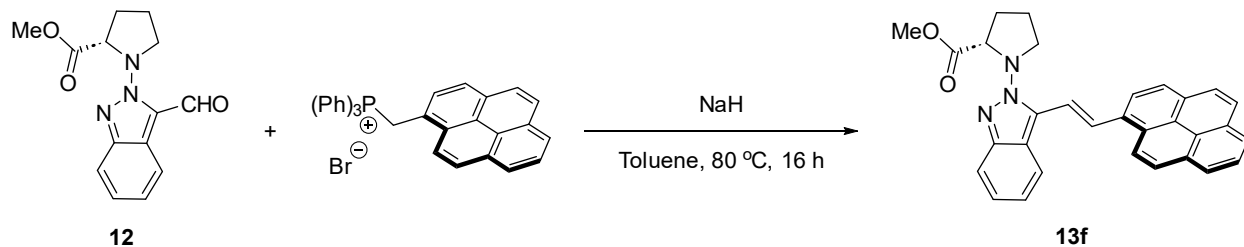


^{13}C NMR spectrum of 13e

Absorbance maximum: 364 nm; Fluorescence emission maximum (excitation at 364 nm): 427 nm. Absorbance normalized to baseline and zoomed for comparative viewing of excitation and emission spectra.



Methyl (E)-3-(2-(pyren-1-yl)vinyl)-2H-indazol-2-yl)-L-prolinate



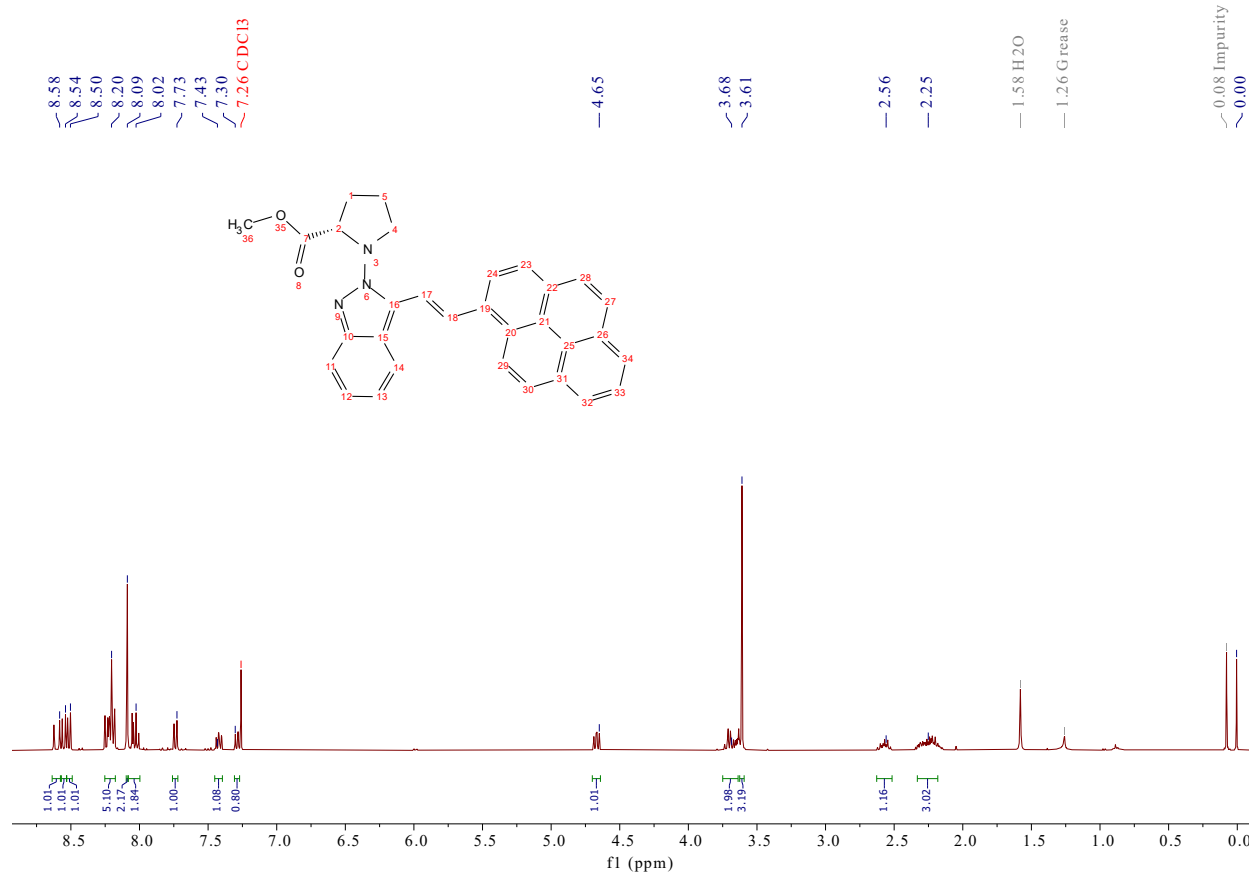
Procedure: A 25 mL Schlenk tube was charged with 334 mg of Triphenyl(pyren-1-ylmethyl)phosphonium bromide salt (0.6 mmol, 3.0 equiv.) and was backfilled with N₂ three times. Then, 2 mL of anhydrous toluene was added under N₂. The resulting mixture was cooled to 0 °C. To this cooled solution, 24 mg of NaH (0.6 mmol, 3.0 equiv., 60 % dispersion in mineral oil) was added. The resulting mixture was stirred for 15 min, and then brought to room temperature and stirred for 1 h. 54 mg of isoindazole 3-carbaldehyde **12** (0.2 mmol, 1.0 equiv.) was added in one portion, and the resulting mixture was heated at 80 °C for 16 h. Upon completion of the reaction, as indicated by TLC, the reaction was quenched with water and extracted with EA (3 × 5 mL). The combined organic fractions were dried under Na₂SO₄, concentrated, and purified on silica using 0-10 % EA in Hexane as the eluent to give 49 mg of the titled product **13f** as a yellow solid (52 %).

Spectral data for 13f

Methyl (E)-3-(2-(pyren-1-yl)vinyl)-2H-indazol-2-yl-L-prolinate. ^1H NMR (400 MHz, CDCl_3) δ 8.65 – 8.60 (m, 1H), 8.59 – 8.56 (m, 1H), 8.54 (d, $J = 8.1$ Hz, 1H), 8.29 – 8.20 (m, 5H), 8.13 – 8.10 (m, 2H), 8.09 – 8.02 (m, 2H), 7.78 – 7.74 (m, 1H), 7.47 – 7.42 (m, 1H), 7.33 – 7.29 (m, 1H), 4.72 – 4.66 (m, 1H), 3.76 – 3.66 (m, 2H), 3.66 – 3.60 (m, 3H), 2.67 – 2.53 (m, 1H), 2.41 – 2.13 (m, 3H).

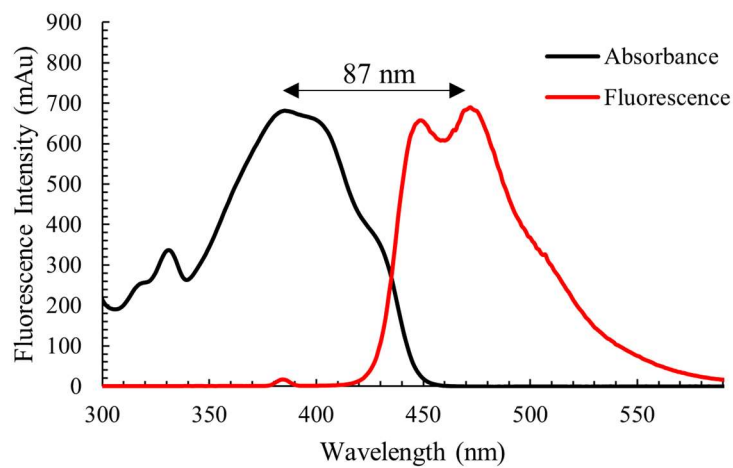
We are still working to obtain the ^{13}C NMR spectrum of **13f**

^1H NMR spectrum of **13f**

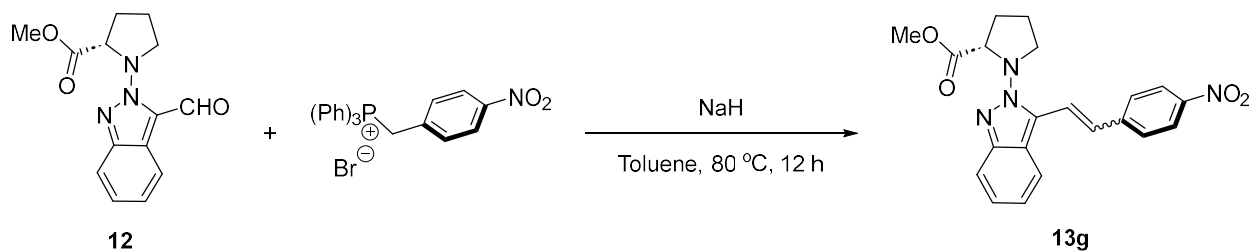


Absorbance maximum: 385 nm; Fluorescence emission maximum (excitation at 385 nm): 472 nm. Absorbance normalized to baseline and zoomed for comparative viewing of excitation and emission spectra.

Fluorescence Spectrum of 13f



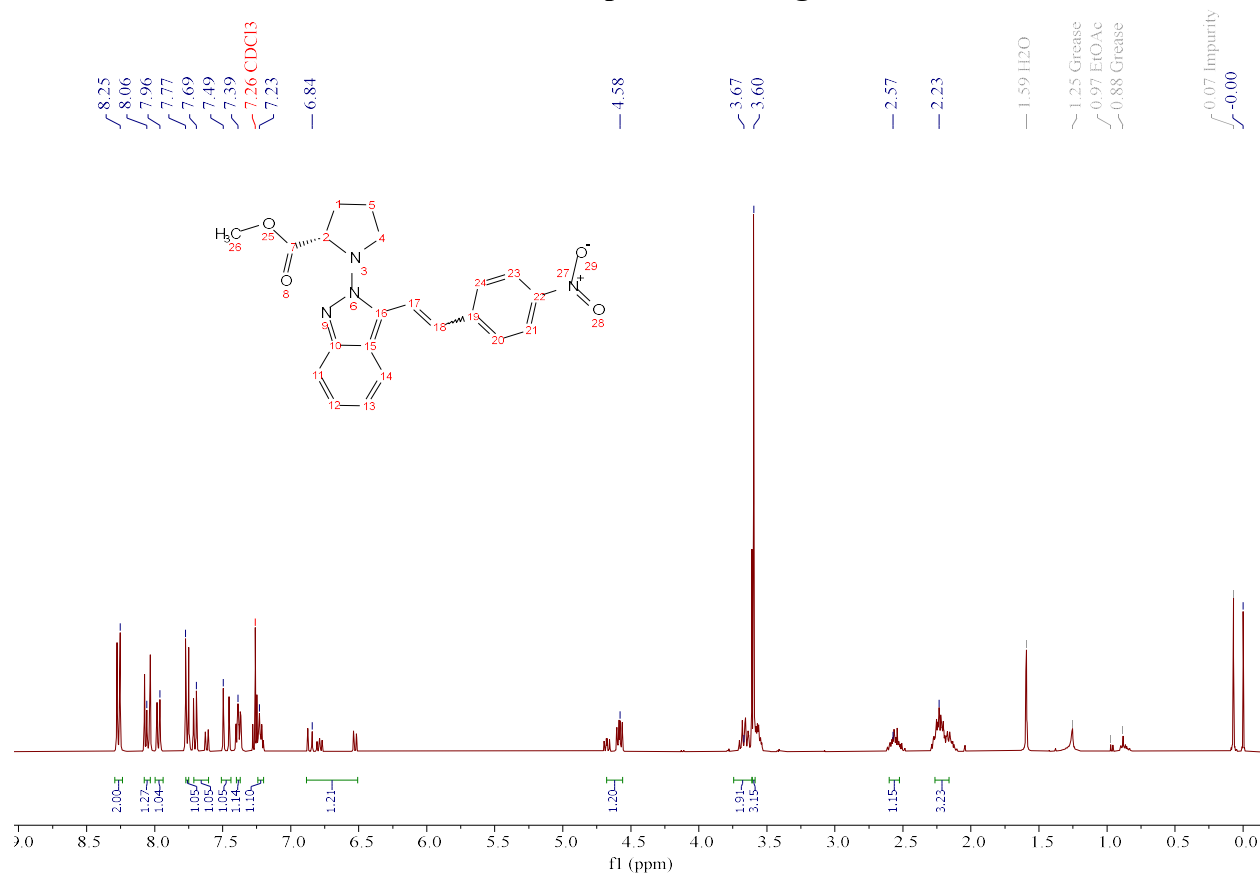
Methyl (3-(4-nitrostyryl)-2H-indazol-2-yl)-L-prolinate

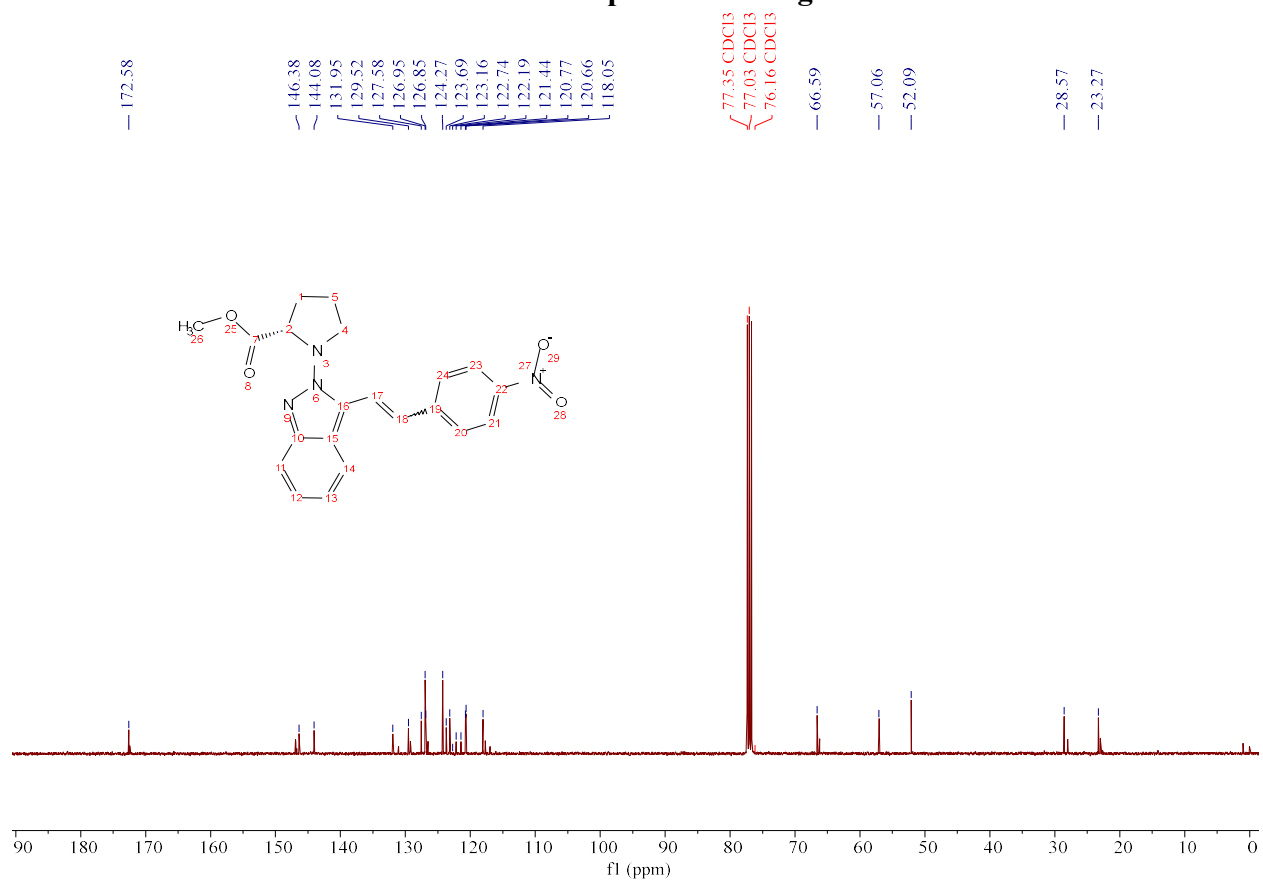


Procedure: A 25 mL Schlenk tube was charged with 286 mg of the (4-nitrobenzyl)triphenylphosphonium bromide salt (0.6 mmol, 3.0 equiv.) and was backfilled with N₂ three times. Then, 2 mL of anhydrous toluene was added under N₂. The resulting mixture was cooled to 0 °C. To this cooled solution, 24 mg of NaH (0.6 mmol, 3.0 equiv., 60 % dispersion in mineral oil) was added. The resulting mixture was stirred for 15 min, and then brought to room temperature and stirred for 1 h. 54 mg of Isoindazole 3-carbaldehyde **12** (0.2 mmol, 1.0 equiv.) was added in one portion, and the resulting mixture was heated at 80 °C for 16 h. Upon completion of the reaction, as indicated by TLC, the reaction was quenched with water and extracted with EA (3 × 5 mL). The combined organic fractions were dried under Na₂SO₄, concentrated, and purified on silica using 0-10 % EA in Hexane as the eluent to give 31 mg of the titled product **13g** as an orange solid (40 %, *E:Z* = 1:1).

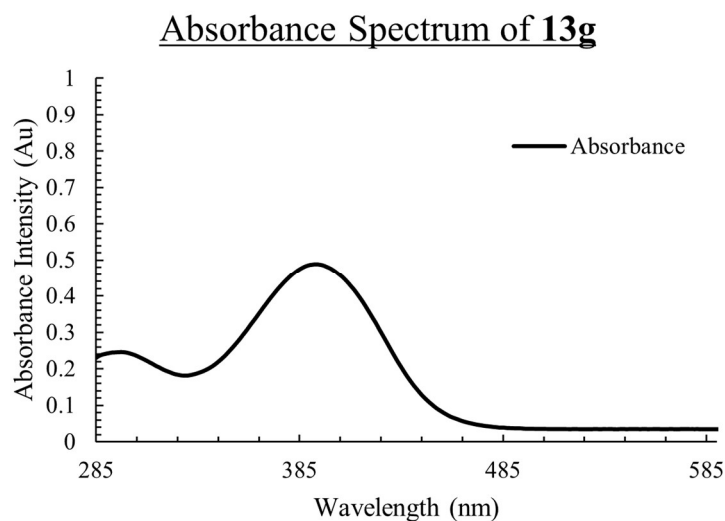
Spectral Data for **13g**

Methyl (3-(4-nitrostyryl)-2H-indazol-2-yl)-L-prolinate. ¹H NMR (400 MHz, CDCl₃) δ 8.29 – 8.23 (m, 2H), 8.10 – 8.01 (m, 1H), 7.99 – 7.95 (m, 1H), 7.79 – 7.73 (m, 1H), 7.72 – 7.59 (m, 1H), 7.51 – 7.43 (m, 1H), 7.41 – 7.35 (m, 1H), 7.25 – 7.19 (m, 1H), 6.88 – 6.49 (m, 1H), 4.71 – 4.54 (m, 1H), 3.75 – 3.61 (m, 2H), 3.61 – 3.55 (m, 3H), 2.65 – 2.46 (m, 1H), 2.31 – 2.08 (m, 3H). ¹³C NMR (101 MHz, CDCl₃) δ 172.6, 146.4, 144.1, 131.9, 129.5, 127.6, 127.0, 126.8, 124.3, 123.7, 123.2, 122.7, 122.2, 121.4, 120.8, 120.7, 118.1, 66.6, 57.1, 52.1, 28.6, 23.3.

¹H NMR spectrum of 13g

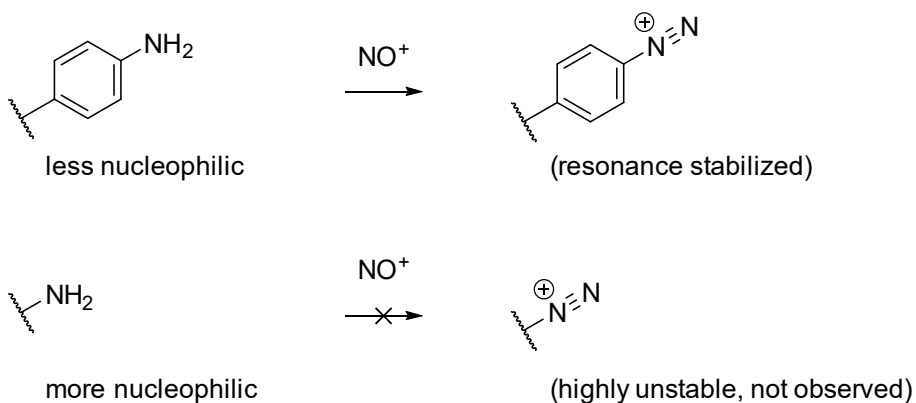
^{13}C NMR spectrum of 13g

Absorbance maximum: 392 nm; No fluorescence was observed for 13g at the excitation wavelength of 392 nm.



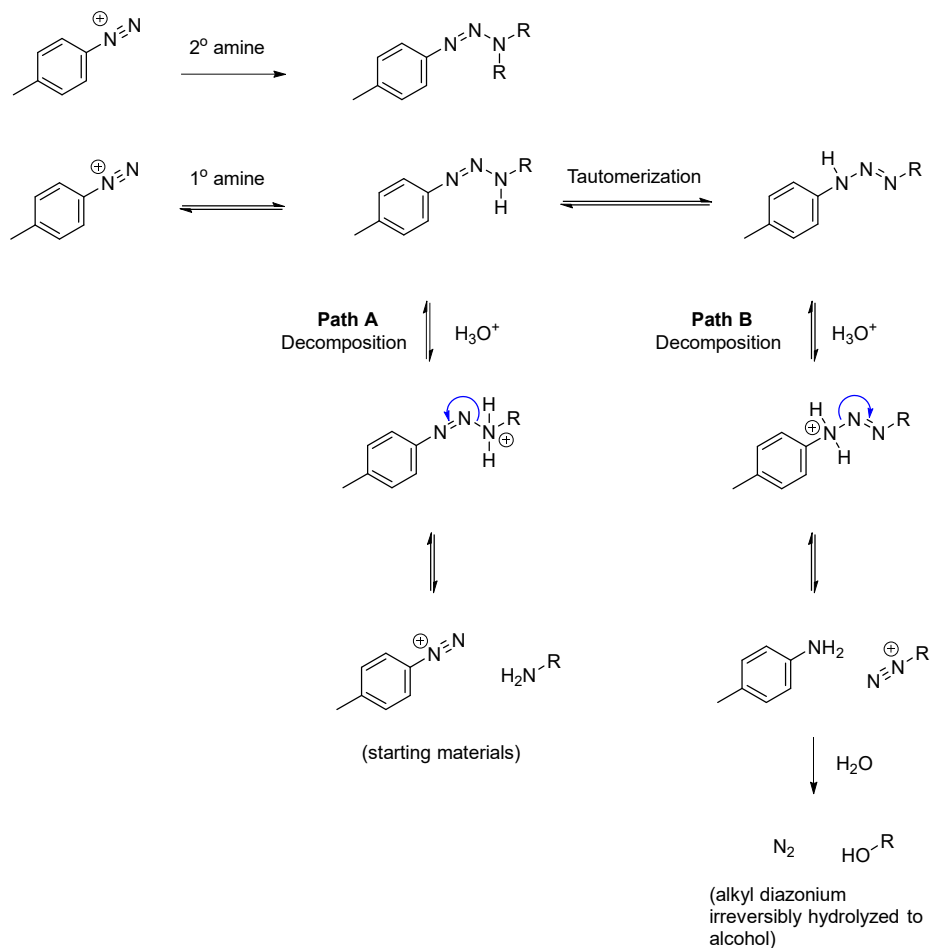
Supplementary Figure 9: Mechanistic considerations for formation of aryl diazonium and triazene

a. Formation of aryl diazonium



Discussion: The formation of the aryl diazonium follows a mechanism shown in the manuscript (Fig. 9). The diazonium ion has not been observed to form on alkyl amines in our reaction conditions. While an alkyl amine is more nucleophilic than an aryl amine due to the electron-donating nature of the aryl amine into the ring, there are one or more high energy transition states that lead to the formation of the alkyl diazonium. This poses an insurmountable barrier given the reaction temperature (0 °C) and short reaction time (10-15 min) to the formation of the alkyl diazonium.

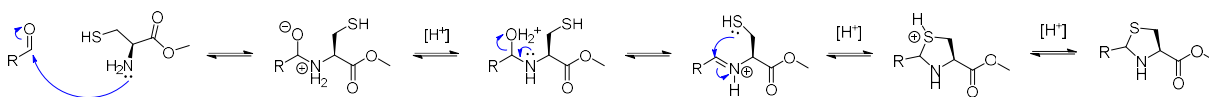
b. Stability of 2° triazene as compared to 1° triazene



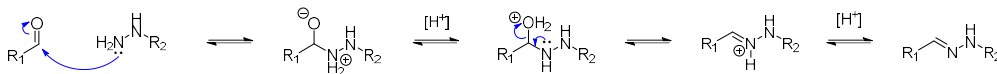
Discussion: a 2° amine is more nucleophilic than a 1° amine owing to the increased electron density afforded by hyperconjugation with the alkyl groups, which may partially explain the preferential reaction of 2° amines with the aryl diazonium. However, the aryl diazonium is a good electrophile and a 1° amine will conceivably react with it to form the triazene. Despite this, in our previous publication, for all peptide examples, the diazonium was observed to react selectively with the secondary amine, indicating a reversibility of the triazene formed from the 1° amine. Path A and B showcase the two decomposition pathways of the triazene from 1° amines.³ The triazene from the 1° amine can tautomerize into a second isomer that follows path B to give the alkyl alcohol as an irreversible product. We demonstrated in our previous publication that in the absence of a 2° amine, the aryl diazonium will slowly give the alkyl alcohol because of the irreversible nature of the formation of the alkyl alcohol. In short, when both a 1° and 2° amine source are present, the triazene selectively forms with the 2° amine.

Supplementary Figure 10: Mechanisms for derivatization of aldehyde from Figure 14

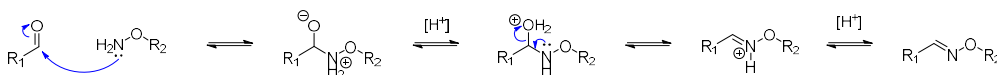
a) thiazolidine from cysteine



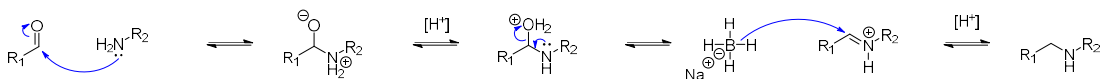
b) hydrazone from hydrazine



c) aldoxime from hydroxylamine

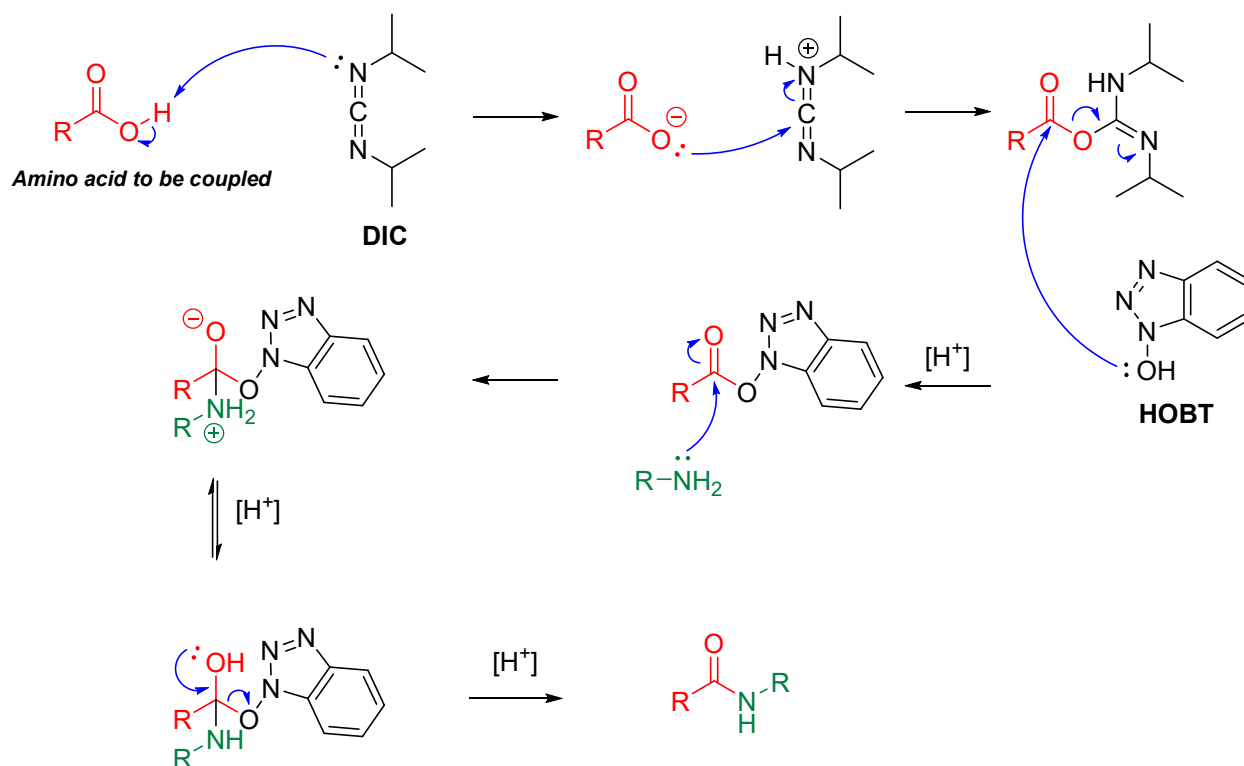


d) amine from reductive amination

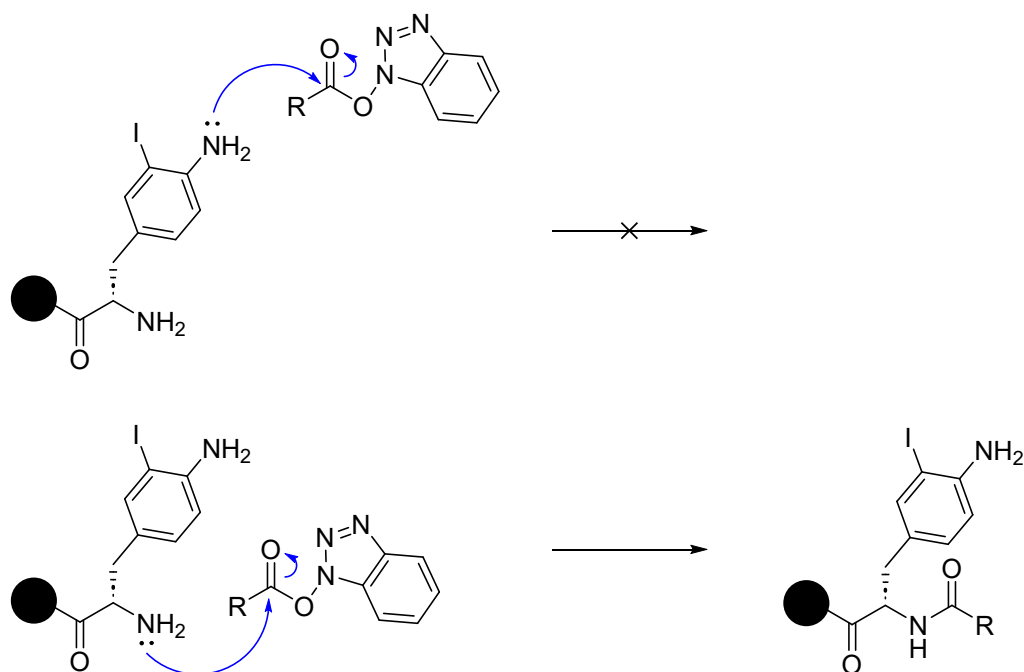


Supplementary Figure 11: Amino acid coupling mechanism and discussion

a) HOBT / DIC coupling mechanism



b) Aryl amine concern during SPPS



Discussion: As discussed in Chapter 1, there was a concern that the aryl amine would compete with the free N-terminus to react with the activated ester during amino acid coupling (Supplementary Fig. 11b). HRMS of the test cleavage product after Sonogashira coupling (Supplementary Fig. 3) and HPLC after chain elongation and cleavage both confirmed that the electron deficient aryl amine did not undergo coupling.

References

- (1) Chan, W. C.; White, P. D. *Fmoc solid phase peptide synthesis: A practical approach* (Oxford Univ. Press, New York, 2000).
- (2) Stathopoulos, P.; Papas, S.; Tsikaris, V. C-Terminal N-Alkylated Peptide Amides Resulting from the Linker Decomposition of the Rink Amide Resin: A New Cleavage Mixture Prevents Their Formation. *J Pept Sci* **2006**, *12* (3), 227–232. <https://doi.org/10.1002/psc.706>.
- (3) Farnsworth, D. W.; Wink, D. A.; Roscher, N. M.; Michejda, C. J.; Smith, R. H. Jr. Decomposition of Pyridinyltriazenes in Aqueous Buffer: A Kinetic and Mechanistic Investigation. *J. Org. Chem.* **1994**, *59* (20), 5942–5950. <https://doi.org/10.1021/jo00099a024>.